Summer 2014

Analysis of a ventilation network in a multiple fans limestone mine

Ali Haghighat

ANALYSIS OF A VENTILATION NETWORK

IN A MULTIPLE FANS LIMESTONE MINE

by

ALI HAGHIGHAT

A THESIS

Presented to the Faculty of the Graduate School of the

MISSOURI UNIVERSITY OF SCIENCE AND TECHNOLOGY

In Partial Fulfillment of the Requirements for the Degree

MASTER OF SCIENCE IN MINING ENGINEERING

2014

Approved by

Dr. Stewart Gillies, Advisor
Dr. Jürgen Brune
Dr. Kelly Homan

ABSTRACT

As mining progresses the total resistance of an excavation is increased, the mine characteristic curve becomes steeper, and the operating point moves up the fan curve, reducing the total air quantity and increasing the system pressure. For multi-level ventilation networks with a number of fans the process can be tedious, and on a count of numerous dependent factors the optimal combination of fans is very hard to be achieved. The design of a ventilation network in conjunction with multi surface fans and booster fans entails a complex procedure.

The objective of this study is to provide a plan to improve the ventilation network of a mine for use in the future with consideration to the source of losses through the network, design of network with multi fans and fire analysis. The guidelines listed in this paper were formulated based on current U.S. and international standards, safe operating practices developed by the mining industry, and recommendations provided by fan manufacturers. The problems proposed can be solved using ventilation and fire simulators and usage of computational fluid dynamics. Some key design factors which, if not accounted for properly, may result in ventilation system inefficiencies are shown.

A pressure and quantity ventilation survey has been conducted. The Hardy Cross method using switching parameters has been found to be a good tool to solve a multi fan network. The modified Hardy Cross method is faster and more flexible than other methods. Ventsim Visual software modeling has been used for network analysis to determine suitable surface and booster fans locations, blade settings, and speeds.

No underground peril has greater potential for large loss of life than a mine fire or explosion. A study has been carried out in order to get a better understanding of fire behavior in unpredicted incidents. A Bobcat vehicle burning at the working faces has been investigated. Various possible ways to control the fire have been considered.

Main mine fans are often connected to underground workings through bends or elbows. These connections may include damper controls or louvers. Leakage and shock losses in different parts of mine airways are of major concern. Comprehensive analyses has been undertaken of these ventilation shock losses experimentally, numerically and computationally to increase understanding and optimize air flow through the mine.

ACKNOWLEDGMENTS

I would like to extend thanks to Dr. Stewart Gillies, my advisor, for his technical knowledge and constant encouragement. I would like to express my sincere gratitude to the examining committee members: Dr. Jürgen Brune, Department of Mining Engineering of Colorado School of Mine and Dr. Kelly Homan, Mechanical Engineering department of Missouri S&T, for their support and guidance.

I would like to further extend my appreciation to Missouri S&T Experimental Mine personnel, specifically Mr. Jimmie Taylor and Rock Mechanics and Explosives Research Center staff for their patience and cooperation. It was a great pleasure working with Michael Bassett, John Tyler, Samuel Weeks and all others during my graduate study. I also would like to extend my thanks to Ms. Diane Henke, Ms. Kathleen Morris, Ms. Shirley Hall and Ms. Judy Russell for their patience and support.

I would like to show my appreciation to the National Institute for Occupational Safety and Health (NIOSH) for funding my research and education. I would like to express my deepest appreciation to my friend Arash Habibijavanbakht and his spouse Laura for their constant support and guidance. My abundant thankfulness to my brother Mohammad and his wife Maryam for guidance and advice that I undertake graduate study. Finally I would like to express my thanks to my mother Mahnaz and sisters and their husbands for keeping me grounded.

I would like to dedicate this thesis to my family, especially my mom, for her understanding, encouragement, and full emotional support of my graduate study. In addition I also would like to dedicate this thesis to the memory of my father, Karim.

TABLE OF CONTENTS

LIST OF ILLUSTRATIONS

Page

LIST OF TABLES

Page

1. INTRODUCTION

1.1. INTRODUCTION

A ventilation system is composed of a fan or fans and a set of connected mine openings. A single-fan network can be easily divided into two main ventilation components, the fan and the connected mine openings (or branches). By dividing the system in this fashion two characteristic curves may be drawn, the fan curve and mine characteristic curve. The mine characteristic curve, according to Atkinson's equation, in a single fan system is a strictly increasing function at a given specific air weight and a constant fan speed. However, this relationship holds true for a ventilation system with a single fan, but generally cannot be directly applied to multiple-fan networks because of the multiple pressures and air quantities that are associated with the different fans in the network and their interaction with each other (Wang, 1984b). Accordingly, each fan in a multiple-fan system has its own mine characteristic curve or subsystem curve associated with it. Many researchers have studied the interaction of fans in multiple-fan systems. The effect in behavior of usage of multiple fans is seen as an irregularity in the shape of each fans subsystem curve and in the resulting number of operating points in the system. This phenomenon may occur with many different axial flow fans, especially if one or more of those fans are operating outside of its design range. As a result mine fans may operate frequently between these operating points which appears as a considerable throb and pulsation accompanied with noise, rumbling and high vibration as described by Harrison and Kutay, 1986.

1.2. PROBLEM STATEMENT

As mining progresses the total resistance of an excavation is increased, the mine characteristic curve becomes steeper, and the operating point moves up the fan curve, reducing the total air quantity and increasing the system pressure. The design of a ventilation network in conjunction with multi surface fans and booster fans entails a complex procedure. Besides main mine fans are often connected to underground workings through bends or elbows. These connections may include damper controls or

louvers. As air progresses through the ducts imposed pressure by the main mine fan is dropped, the velocity is decreased and needful air quantity problem at working faces will emerge.

Unfortunately, the effects of mine fires on the underground ventilation system and the distribution rate of noxious gases and anticipation of fires before the event is extremely difficult, not only the location (which to some degree may be predicted using risk assessment techniques on possible combustible sources), but also to the nature, size and behavior of the fire. Therefore assessments have relied largely on empirical information and experimental precedents. Fires and explosions are significant contributors to fatalities and high potential incidents in the world mines. MIHSC (2005) conducted a detailed review of safety incidents in the Australian mining industry over a two-year period from July 2002 and found a high potential incidence rate per million work hours of four and nine respectively for coal and hardrock mines from fires alone. Major explosions in coal mines are not uncommon events in first world countries (Pike River in 2010 and several in the USA in the past ten years); major fires in underground hardrock mines are also not infrequent, with at least two fires widely reported in Australasia in the public media in the past 18 months (Broken Hill truck in fuel bay in late 2011 and Waihi truck fire in mid-2012), but there have been many others that have not had such a high public profile as described by Brake, 2013.

1.3. ANALYSIS TECHNIQUES

Research defining how system pressure, air power, and quantity are affected by multi fans network; describing how system efficiency and network power cost are affected by the location, placement, and size of the booster and surface fans; and identifying the relationships between booster fans and main surface fans in ventilation systems that are consistent with U.S. mining conventions is presented in this study. Besides research is going to clarify how percentage of noxious gases, psychrometric information of the mine, heat in unforeseen fire event is consistent with the knowledge about natural ventilation pressure, time, location of event and the procedures for controlling the fire intensity; and identifying the percentage of toxic gases has been

controlled according to the U.S. mining conventions is presented in this study. Research explaining how ventilation network pressure and velocity through ducting are affected by losses which are caused by different bends and modulators such as elbow and louvers; and analyzing the shape, size; bend angle of these parts to optimize the air quality at the mine inlet shaft has been undertaken.

1.3.1. Network Modeling Using Ventilation Software. Numerical modelling software (Ventsim) has been used for network analysis to determine the optimum surface and booster fans locations, blade settings, and speeds. Both natural and mechanical induced ventilation pressures have been taken into account. Numerous parameters such as efficiency, air quantity, total pressure, density and temperature have been considered to select the most appropriate surface fan taking into account the effects of other fans. This study has been employed to maximize the networks efficiencies and air flow quantities at determined working faces and understand the minimization of annual network power costs. Different locations for surface fans and use of booster fans operating at varying blades angles have been examined in series or parallel connections. Air pressure and quantity surveys have been used to acquire performance specification. The main fan selection has been carried out according to the mine required performance specifications and fans' characteristics. As part of this study the ventilation model has been expanded for the next 100 years and simulations have been conducted to design the future ventilation network plan. In addition, a cost study analysis has been done to evaluate the optimal solution for the future of the ventilation plan.

1.3.2. Fire Modeling Using VENTFIRE Software. Numerical modelling software (VentFIRE) has been used to investigate fire behavior through the airways on future layout of mine ventilation network. Both natural and mechanical induced ventilation pressures have been taken into account. . Heat simulation and dynamic simulation has been calibrated for fire simulation commencement. According to the most usable vehicle in that mine a Bobcat burning, has been investigated at working faces. Numerous parameters such as amounts of CO, CO_2, O_2, temperature behavior, heat and airflow direction have been investigated during the real time. Various options have been considered to decrease the amount of perilous gases at determined monitored stations in all scenarios. Surface and booster fans have been turned off or left on according to the

least amount of hazard accomplishment. The optimum procedure for mitigation of hazards, temperature and toxic gases has been selected as the most advantageous plan in the mine.

1.3.3. Computational, Experimental and Numerical Modeling Analysis. Computational fluid dynamics (CFD) exercises have been conducted to gain understanding of flow behavior through ducting. Fluent 14 has been applied in order to investigate pressure drops across louvers and the elbow in mine's duct. The model has been used to predict possible locations and leakage flow rates for numerous boundary conditions and geometries over the elbow and inlet shaft. A series of simulations has been performed for optimum design of main fan ductwork by reducing shock loss in the air way. Losses from various elbow's angles and louvers have been calculated numerically by using Bernoulli's equation for incompressible fluid. K Atkinson factors for different angles of elbow and air power losses across louvers have been calculated numerically.

1.4. OBJECTIVES

The objective of this study is to propose a plan to improve a ventilation network of Missouri S&T Experimental Mine for use in the future with consideration to the source of losses through the network, design of network with multi fans and fire analysis.

A first action is to quantify how the efficiency of a ventilation system can be increased with use of an additional main fan. The design of a multi fan future ventilation network can be demonstrated with the use of numerical modelling software. The layout of ductwork, door/stopping positions and fans with different characteristics has been examined. In all simulation scenarios, the interaction of operating main and booster fans with each other and the reversal ventilation network flow has been considered. The required flow rate at identified working faces has been determined. Efficiency, minimum energy losses and annual network power cost determines the best scenario. Designs have been proposed for the ventilation network future plan. The optimum flow rate across working faces is the key criterion selected.

Fire events are the most significant contributors to fatalities and high potential incidents in mines. Data from fire simulators have been used to evaluate numerous options to achieve the acceptable layouts to mitigate the hazards in the Experimental Mine. This study has been carried out in order to get a better understanding of fire behavior in unpredicted incidents. A Bobcat vehicle burning has been investigated at working faces. Numerous parameters such as amount of toxic gases, psychrometric behavior, airflow direction, visibility and produced heat have been investigated. Tire selection has been considered in all simulations. Confining the fire in a limited area with a low monitored amount of gases of CO, CO_2 and a high amount of O_2 at determined stations have been determined as the key criteria amongst all scenarios for selecting the acceptable plan in emergency situations. Various options have been considered to quench produced fires in the mine. The ideal long distance control of fire for mitigation of hazards, temperature and toxic gases has been selected as the most advantageous plan in each scenario. The most dangerous part of the mine has been identified.

Finally, a comprehensive analysis has been undertaken of ventilation shock losses in ducting by experimental, numerical and computational approaches to increase understanding of air flow through the mine. Two approaches have been used to determine shock loss factor across the elbow numerically. Atkinson's friction factor "k" for the mine elbow has been determined. The Bernoulli Equation has been used to calculate pressure loss across the louver at two discrete angles. An approach has been used to determine loss factors (K factors) across the louvers numerically. The CFD exercises have been conducted to gain understanding of flow behavior at various louver blade angles and elbow designs with intention of achieving minimum shock loss and maximum velocity at the inlet shaft.

Different parameters such as velocity inlet and outlet pressure drops have been determined and ideal elbow and louver designs have been selected from use of the experimental, numerical and computational approaches. Experimental design has been compared to the computational and numerical designs. The optimum position of main mine fan has been determined from results of this study.

2. LITERATURE REVIEW

2.1. UNDERGROUND VENTILATION SYSTEMS-BACKGROUND INFORMATION

The design of an underground ventilation system is a complex process due to many interacting development, production and mine support systems. It is important that ventilation system design and other mine support infrastructures must not be treated in isolation during the overall mine design process. However, in the past it has often been the case that the sizes of mining equipment along with the required rate of mineral production and ground stability considerations have dictated the layout of a mine without, initially, taking into account ventilation demands. This usually results in inefficient ventilation systems with high capital and operating costs. In some cases, the results of inadequate planning and incorporation of ventilation system design deficiencies can result in production losses, high costs of reconstruction, poor environmental conditions and tragic consequences to the health and safety of the workforce (McPherson, 1993).

Mine fans are selected for dynamic conditions since the flow and pressure relationships change constantly over the life of the mining operation. The volume requirement is a function of the number of working sections, the extend of idle or inactive areas methane or other strata gas liberation rates, and the quantity and size of diesel equipment operated in the mine. For deeper metal mines, heat and humidity control needed to provide acceptable working conditions also influence the required fan plant capacity. The pressure requirement is a function of the losses associated with the shafts, as well as the configuration and physical characteristics of the ever changing underground mine workings. The selection of a main mine fan is established by several duty points based on the flows and pressure determined by the conditions and factors noted above over the projected life of the mine(Gamble, Ray, Americas, and York, 2009).

A coal mine main fan is one of the largest-power-consuming facilities among various electrical and mechanical equipment. Its power consumption usually accounts for 20% ~ 30% of the mine total. If a few percentage points can be lowered in its energy consumption, energy efficiency will be very substantial. One main reason for the main

fan's high power consumption is its overall low efficiency (Wang, Wei, Yuan and Zhu, 2009).

Mine ventilation essentially deals with the controlled flow of air through mine airways to maintain an acceptable atmospheric environment. Martinson (1976) has defined three elements of ventilation,

1.) An engineering element concerned with establishing quality control (removal of dust and gases), quantity control (regulation of air direction and magnitude) and climatic conditioning (temperature-humidity control),

2.) A biological element in which an understanding of biological response is used in assessing the mine environment, and

3.) A philosophical element requiring judgments as to the degree of risk or worker discomfort that is socially acceptable (Luxbacher and Ramani, 1979).

2.2. EVALUATION CRITERIA OF MINE VENTILATION SYSTEM

As described by Cooke, 1958. The use of ventilation efficiency is considered in two parts: (a) the efficiency of the fans, and (b) the efficient use of the fan quantity and pressure in the underground workings. Since, for evaluation purposes, efficiency must be further defined in terms of cost, Cooke identifies the following cost items to be considered:

- The cost of driving and maintaining roadways;
- The cost of primary ventilation;
- The cost of ancillary underground equipment;
- The cost of power; and
- The cost of the consequences of reduced or inefficient mine ventilation.

In the optimization of coal mine ventilation systems through the evaluation of alternatives, two major cost classifications have been developed as the evaluation criteria. These are the power cost and the capital costs. In addition, a separate classification based only partially on cost is also included: the system shaft requirements (Luxbacher and Ramani, 1979).

2.2.1. Power Cost. In coal mine ventilation, power costs are a continual daily expense. Fan power and air quantity have a cubic relationship and 3/2 power of the system head loss. It is obvious from power considerations alone that only as much air as is required should be circulated through the ventilation system. Consequently, leakage should be maintained at a practical minimum (Luxbacher and Ramani, 1979).

System head loss is much more difficult to analyze. A balance should be maintained between the head loss in the intake and return air courses, either by entry configuration or by shaft placement. In multiple fan mines the system head loss may depend on the zone of influence of each of the fans, which may change as the fan operating conditions (speed and blade angle) are changed (Turpin and Wheyher, 1977).

2.2.2. Capital Cost. Capital cost items include the system main fans and the ancillary underground equipment such as stoppings, regulators, and overcasts. Cost estimates for some of this equipment may be hard to quantify, especially when it is to be used on a comparison basis.

2.2.3. Shaft Requirements. Shaft requirements are considered separate from capital costs for several reasons. Primarily, the high cost for shaft construction has led many companies to attempt to minimize shaft requirements simply to minimize capital outlay. This is despite the fact that most coal companies treat shaft sinking costs as capital expense items and amortize them. Instead, the rehabilitation of old entries or the driving of new entries (with the added benefit of coal production) is often preferred (Luxbacher and Ramani, 1979).

2.3. OPTIMIZATION OF MAIN FANS

After running for a long time, fan impeller, inlet box, air inlet, and fan casing of mine ventilation main fan are corroded seriously. This is a threat to safe operation of main fans, which increases running resistance and reduces efficiency. Therefore, main fan corroded can't meet actual needs of fieldwork (Wang and Shang, 2009).

2.3.1. Main Fans Background in U.S. Great care is usually given in the mining industry to design and installation of main fan assemblage, but less to installation of underground booster fans. The proper design of the primary ventilation fans is critical to

a mine (Krog, 2002). Main mine fan installations at underground U.S. coal mines must be designed to comply with the requirements outlined in 30 CFR (Code of Federal Regulations) part 75. However, very little emphasis is placed typically on the aerodynamic optimization of shaft collar designs, ductworks configurations and the selection of a fan isolation, or "closing door" system. Field testing has shown that poorly designed systems may produce large pressure losses between the shaft and fan inlet, as well as air turbulence problems which adversely impact fan efficiency and sometimes fan structural integrity (Ray, n.d.). Distributing the air adequately through the network with considering the denouement of that on booster fans, Stoppings and the other parts of ventilation circuit is the major concern in conjunction with optimization of surface fan.

2.3.2. Location of Main Fans. In the majority of the world's mines, main fans are sited on surface. In the case of coal mines, this may be a mandatory requirement. A surface location facilitates installation, testing, access and maintenance while allowing better protection of the fan during an emergency situation. Siting main fans underground may be considered where fan noise is to be avoided on surface or when shafts must be made available for hoisting and free of airlocks. A problem associated with underground main fans arises from the additional doors, airlocks and leakage paths that then exist in the subsurface. In designing the main ventilation infrastructure of a mine, a primary decision is whether to connect the main fans to the upcast shafts, i.e. an exhausting system or, alternatively, to connect the main fans to the downcast shaft in order to provide a forcing or blowing system (McPherson,1993). In U.S mines the most common system is exhausting system.

Blower systems generate pressure higher than atmospheric and this prevents gases trapped in the caved area (gob) from entering the mine atmosphere and exhaust systems from pressures lower than atmospheric and this tends to draw gases into the mine atmosphere where they can be diluted (McPherson,1993). Blower systems have several disadvantages. Because they operate at high pressure near the intake, air lock doors are required and these doors can contribute to excessive air leakage and lower system efficiency. Also, in blower systems, if the fan fails, the relative pressure drops and large amounts of gas can be liberated (Hartman et al, 1997). Possible location of main fans has been shown in Figure 2.1.

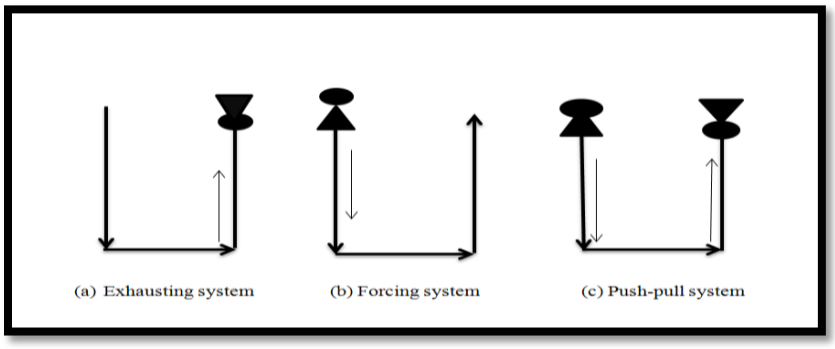

Figure 2.1. Possible locations of main fans

Airflow direction is affected by the location of the main fan which, in turn, will significantly impact the other aspects of operation or transportation. An antitropal system is one in which the airflow and transported rock moves in opposite directions, implying that the mineral transportation is carried out in intake airways. This tends to put restrictions on the air velocities in intake airways so that dust and other gases will not be too excessive. Conversely, a homotropal system is one where the airflow and the mined rock move in the same direction, or the haulage is carried out in return airways. This system will ensure that dust, heat, and other pollutants from broken rock will be vented directly to the outside. In addition, this system also has the advantage in case of fire occurring in the haulageway.

Another factor in airflow direction is the inclination of the airway. An ascensional ventilation is when the airflow moves upwards through inclined workings. This takes advantage of the natural ventilation effects caused by the added heat to the air. Descensional ventilation may be employed on a more compact system, with both air and conveyed materials moving downhill.

It is the pressure difference that causes air to flow underground, regardless of how this pressure difference is generated. There are different merits and drawbacks in each system. A particular system must be selected to accommodate the specific mining situation, and not the ventilation designer's pet theories. The following is a list of pros and cons for both arrangements (Tien, 1978).

2.3.2.1 Exhausting system.

2.3.2.1.1 <u>Advantages.</u>

- When main fan stops, underground pressure builds up to atmospheric. The increase in pressure slows gas emissions from the gob and prolongs the time required for the gas to reach active workings.
- The haulage roads, where most travel is done, are kept free from dust, gas, and smoke. This permits the men to perform their work in fresh air.
- In the event of a fire or explosion, exhausting ventilation enables the rescue work to proceed more rapidly, because the fresh air is on the haulage road, which provides an easy route for carrying material and equipment to make mine repairs.
- Both intake airways and track entries serve as escapeways, if stopping lines are well maintained.
- Greater power savings are possible if mine openings are small. This is due to the potentially greater recovery of velocity pressure through the use of discharge evasè (gradual expansion ducts) on exhaust fans.

2.3.2.1.2 <u>Disadvantages.</u>

- It reduces temperatures in the belt slope, slope bottom, and main haulage line. During winter, the belt sprinkler system, damp coal on the belt rollers, and water lines along the haulageway can freeze. The temperature also is uncomfortable for the people working in these areas.
- It is more difficult to detect a fire in belt and track entries since the air is carried directly to the return airways.
- Dust produced at the portals and along the haulage road contaminates the intake air stream. Similarly, fire in the belt and track entries can be carried to the working areas.
- d) Contaminated air goes through the fan, corrosive particles settle on the fan blades and corrodes them, reduces effective air passage area, and can throw the fan out of balance.

2.3.2.2 Blowing system.

2.3.2.2.1 <u>Advantages.</u>

- It applies a continuously decreasing overpressure from the air intake portal to the discharge opening. This characteristic produces airflow from intake airways to the return and prevents contaminated flow into working areas from idle areas and return airways. In fact, the blowing system may be the only practical method of ventilation in shallow mines having fractured ground, as well as areas of contiguous mining where there may be ground cracks into abandoned mines.
- The haulage roads and hoisting shaft stay free from ice, making it more comfortable for the men in winter.
- A fire in any part of the mine is soon evident, due to leakage, to anybody working in the air current coming away from the face area.
- Only outside air, non-corrosive and with normal moisture content, goes through the fan.
- Fan unit is cheaper because of a shorter fan duct (diffuser).

2.3.2.2.2 <u>Disadvantages.</u>

- Products of combustion from a mine fire or explosion are carried into the neutral escape-way. Thus, fire-fighting and rescue work are more difficult because access is often blocked by smoke. Ventilation reversal, in these cases, may endanger the men.
- Dust, smoke, and other impurities are carried away from the face area and along the haulage road. Methane tends to accumulate in pockets in the roof, sometimes causing slight explosions.
- Since neutral air flows away from working sections to the slope bottom, any accumulated air contaminants converge on workmen in the slope bottom area.
- Shock losses are greater. It requires a distance of 30 times the duct diameter away from the pressure jet for the air velocity to lose 90% of its original velocity. For an exhausting system, only one duct diameter distance is required to lose 90% of its velocity. As result, pressure loss caused by shock, which is in addition to frictional loss, is considerably more in a blowing system.
- Dirt and dust from outside will settle on the fan blades.

2.3.2.3 Push-pull (combination) system. In the push-pull system, it is easier to get air to difficult places. The disadvantage of this system is that it is harder to balance the ventilation system, resulting in neutral spots in the mine. According to recent survey, the majority of the underground coal mines in the U.S. use exhausting ventilation as their main ventilation system.

In the more general case of multi-shaft mines, the use of multiple main fans (whether exhausting, forcing or push-pull) offers the potential for an improved distribution of airflow, better control of both advantages may not always be realized as a multi-fan system requires particularly skilled adjustment , balancing and planning (McPherson,1993).

2.4. FEDERAL REGULATIONS

2.4.1. Main Mine Fan Installation Design. The design of main mine fan installations at underground mines must comply with requirements of the mine safety and health administration of the United States Department of Labor as outlined in the Title 30 CFR (Code of Federal Regulations) part 75 ("Mandatory safety standards – Underground Coal Mines")[3] or part 57 ("safety and health standards – Underground Metal and Non Metal Mines")[4]. Part 75 contains stricter regulations pertaining to fan installations than part 57 due to the presence of methane gas, which is explosive in concentrations of 5 to 15 percent, in underground coal mines. Stipulations regarding main fan installations contained in part 75 include the following:

2.4.1.1 Offset distance. Fans cannot be within 4.5 m of the mine or shaft opening.

2.4.1.2 Explosion doors or weak walls. To protect the fan from a possible underground methane explosion, doors or weak walls in line with the direction of the explosive forces must be provided to allow pressure relief in a direction away from the fan installation.

2.4.1.3 Fan motor location. The drive motor for a main exhaust fan must be located outside of the return airstream to prevent a methane ignition caused by arcing from the motor. Locating the motor outside of the airstream requires a minimum of a 45-

degree turn in the inlet ductwork to the fan, as illustrated in the coal mine exhaust fan installation.

2.4.1.4 Self-closing doors. Fans at mines with more than one main mine fan must be equipped with self-closing doors or dampers in the connecting ductwork to prevent air reversals through idle fans (Gamble et al., 2009).

The installation of main mine fans underground is prohibited by 30 CFR part 75.310, (a)(1). Providing explosion doors or weak walls in line with a possible underground explosion and offsetting the fan 4.5 m from the edge of the shaft preclude the installation of the fan directly over the shaft. In addition, 30 CFR part 75.507-1 specifies that all electrical equipment used in return air courses be permissible, which requires locating the fan motor outside of the airstream exhausted through the fan(Ray, n.d.).

2.4.2. Ventilation Regulations. In the United States, coal mines are required to use surface fans for ventilation, and with the exception of anthracite mines, the use of booster fans is prohibited. There are fewer than 64 surface and underground anthracite coal mines in the United States and only 160,000 tons of coal are produced from underground anthracite mines, which accounts for less than 1% of the total underground coal production.

Underground anthracite mines make up a very small sector of the underground coal industry and because booster fans are prohibited in all underground coal mines except anthracite mines, booster fans are illegal in the vast majority of underground coal mines in the United States. In contrast, booster fans are permitted in coal mines in both Australia and the United Kingdom. In Queensland, Australia, mine operators must have a principal hazard management plan that defines procedures for using booster fans and action required if methane levels reach 1.25% or higher. In the Australian state of NSW, which contains a high concentration of underground coal mines, booster fans can only be installed if the installation and operation of the fan have been approved by the mine inspectorate (Wempen, 2012).

Although booster fans are allowed in all underground mines in the world, main surface fans are the primary source of ventilation. As such, given their critical life safety function, failure of these fans is given important consideration including fail safe power systems, failure warning systems, and backup fans. Main fan failure is particularly

significant in systems using booster fans because if the main fan is disabled, a large amount of recirculation is likely to occur. The United States, the United Kingdom, and Australia all have regulations related to main fan failures. In the United States, if a surface fan stops, all the electrically powered and mechanized equipment must be disabled, and if the fan is stopped for more than 15 minutes and ventilation is not restored, the mine must be evacuated. Backup fans can be used to provide adequate ventilation in the event of a fan failure, but they are not required, and few U.S. mines maintain backup fans. In Australia, requirements in the event of a main fan failure are similar to the requirements in the United States. In the United Kingdom, mines are required to maintain standby surface fans that are capable of providing adequate airflow to allow a mine to be safely evacuated in the event of a main fan failure. Although it is not required, most mines in the United Kingdom maintain a standby fan that is capable of producing full volume flow. Like Australia, the failure of a main fan does not immediately require mine evacuation. In addition to regulations regarding fans in underground coal mines, regulations defining adequate airflow in development areas and limiting contaminant concentrations throughout a mine are important because they help to define the necessary air capacity of ventilation systems. Because the method of coal production can affect the amount of dust produced and the volume of gas liberated, the United States specifies different air quantities for continuous miner and long wall mining methods: a minimum, 4.25 m^3/s of airflow is required at the last open crosscut of each set of entries in continuous miner sections and 14.16 m^3/s of airflow is required at a long wall working face. In New South Wales, continuous miner sections must maintain 0.3 m^3/s for each square meter of roadway cross-section and long walls must maintain 4 m^3/s for each meter of extraction height. Queensland requires a velocity of 0.3 m/s in all areas that are identified as explosion risk zones (ERZ), including the working sections, where the concentration on methane is between 0.5% and 2% (Moreby 2009).

Regardless of the air quality, ventilating multiple working sections with the same intake air is prohibited in coal mines in the United States and in Australia. In addition to the use of prescribed flow rates, the United States and Australia also require that contaminants be limited to acceptable levels. Australia's limits for methane, oxygen, and carbon dioxide are identical to the limits required in the United Kingdom. In the United

States, the eight-hour time weighted average (TWA) exposure to carbon dioxide is 0.5% with a 15-minute short term exposure limit (STEL) of 3% by volume. Oxygen must be maintained at 19.5% by volume. Methane concentrations in the intake airways must be maintained at less than 1% by volume, return airways must be maintained at less than 1.5% methane by volume, and bleeders must be maintained at less than 2% methane by volume. Maximum allowable levels of gas concentrations in the United Kingdom, Australia, and the United States are shown in Table 2.1 (Moreby, 2009).

Table 2.1. Gas concentration limits as a percentage by volume

			CH4%	
	Co_2%	O2%	Face	Return
United State	0.50	19.5	1.00	1.50
Australia	1.25	19.0	1.25	2.00
United Kingdom	1.25	19.0	1.25	2.00

2.4.3. Ventilation Controls. Within the primary and auxiliary ventilation systems there are two types of controls, active control (i.e. fans) and passive controls (i.e. doors and regulators). Presently, both controls can be installed easily and cost effectively. Primary and auxiliary fans can be fitted with soft starters and variable frequency drives (VFDs) and their airflow delivery controlled through either variable pitch or rotational speed. Furthermore, most commercial ventilation doors can be adapted in order to allow variable amounts of airflow along the development and haulage drifts. Some ventilation doors can also act as regulators when partially open; alternatively, specific regulators with a finer control of volume may be required (Fink and Beatty, 1987), (Allen and Keen, 2008).

2.5. AXIAL FANS

2.5.1. Axial Impeller. Axial fans of acceptable performance did not appear until the 1930's. This was because of a lack of understanding of behavior of air flow over axial fan blades. The early axial fans had simple flat angled blades and produced very poor efficiencies. The growth of the aircraft industry led to intensive studies of airfoils for the wings of airplanes (McPherson, 1993). A fixed bladed axial fan of constant speed has a rather limited useful range and will maintain good efficiency only when the system resistance remains sensibly constant. This can seldom be guaranteed over the full life of a main mine fan. Fortunately, there are a number of ways in which the range of an axial fan can be extended;

(a) The angle of the blades may be varied.

(b) The angle of the inlet and /or outlet guide vanes may also be varied, with or without modification to the impeller blade angle.

(c) The pitch of the impeller may be changed by adding or removing blades. The impeller must, of course, remain dynamically balanced. This technique can result in substantial saving in power during time periods of relatively light load.

(d) The speed of impeller may be changed either by employing a variable speed motor or by changing the gearing between the motor and the fan shaft. The majority of fans are driven by A.C. including motors at a fixed speed. Variable speed motors are more expensive although they may produce substantial saving in operating cost (McPherson, 1993).

2.5.2. Various Losses in Axial Fans. The losses in an axial fan may be divided into recoverable ad non-recoverable groups. The recoverable losses include the vortices or rotational components of velocity that exist in the airflow leaving the fan. We have seen that these losses can be recovered when operating at the design point by the use of guide vanes. The non-recoverable losses include friction at the bearings and drag on the fan casing, the hub of the impeller, supporting beams and the fan blades themselves. These losses result in a transfer from mechanical energy to heat which is irretrievably lost in its capacity for doing useful work (McPherson, 1993).

2.6. MAIN FAN ENERGY CONTROL METHODS

2.6.1. Outlet Dampers. Outlet dampers increase system pressure and reduce air quantity, effectively increasing system resistance and reducing fan power.

2.6.2. Fan Speed. Fan speed can be controlled by electronic, hydraulic or mechanical variable speed drive [VSDs]. VSDs have gained wide acceptance and in some cases have been applied to control main mine fans. While these systems can find application for new installations they are in general, because of cost and complexity, unsuitable for retrofit of existing main fans.

2.6.3. Inlet Guide Vanes [IGV]. Pre-rotational guide-vane controls involves Fitting adjustable vanes into the air stream at the fan inlet. The guide vanes generate a controllable swirl in the air as it enters the impeller. If swirl is in the same direction as the rotating fan impeller then the effect and work done by the impeller is low- hence part load. If swirl is in the opposite direction then the effect and work done by the impeller is high- hence full load.

2.6.4. Theory. Total pressure rise across any fan impeller- axial, mixed flow or centrifugal- is given [ignoring losses] by the following equation (Stebbins, 2005):

$$\Delta p = U2V2\cos\alpha 2 \; - U1V1\; cos\alpha 1 \qquad (2.1)$$

where U, V and α are shown in the velocity triangles of Figure 2.2 (Plessis and Marx, 2008).

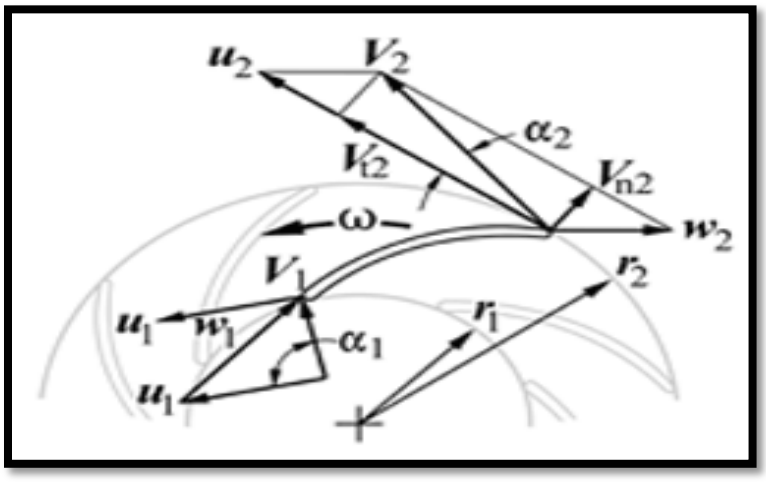

Figure 2.2. Centrifugal impellor velocity triangle

2.7. METHOD OF SOLVING MINE VENTILATION NETWORKS

There are basically two sets of solving fluid networks:

- "Analytical" methods, which involves the formulation of the governing laws into sets of equation that can be solved analytically in order to obtain a solution, and
- "numerical" methods, which become very popular with the availability of personal computers, which were then used to solve the equations through iterative procedures (Eng, 2009).

2.7.1. Analytical Methods. The "equivalent resistances" of a ventilation network is the most elementary method of solving and balancing a ventilation system. If two or more airways are connected in series or in parallel then each of those sets of airway resistances may be combined into a single "equivalent" resistance. The concept of equivalent resistances is particularly useful when combining two or more airways that run parallel to each other. Through this technique, thousands of such branches that may exist in a mine can be reduced to hundreds, thus simplifying the network schematic, reducing the amount of data needed to be processed and consequently, minimizing the time of solving and balancing a ventilation system (McPherson, 1993).

2.7.2. Numerical Methods. The method that is most widely used in computer programs for ventilation network analysis was originally developed for water distribution systems by professor Hardy Cross at the University of Illinois in 1936. This was modified and further developed for mine ventilation systems by D. R. Scott and F. B. Hinsley at the University of Nottingham in 1951 (McPherson, 1993).

2.8. VENTILATION NETWORK ANALYSIS

2.8.1. Background. Network analysis of mine ventilation systems actually dates back to 1854 when Atkinson solved a small network problem using a method of succession approximation. Network analysis is still done using a method of successive approximation developed the Hardy Cross method by Professor Cross in 1936 and adapted and modified by Scott and Hinsley (1951) for the solution of ventilation network problems (Luxbacher and Ramani, 1979). An important component in the design of a new mine is the determination and distribution of the required air volumes to the

production areas and throughout the mine. During the life of an underground operation, it is important to plan ahead in order that new fans, intake and exhaust raises and other new infrastructures are available in a timely manner in order to efficiently provide the required airflow to the underground workings. Due to the dynamic nature of the underground operations with new orebodies and their production blocks under continuous development as older ones approach the end of their operating life, mine ventilation planning would also need to be a continuous process (Eng, 2009; McPherson, 1993).

Ventilation network analysis is a generic term for a family of techniques that enable quantitative determination of the distribution of airflow and the operating duties of the fans in a ventilation network where the resistances of all branches are known. In a given network there are theoretically, an infinite number of combinations of airway resistances, pressure generators and regulators that will give a desired airflow distribution. However, practical consideration can limit the number of acceptable solutions. The techniques of network analysis that are applicable and useful for industrial applications must be flexible and converge to a solution in a short time period in order to allow multiple alternative solutions to be investigated (McPherson, 1993).

First attempts to use digital computer methods to solve mine ventilation networks occurred in Belgium, Germany and Japan in the late 1950's. The first reported use of digital computers in the United States was by Hartman and Trafton (1963) at Pennsylvania State University who developed a program capable of solving free splitting network problems. This program was extended the following year to handle fans external to the network (Trafton and Hartman, 1964). At approximately the same time and independently, computer programs for network analysis were being developed in England (Luxbacher and Ramani, 1979).

2.8.2. Computational Fluid Dynamics. Computational Fluid Dynamics (CFD) is a rapidly developing numerical technique by which many complicated fluid flow problems can be solved with a computer economically, and within a relatively short time. CFD can be described (Anderson, 1995) as "the art of replacing the partial derivatives in the fluid motion equations with discretized algebraic form, which, in turn, are solved to obtain the flow field values at discrete points in time and/or space". CFD embraces a variety of technologies, including mathematics, computer science, engineering and

physics, and the disciplines have to be brought together to provide the means of modeling fluid flows. The applications of the CFD technique in mine ventilation can help engineers to analyze complex air flow fields and contaminant transport in order to design more economical and safer ventilation systems. In the last few years many attempts have been made to solve mine ventilation problems with the CFD technique and numerous papers have been published concerning these studies. Generally, these problems can be classified as follows:

2.8.2.1 Contaminant transport (gas-particle flow). CFD simulations help to study face ventilation at a continuous miner section using novel methane dust control systems for extended cuts or for long wall faces. Such studies are useful in determining the appropriate measures for dust suppression and safe positions for operators (Heerden and Sullivan, 1993; Srinivasa, et al, 1993).

2.8.2.2 Air flow fields study (flow patterns). These simulations have been performed to predict the flow fields across certain main airways such as shafts, drifts and main fan ductworks. Optimal designs can be obtained from the simulations (Greyvenstein, et.al. 1993; Oberholzer and Meyer, 1995).

2.8.2.3 Heat transfer between air flow and strata during a mine fire and mine fire development. In 1994, Lea used CFD to simulate an open mine fire development and heat transfer between the tunnel (opening) walls and air flow. Recent developments in CFD software along with the progress of computer technology suggest that this technique is becoming a very important tool for both research and design. Although CFD has many advantages, it does not eliminate the need for experimental studies (which are often expensive and time consuming) for verification of the numerical analysis (Wala, Yingling, Zhang and Ray, 1993).

2.8.3. Fan Selection Procedure. The procedure applied in this study is the one developed at the University of California, Berkeley. This is an empirical approach which, by using a ventilation simulator, allows optimization of a power consumption function subject to a set of linear relationships between fan pressures and regulator resistances. Here, it is assumed that the ventilation system consists of a network of airways, a number of working areas with fixed airflow requirements, and a set of main fans of unknown

pressures. This procedure can be summarized by the following two routines for a two fan system of one main fan and one booster fan:

2.8.3.1 Single fan system. The process is initiated by assigning a trial pressure to this fan, solving the network for airflow rates and pressure drops, and evaluating the resulting regulator resistances. These resistances are arranged in decreasing order of magnitude and evaluated by applying the following criteria. If the smallest resistance is positive, then the fan is oversized. To achieve an improved condition, the trial pressure should be decreased by a fixed amount and the process repeated. If the smallest resistance is negative, then the fan pressure is inadequate. This should be increased by a fixed amount and the process repeated to achieve an improved condition. If the smallest resistance is equal to zero, then the trial pressure is the lowest fan pressure that minimizes the input power requirement. In most cases, the solution to the problem can be achieved after three iterations.

2.8.3.2 Two fans system. At this stage, the single fan system is modified to include another booster fan. The network is then solved for the best combination of fan pressures. The procedure is initiated by assigning a fixed pressure to the booster fan and varying the main fan pressure for a given range. For every pair of fan pressures the network is solved for flow rates, pressure drops, and a set of regulator resistances. By applying the evaluation criteria described previously, a local optimal solution to the problem can be determined at this stage, the total power consumed by the two fans can be calculated. The procedure is repeated for other booster fan pressures and a set of local optimal locations determined. These results can then be plotted as pressure-power graphs, and used to determine the global solution to the problem, namely a pair of fan pressures that satisfies the air flow requirements at the workings and minimizes the total power consumption.

For large networks this procedure can be quite time consuming and complex, especially for networks with multiple surface fans. A more robust and efficient approach to these types of problems will be sought in this project (Calizaya, City, Stephens and Gillies, 2010).

2.9. VENTILATION NETWORK IMPROVEMENT WITH CONSIDERATION OF SURFACE FAN

There are four fundamental ways that contribute to the optimization of ventilation network;

- Optimization of fans equipment
- Auxiliary ventilation system installation
- Adding booster fan
- Modification of airways

2.9.1. Fans Body Optimization. The value of analyzing the precise cause of fan's degeneration – whether it is wear, corrosion or temperature – appears over the long term in capital expenditure savings. The approach from an engineering standpoint is to assess the cause of the fan's degeneration and use the information to repair or replace the fan with an improved model. In many cases repair proves the more economical solution in the short and the long term (Rape, 2005). Generally, sets of operational possibilities have been allocated to optimize the fan's body

- Replacing fan impellers
- Removing the original motor, replacing with the new motor with higher power.
- Replacing the drive shaft, casing, air inlet and air outlet
- Adjusting thyristors unit correspondingly according to the new motor operating parameters
- Installing and modifying oil pumps and layout of lubricating oil road according to design
- Repairing anti-corrosion coating damaged for welding and other reasons in installation process according to anti-corrosion coating technology
- According to new layout and operation mode of equipment, expand on-line detection system to upgrade and improve it.

2.9.2. Auxiliary Fans. As described by Wallace, 2001. Ideally, an "auxiliary" ventilation system which can consist of a large number of auxiliary ducting systems (steel/fiber/fabric) and auxiliary fans through which fresh air is delivered to the production areas and should have no impact on the distribution of airflow within the mine's primary

ventilation system. This is important because it would allow the auxiliary ventilation system to be planned and designed independently from the mine's primary ventilation system. Auxiliary ventilation systems that are used to supply fresh air to the working faces and dead-end headings can be classified into three basic types, namely: "line brattices", "fan and duct" and "ductless" systems. Generally, the use of "line brattices" is common in underground operations employing the room-and-pillar mining method and its variations. Two major disadvantages of employing a "line brattices" system are the relatively high frictional and shock pressure losses at their "inbye" locations and potential for increased leakage throughout the auxiliary system.

Where dust is the main contaminant, an "exhausting" fan-duct auxiliary ventilation setup may be preferred. With this setup, the polluted air at the face is immediately drawn into the auxiliary ducting system at the face, allowing fresh air to flow along the dead-end heading or along the production draw-point's haulage drift. However, an exhausting fan-duct auxiliary system would need to employ more expensive rigid ducts (such as steel ducts) or spiral type flexible ducts (Hartman et al, 2006).

2.9.2.1 Auxiliary fans installation. Coal mine ventilation systems are often subject to high leakage rates. As a result, changes in airflow resistance will strongly affect the efficiency with which air is delivered to the working place. One major source of airflow resistance is the line brattice used to direct air from the last open crosscut to the working face. Substituting auxiliary fans for brattice eliminates this source of resistance, with improvements in system efficiency and cost(Wallace, McPherson, Brunner and Kissell, 1990).

2.9.3. Booster Fans. A booster fan is an underground fan installed in series with a main surface fan and used to boost the air pressure of the ventilation air passing through it. Currently booster fans are used in almost all foreign major coal mining countries requiring this form of ventilating air motivation including the United Kingdom, Australia, Poland, South Africa and China. In the United States they are used in a significant number of metal and non-metal mines, however, due to concerns of uncontrolled recirculation, coal mine operators have not been allowed to use them.

The purposes of booster fans is to overcome a fraction of the mine's frictional losses in a similar manner to surface fan overcoming all losses within a mine. Booster

fans may, for example, be located in individual gate road(s) to boost panels or in main return headings to boost the entire mine circuit. It is the second application that is likely to become more common. Some of possible advantages of booster fans identified are:

- reduced intake to return pressure differentials and hence reduced leakage and need for airlocks;
- reduced surface fan pressures, allowing existing installations to remain in place;
- as an alternative to avoid potentially more expensive options such as shafts, additional headings or prohibitively large surface fans; and
- As a method to be used to boost single panel(s) rather than the whole mine to minimise regulation and hence mine resistance.

Use of booster fans can lead to lower operating electricity power costs as they augment mine fan power and do not destroy energy as occurs with use of mine regulators. As such, they are a better alternative approach to balancing or controlling airflow through mine parallel splits. They may extend life of mine fan duty as they augment mine fan power. Their introduction allows deferral of installation of a new ventilation shaft or other major capital facility (Habibi and Gillies, 2012).

However there are various disadvantages of booster fans:

- Capital cost of booster fans will certainly be greater in comparison with alternatives such as regulator installation.
- Monitoring of their off/on status is required particularly in gassy atmospheres. Automatic shut-off is required if the main fans stop to avoid underground recirculation.
- Shut off of either main surface or booster fans can trigger a requirement of withdrawal of all miners to the surface whether the shut off is caused by an electronic fault or a serious system failure.
- Their use in a gassy atmosphere may require flame-proof electrical components or placement of electric motors in intake air. This may necessitate use of extended drive shafts from intake to return air sides of a bulkhead.
- If used in a gassy atmosphere the fan must be designed with anti-sparking characteristics. This means using stainless steel rotor and blades and that the most commonly used axial fan impeller material, aluminum cannot be used.

- The layout of parallel intake and return airways in collieries does not usually lend itself to the use of boosters. Most colliery panels comprise multiple intake airways and multiple returns in parallel. If one fan is used all return air to be boosted must be directed to one single airway.
- Coal mine roadways are usually wide openings with limited vertical dimensions. This shape does not lend itself to the accommodation of a large fan and therefore, a considerable amount of site preparation and removal of roof material is usually required.
- Competent stoppings are required where high air pressures occur downstream of fans to reduce leakage of return air into intakes and avoid recirculating flows.
- In the event of some emergency situations such as an underground fire or serious roof fall, it may become critical to control the fan. This requires remote surface control equipment. There must also be proper warning devices on the surface to indicate a stoppage of the booster fan**.**

The installation of booster fans in the main returns of coal mines poses several unique challenges. The first and foremost is installing fans in such a way that methane in the returns does not pose an explosion hazard. The simplest solution would be to install the fan with an explosion-proof motor. This, however, is normally not an optimal solution due to the cost of the motors. Another solution would be to situate the fans such that a system of belts and drive shafts will be used to transfer power from the motor located in the intake airway to the fan located in the return entries (Gillies, 2010).

Before any booster fan installation is considered, alternate options should be evaluated carefully. Options such as upgrading the main fan, repairing damaged bulkheads, and slashing high resistance airways should be considered first, then the possibility of using booster fans. Planning for the usage of booster fans in existing mines almost always starts with ventilation surveys and estimation of airflow requirements. This is followed by network modeling and simulation exercises for different ventilation strategies (Calizaya, 2009). Booster fan can reduce the pressure required from the main fan and decrease the system leakage and total required air power (Martikainen et al, 2010). It can be seen that with the use of available technologies booster fan installations have been operated in controlled and safe manner in Australia and the United Kingdom

and other major coal mining countries (Gillies and Calizaya, 2012). The use of booster fans in coal mines is not as common as the usage of them in metal and non-metal mines in U.S.

The use of booster fans to assist in panel ventilation is less widespread. Only one coal example is known from the literature (Ashelford, 2009); however in metal and nonmetal mines booster fans are quite common. In general these installations are similar to installations in the mains with the fans situated in the return airways and the motors placed on the other side of the bulkheads in the intake airways. The final example of booster fan installations are those that are seen in controlled recirculation. The primary examples of this method are in collieries in Britain. While generally prohibited; this practice has been allowed on a case by case basis. These systems are used in mines where the surface fan can meet the statutory ventilation requirements, the mine is non-gassy and additional airflow is desired at the face to reduce dust, heat or other environmental nuisances. These systems are primarily located in a small drift driven next to the intake that is connected through a series of overcasts to the primary exhaust airways. Monitoring is done both in the return before the recirculation split as well as after the recirculation split in the intake. The monitoring systems are preset so that if methane or carbon monoxide levels increase in the recirculation split increase the recirculation fan will shut down automatically (Gillies, Slaughter and Wu, 2010).

2.9.3.1 Recirculation. Recirculation is discussed in two forms: controlled recirculation and uncontrolled recirculation. In controlled recirculation systems, a portion of the return air is purposefully directed into the intake air and transmitted to the production areas and the quantity of recirculated air is closely monitored and managed (Calizaya, 2009).

Controlled Recirculation can increase the capacity of a ventilation system by increasing the air quantity and air velocity near the production areas (Marks 1989).

Uncontrolled recirculation occurs when air is leaked from the return airway to the intake airway but the leakage is not expected or planned and the quantity of recirculating air is not managed, so there is the potential for a buildup of harmful air contaminants including gasses, dust, and heat in a section of the mine. Controlled recirculation systems are used commonly in deep mines and mines that require heating or cooling of air. In

these mines, recirculation is used to increase face velocities and to help manage cost associated with conditioning the air (Aldred et al. 1984; Fleetwood et al. 1984; Rose 1992; Hardcastle and Kocsis 2004). In addition, although air recirculation is prohibited in coal mines in the United States, controlled recirculation has been used successfully in coal mines in the United Kingdom, South Africa, and India (Robinson and Harrison 1987; Kumar et al. 1991; Meyer 1993) (Wempen, 2012)

2.9.4. Modification of Airways. At a point in the mines life where the main fans are operating close to their stall point or an unstable region of the operating curve several options must be considered to prolong the operation's life or provide the option to extend workings into new areas. This includes consideration of the ability to increase the duty of the main fan installation with an associated increase in power consumption, whether new main fans are required or use of additional ventilation infrastructure such as a new shaft or an increased number of roadways underground. Each of these options can be assessed in terms of required capital and operating revenues (Jobling et al, 2001).

2.10. PURCHASING A MAIN FAN

The results of ventilation network planning exercises will produce a range of pressure-volume duties required of any new major fan that is to be installed. The process of finding and ordering the fan often commences with the ventilation engineer perusing the catalogues of fan characteristics produced by fan manufacturers. Several of those companies should be invited to submit tenders for the manufacture and, if required, installation of the fan. However, in order for those tenders to be complete, information in addition to the required pressure-volume range should be provided by the purchasing organization.

- The mean temperature, barometric pressure, humidity and, hence, air density at the fan inlet should be given. This allows data based on standard density to be corrected to the psychrometric conditions expected in the field.
- In many cases of both surface and underground fans, noise restrictions need to be applied. These restrictions should be quantified in terms of noise level and, if necessary, will respect to direction.

- A plan and sections of the site should be provided showing the proposed fan location and, in particular, highlighting any restrictions on space.
- The request for a tender must identify and, whether possible, quantify the concentrations and types of pollutants to be handled by the fan. These include dusts, gases, water vapor and liquid water droplets. In particular, any given agents of a corrosive nature should be stressed. The purchaser should further indicate any preference for the materials to be used in the manufacture of the fan impeller and casing. Specifications on paints or other protective coatings might also be necessary.
- Any preference for the type of fan should be indicated. Otherwise, the manufacturer should be specifically invited to propose one or more fans that will meet the other specifications.
- The scope of the required tender should be clearly defined. If the contractor is to be responsible for providing, installing and commissioning the new fan, the individual items should be specified for separate costing.
- The motor, transmission, electrical switchgear and monitoring devices may be acquired and installed either by the provider of the fan or separately. In either case, the voltage and any restrictions on power availability should be stated.
- Areas of responsibility for site preparation and the provision and installation of ducting should be identified (McPherson, 1993).

Mine fans are purchased with less detailed specifications. Typically the performance specifications are utilized (the mine airflow quantity and total pressure requirements over the life of the fan are provided) and the detailed design of the fan is up to the selected fan manufacturer. The mine owner may provide specifications for ductwork and closing doors or dampers purchased from the fan manufacturer, or may also leave the detailed design of those components up to the manufacturer. Negotiations regarding terms and conditions and exceptions to the specification are always part of the contracting process (Gamble and Ray, 2009).

2.11. FIRE IN MINES

The main problem with many mines today is that they are complex often with multiple shafts, ramps and drifts making difficult to control the way the smoke and heat spread in the instance of a fire. The ventilation strategy is of the greatest importance in cases requiring fire and rescue strategies. Experience of attacking fires in real life is little. New knowledge about fire and smoke spread in complicated mines consisting of ramps is therefore of importance in order to make reasonable strategies for the personnel of the mining company and the fire and rescue services. The main experience from fighting mine fires comes from old coal mines (Hansen, 2009).

2.11.1. The Effects of Fire on Ventilation Network. Fires produce large amounts of very hot, very low density gas. This results in four main effects on the ventilation system (Hansen, 2010b; Gillies et al, 2004):

1. A throttling or choking effect caused by the volume increase of the air passing through the fire zone resulting in higher wind speeds downwind and therefore higher frictional pressure losses.
2. A chimney or natural draft or natural ventilation effect caused by the increased buoyancy of the 'air' downwind of the fire effectively giving rise to very large (and potentially unstable) natural ventilation pressures (NVPs) in various parts of the ventilation circuit .
3. Flow reversals: these have been experienced in practice and also shown theoretically via modelling. As an example, in the Belmont fire of 1911, the US Mine Rescue Association stated that in a fire, 17 men lost their lives. The fire should not have been a serious one; little damage to the mine resulted. It was discovered while it was still small and was attacked for some time at close quarters, yet the unfamiliarity of the men with fire-fighting methods, together with a reversal of the air currents, permitted an insignificant blaze to develop into an appalling disaster.
4. Rollback or the localized reversal of airflow direction above a fire usually characterized by smoke near the roof moving backwards against the general flow of air over the fire. This is primarily a convection issue with hot, low density gases produced by the fire rising and expanding ('mushrooming') above the fire.

The intensity of a fire or heat release rate is largely determined by the rate at which air oxygen can reach the fire and the surface area and type of fuel available for burning. Within limits, if more oxygen reaches at the fire, the intensity of the fire increases and vice versa (Brake, 2013).

2.11.2. Classification of Fire. A classification used in fire chemistry literature is the 'equivalence ratio' which is defined as the actual fuel/ air (oxygen) mass ratio divided by the stoichiometric fuel/air (oxygen) mass ratio (Karlsson and Quintiere, 1999). A ratio less than one means the fire is fuel-rich (poorly ventilated) and greater than one means it is oxygen-rich (well ventilated). If the equivalence ratio is exactly one (the stoichiometric condition), then in theory the fuel and oxygen would exactly consume one another with none of either left over.

The size and nature of a mine fire depends on:

- how long it has been burning
- what is burning
- whether the fire has been spontaneous or was externally initiated
- the air flow to the fire (supply of oxygen)
- the geometry and composition of the material
- where the heat goes.

2.11.3. Fire Risks in Hardrock Mines. There is substantial data available regarding the incidence of underground mine fires. In the USA, NIOSH (De Rosa, 2004a; De Rosa, 2004b) compiles regular reports on coal and non-coal mine fire statistics.

In a hardrock mine, the three most critical fire risks are probably:

1. Mobile diesel equipment fire: fires on underground mobile equipment are (unfortunately) still relatively common. Most of these are relatively minor and are extinguished either via on-board suppression systems or portable extinguishers. Major fires (where the vehicle is destroyed) are infrequent but by no means 'incredible'. From this author's experience, the two most common incidents where the vehicle is destroyed are:

- fire during vehicle refueling.
- fire due to vehicle rollover.

2. Magazine fire: magazine fires can be especially significant as it common for them to be located adjacent to major intakes, there are often large quantities of explosives stored underground, they have limited direct exhaust or none at all, explosives are oxidizing agents (which means they do not need an external source of oxygen to burn) and there is the risk of detonation if the explosives catch fire.

3. Conveyor fire: as the potential fuel load for a conveyor fire (the belt) is spread out over the length of the conveyor, and the conveyor may be moving when it catches fire (making the fire mobile), a conveyor fire can result in a large area being directly affected and a lengthy process to contain or extinguish the fire (Brake, 2013).

2.11.4. Fire Management. Fire management in an underground mine has several key principles (DME, 1997; Thyer, 2002):

- Prevent the start of the fire using equipment specifications, fire suppression systems, careful materials selection and careful consideration of ignition sources.
- Detect the fire early and provide effective systems to isolate and/or reduce the impacts of the fire. This includes fire suppression systems, fire containment systems, and an effective ventilation system that prevents or reduces the toxicity of products of combustion entering the main mine workings.
- Provide warning for persons underground and effective egress and entrapment/refuge systems so that personnel can wait safely until the fire is extinguished or they are rescued.

2.11.5. Stages of Mine Fire. A fire goes through three principal stages:

- Growth stage

In this stage, the fire starts and its intensity increases until it reaches a maximum determined by either the limit on fuel that is available at any time to be burned, or the oxygen available. In a fire in a constrained area, the end of the growth stage is often characterised by flashover, when the hot gases and radiation have heated the temperature of the remaining combustible materials to their auto-ignition temperature and, effectively, these explode simultaneously into flame.

- Peak intensity stage

In this stage, the fire burns at roughly the same peak intensity with the rate (of intensity) determined by either the available fuel or the available oxygen. This is the phase with the maximum heat production, maximum temperatures and maximum impact on the ventilation system.

- Decay stage

In this stage, the fire is starting to reduce in intensity of its own accord as it is starting to run out of fuel. However if the fire is partially oxygen constrained, then if more oxygen is suddenly made available (eg by opening fire doors), the fire may flare up again. It is often in the decay stage of the fire life that firefighting attempts may be made to hasten the extinguishment of the fire (Brake, 2013).

2.11.6. Toxic Gases Codes. A CO concentration of 1200 ppm is considered to form an immediate danger to life or health which is the benchmark for emergency egress whilst the immediate danger to life or health for CO_2 is 4%. The National Occupational Health and Safety Commission in Australia (NOHSC) recommends any CO exposure (in an occupational not emergency setting) to not exceed 100 ppm CO for a 30 minute duration and on no account to exceed 400 ppm CO. All exposure limits should be adjusted where the oxygen partial pressure varies significantly from the sea level standard. In the USA Time Weighted Average (TWA) for CO and CO_2 are determined at 0.005% and 0.5% respectively.

2.12. CONCLUSION OF SECTION

The literature review has drawn on background information from categories of underground ventilation system, evaluation criteria of mine ventilation system, main fans installation design and optimization, main fan energy control methods, ventilation network analysis approaches and fire management to allow a full understanding of the new material developed in the subsequent chapters. It has also demonstrated that complex fluid flow problems can be solved by CFD approaches in order to design more economical and safer ventilation systems. Finally, the literature review shows that

underground fires which have been initiated by mobile equipment are still relatively common and likely to be underestimated.

3. FUNDAMENTAL EQUATIONS

3.1. SHOCK LOSS

Whenever the airflow is required to change direction, additional vortices will be initiated. The propagation of those large scale eddies consumes mechanical energy (shock losses) and, hence, the resistance of the airway may increase significantly. This occurs at bends, junctions, changes in cross-section, obstructions, regulators and at points of entry or exit from the system. The effects of shock losses remain the most uncertain of all the factors that affect airway resistance. This is because fairly minor modifications in geometry can cause significant changes in the generation of vortices and, hence, the airway resistance. Analytical techniques may be practice, scale models or computational fluid dynamics (CFD) simulations that may be employed to investigate the flow patterns and shock losses (McPherson, 1993).

These occur in mine ventilation systems in addition to friction losses and:

- Where airflow direction changes;
- Where airway area changes;
- Where there are obstructions in airways;
- Fan inlet/discharge;
- Air splits and junctions;
- Where two airways with different cross sectional

There are two methods that may be used to assess the additional resistance caused by shock losses

3.1.1. Shock Loss Factor. In text books on fluid mechanics, shock losses are often referred to in terms of the head loss or drop in total pressure, P_{shock} caused by the shock loss. This, in turn, is expressed in terms of 'velocity heads'

$$\mathbf{P}_{\text{shock}} = \frac{X\rho u^2}{2} \tag{3.1}$$

where

ρ= air density $(\frac{\text{kg}}{m^3})$

u = mean velocity of air (m/s) and

X = shock loss factor (dimensionless)

The shock loss factor can be converted into an Atkinson type of resistance, R_{shock}, by re-writing equation (3.1) as a square law

$$P_{shock} = X\frac{\rho}{2}\left(\frac{Q^2}{A^2}\right) = R_{shock}\,Q^2 \quad Pa \tag{3.2}$$

where

$$R_{shock} = \left(\frac{X\rho}{2A^2}\right) \quad \frac{Ns^2}{m^8} \tag{3.3}$$

If rational resistances (*Rt*) are employed then the density term is eliminated and the corresponding shock resistance becomes simply

$$R_{t,\,shock} = \left(\frac{X}{2A^2}\right) \quad m^{-4} \tag{3.4}$$

The major cause of the additional resistance is the propagation of vortices downstream from the cause of the shock loss. Accordingly, in most cases, it is the downstream branch to which the shock resistance should be allocated. However, for junctions, the cross-sectional area used in equations (3.3) and (3.4) is usually that of the main or common branch through which all of the local air-flow passes.

One of the most comprehensive guides to the selection of X factors is contained within the Fundamentals Handbook of the American Society of Heating, Refrigerating and Air Conditioning Engineers (ASHRAE). Similar design information is produced by corresponding professional societies in other countries. An appendix is given at the end of this chapter which contains graphs and formulae relating to shock loss factors commonly required in subsurface ventilation engineering (McPherson, 1993).

3.2. EQUIVALENT LENGTH

Suppose that in a subsurface airway of length *L*, there is a bend or other cause of a shock loss. The resistance of the airway will be greater than if that same airway contained no shock loss. We can express that additional resistance, Rshock, in terms of the length of

corresponding straight airway which would have that same value of shock resistance. This "equivalent length" of shock loss, may be incorporated into equation (3.3) to give an Atkinson resistance of

$$R = K\,(L + Leq)\left(\frac{Per}{A^3}\right)\left(\frac{\rho}{1.2}\right) \qquad \mathrm{Ns^2/m^8} \qquad (3.5)$$

The resistance due to the shock loss is

$$R = K\,Leq\,\left(\frac{Per}{A^3}\right)\left(\frac{\rho}{1.2}\right) \qquad \mathrm{Ns^2/m^8} \qquad (3.6)$$

where per and A are perimeter and area of cross section respectively.

Equation (3.5) gives a convenient and rapid method of incorporating shock losses directly into the calculation of airway resistance. The relationship between shock loss factor, *X*, and equivalent length, *Leq* is obtained by comparing equations (3.3) and (3.6). This gives

$$R_{shock} = \frac{X\rho}{2A^2} = \mathrm{K}\,Leq\,\left(\frac{Per}{A^3}\right)\left(\frac{\rho}{1.2}\right) \qquad \mathrm{Ns^2/m^8} \qquad (3.7)$$

or

$$\mathrm{Leq} = (1.2\mathrm{X}/2\mathrm{K})\,(\mathrm{A}/\mathrm{per}) \qquad \mathrm{m} \qquad (3.8)$$

The equivalent length can be expressed in terms of hydraulic mean diameters, d = 4A/per, giving

$$\mathrm{Leq} = \left(\frac{1.2\mathrm{X}}{8\mathrm{K}}\right)\mathrm{d} \qquad \mathrm{m} \qquad (3.9)$$

leading to a very convenient expression for equivalent length

$$\mathrm{Leq} = 0.15\,\frac{\mathrm{X}}{\mathrm{K}}\,\text{hydraulic mean diameters} \qquad (3.10)$$

Reference to Appendix A5 for *X* factors in McPherson book, together with knowledge of the expected friction factor and geometry of the planned airway, enables the equivalent length of shock losses to be included in airway resistance calculation sheets, or during data preparation for computer exercises in ventilation planning.

When working on particular projects, the ventilation engineer will soon acquire knowledge of equivalent lengths for recurring shock losses. For example, a common rule

of thumb is to estimate an equivalent length of 20 hydraulic mean diameters for a sharp right angled bend in a clean airway (McPherson, 1993).

3.3. PRESSURE LOSS IN BENDS

The pressure loss of a contracting cross section can be significantly reduced. In elbows the airflows streamlines are curved and centrifugal forces cause a pressure increase near the outer wall of elbow. The pressure increases while the fluid enters the elbow.

The head loss in long, straight sections of airways can be calculated by use of the friction factor obtained from either the Moody chart or the Colebrook equation. Bends in airways and ducts produce a greater head loss than if the pipe were straight. The losses are due to the separated region of flow near the inside of the bend (especially if the bend is sharp) and the swirling secondary flow that occurs because of the imbalance of centripetal forces as a result of the curvature of the pipe centerline. These effects and the associated values for large Reynolds number flows through a bend are shown in Figure 3.1. The friction loss due to the axial length of the pipe bend must be calculated and added to that given by the loss coefficient (White, 2007).

For situations in which space is limited, a flow direction change is often accomplished by use of miter bends, as is shown in Fig. 3.2. a and b, rather than smooth bends. The considerable losses in such bends can be reduced by the use of carefully designed guide vanes that help direct the flow with less unwanted swirl and disturbances.

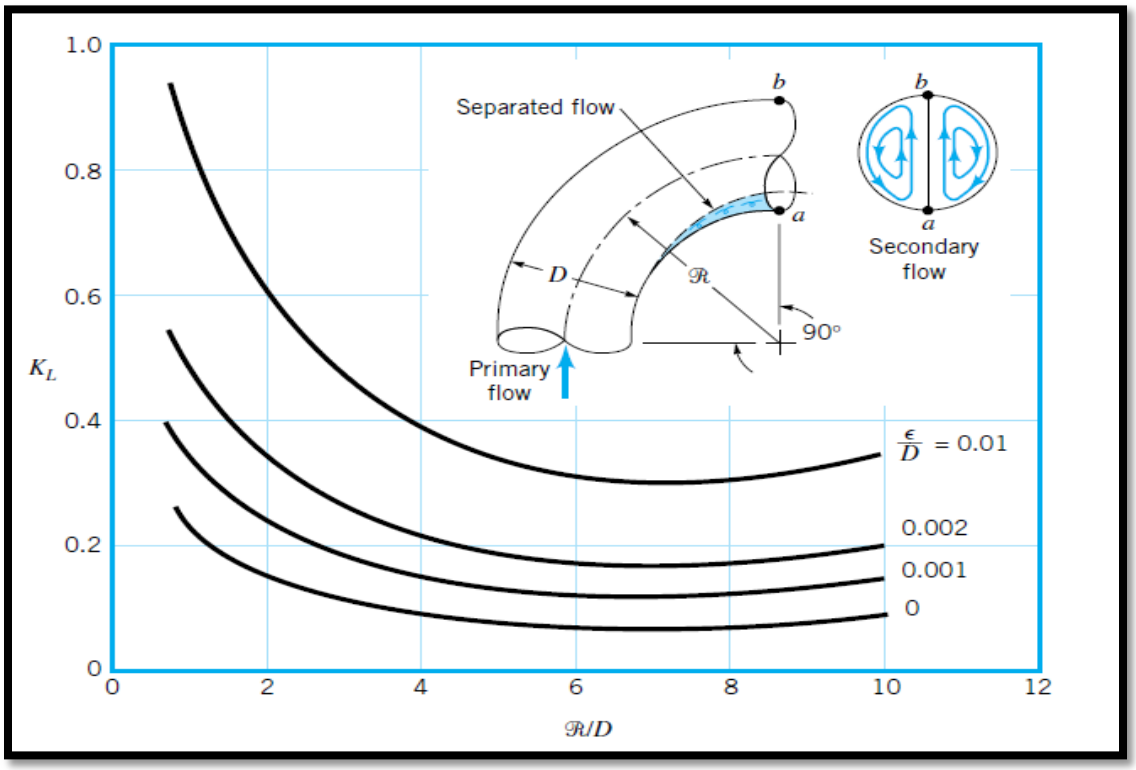

Figure 3.1. Character of the flow in 90 degree bend and the associated loss coefficient

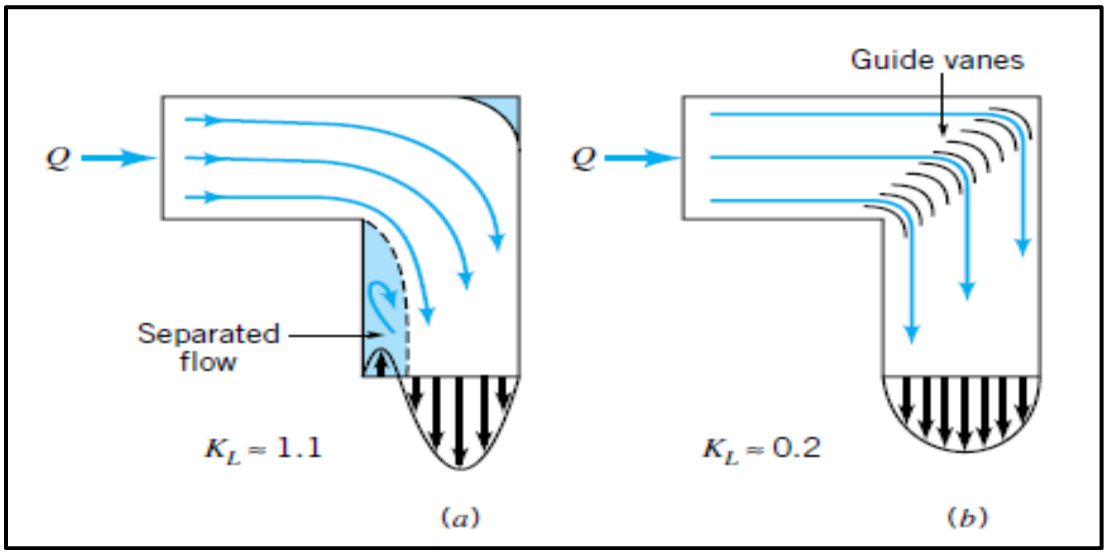

Figure 3.2. Character of flow in a 90 degree elbow and associated loss coefficient: (a) without guide vanes, (b) with guide vanes

The pressure decreases the inside of the elbow. This condition may lead to a separation and turbulence and corresponding losses in flow energy. The magnitude of

these losses to a large extend depend on the sharpness of the curvature. The main portion of flow pressure losses in curved tubes is due to formation of eddies at the inner wall. Rounding of the elbow corners makes the flow separation much smoother and consequently lowers the resistance.

3.4. ATKINSON'S EQUATION, DYNAMICALLY

Mine ventilation systems are treated almost exclusively as systems of incompressible fluid flow and are described most often through Atkinson's equation, commonly given by:

$$\Delta p = \frac{KO(L+L_e)Q^2}{A^3} \tag{3.11}$$

where

ΔP = pressure difference, Pa

K = friction factor, kg/m^3

O = perimeter, m

L = length, m

Le = equivalent length to account for shock losses, m

A = cross-sectional area, m^2

Q = volumetric flow rate, m^3/s

The parameters in brackets in Equation (3.11) are generally referred to jointly as resistance, R, with units of Ns^2/m^8 (Hartman et al. 1997). The volumetric flow rate in Equation (3.11) is calculated using:

$$Q = VA \tag{3.12}$$

where

Q = volumetric flow rate, m^3/s

V = velocity, m/s

A = cross-sectional area, m^2

The dynamic pressure represents kinetic energy that has to be supplied to maintain flow and is lost to the system at discharge. An equation for dynamic pressure is as following:

$$P_K = \frac{\rho v^2}{2} \tag{3.13}$$

where

P_K = dynamic pressure (Pa)

ρ = fluid density (kg/m^3)

V = velocity (m/s)

The resistance is directly proportional to airways length and inversely proportional to airways cross sectional area. Over 70% of typical mine resistance is due to friction between air and rock that forms the airways (Ramani, 1992).

3.5. KIRCHHOFF'S LAWS

The fundamental laws governing the behavior of electrical circuits have been extensively applied in ventilation circuit analysis. According to Kirchhoff's first law also known as Kirchhoff current law (KCL), the quantity of air leaving a junction must equal the quantity of air entering a junction (Hartman, 1997). In other words, the conservation of mass equation must be satisfied. Therefore:

$$\sum Q = 0 \tag{3.14}$$

Where

Q = Volumetric flow rate, (m^3/s)

Kirchhoff's second law, also known as Kirchhoff's voltage law (KVL) states the sum of the pressure drop (change) around any closed ventilation circuit must be zero. Natural ventilation pressure can work with the ventilation system as a positive or

negative pressure source (McPherson, 1993). The Kirchhoff's second law can be written as:

$$\sum p_i = p_f \pm p_n \tag{3.15}$$

where

p_i = pressure difference in ith branch of a closed circuit, (kPa)

p_f = pressure increase due to fan, (kPa)

p_n = natural ventilation pressure, (kPa)

3.6. FAN EFFIECIENCY

In mine ventilation systems, fans are used to generate a pressure difference (Δp) that drives airflow (Q). The pressure difference and air quantity define the power consumed by the ventilation system through the following relationship:

$$\mathrm{P} = Q\ \Delta p \tag{3.16}$$

where

P= power, kW

Q = volumetric flow rate, m^3/s

Δp = pressure difference, Pa

In this form, power is generally referred to as the air power, because it identifies the power provided by the fan to the air, neglecting the overall fan efficiency where overall fan efficiency is given by

$$\eta = \left(\frac{p}{p\ i}\right) * 100 \tag{3.17}$$

where

η = overall fan efficiency, %

P = air power, kW

Pi = input power, kW

Power consumption is an important factor that directly affects the cost of operating a ventilation system (De Nevers, 2000).

3.7. FOURIER'S LAW OF HEAT CONDUCTION

When steady heats flux, q, passes through a slab of homogeneous material, the temperature will fall from θ_1 at entry to θ_2 at exit (Figure 3.3). Planes of constant temperature, or isotherms, will exist within the material. Figure 3.3 also shows two isotherms at a short distance, dx, apart and with temperatures θ and θ+ dθ. The heat flux, q, is proportional to both the orthogonal area, A, through which the heat travels and the temperature difference, dθ, between isotherms. It is also inversely proportional to the distance, dx, between those isotherms.

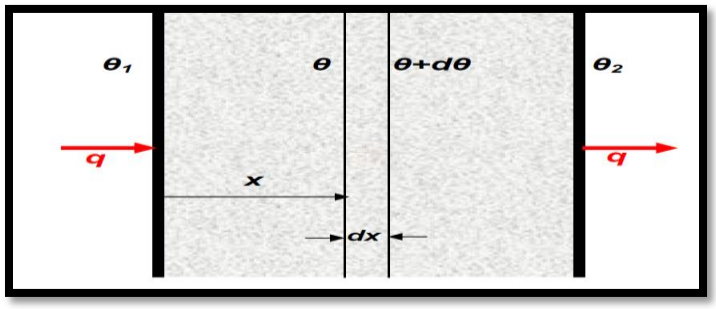

Figure 3.3. Fourier's law of heat conduction

Hence

q is proportional to –A (dθ/dx)

where

q = heat flux (W)

A = area through which q passes (m^2),

θ = temperature (˚C) and

x = distance (m)

The negative sign is necessary since θ reduces in the direction of heat flow, i.e. dθ is negative. To convert this relationship into an equation, a constant of proportionality, k, is introduced, giving

$$q = -k\,A\,(d\theta/dx) \tag{3.18}$$

k is termed the thermal conductivity of the material and has units of W/(m°C). To be precise, k is a slowly changing function of temperature. It may also vary with the mechanical stress applied to the material. In the strata around mine openings, the effective thermal conductivity of the strata can be significantly different from those given by samples of the rock when measured in a laboratory test. The reasons for such differences include natural or induced fractures in the strata, variations in mineralogy that may be direction dependent, movements of groundwater, radioactive decay and local geothermal anomalies (McPherson, 1993).

3.8. THREE DIMENSIONAL TRANSIENT HEAT CONDUCTION

Analytical solution of the three dimensional transient heat conduction equation as obtained by Carslaw and Jaeger (1956).

$$G = \frac{4}{\pi^2}\int_0^{\infty} \frac{e^{-V^2 T}}{[\mathrm{I0}\,(V)+V\,/D\mathrm{I1}\,(V)]^2+[\mathrm{Y0}\;\;(V)+V\,/D\mathrm{Y1}\,(V)]^2\;V}\;dV \tag{3.19}$$

where I_0, I_1, Y_0 and Y_1 are Bessel functions and V is the variable of integration.

3.9. GIBSON'S ALGORITHM

Gibson's algorithm for the numeric determination of dimensionless temperature gradient, G is enclosed as following:

Enter

α (rock diffusivity, m^2/s)

t (age of airway, seconds)

r_a (effective radius of airway = perimeter/(2π), meters

k (thermal conductivity of rock, W/(m°C)).

Then

$F = \alpha t / r_a^2$ (Fourier Number)

$B = h r_a / k$ (Biot Number)

$x = \log_{10}(F)$

$y = \log_{10}(B)$

$c = x\,(0.000104\,x + 0.000997) - 0.001419$

$c = -\{x\,[\,x\,(xc - 0.046223) + 0.315553] + 0.006003\}$

$d = y - (x\,(4x - 34) - 5) / 120$

$d = 0.949 + 0.1 \exp(-2.69035\,d^2)$

$m = \mathrm{sqr}\,[(y - c)^2 + ((216 + 5x) / 70)\,\{0.0725 + 0.01 \tan^{-1}(x / 0.7048)\}]$

$n = (y + c - m) / 2$

$G = 10^n / d$

In the turbulent boundary layer (and within the mainstream), heat transfer is assisted by eddy action and the equation becomes:

$$q = -(k_a + \rho_a C_p E_h)\, d\theta / dy \quad W/m^2 \tag{3.20}$$

where ρ_a = air density (kg/m^3)

C_p = specific heat (1005 J/kg°C for dry air) and

Eh = eddy diffusivity of heat (m^2/s)

The term $\rho_a C_p$ ($J/m^3°C$) is the amount of heat transported in each m^3 for each Celsius degree of temperature difference while *Eh* (m^2/s) represents the rate at which this heat is transported by eddy action. The product $\rho_a C_p E_h$ is much larger than k_a.

In order to combine heat transfer and momentum transfer, Reynolds divided equations (3.21) and (3.22), giving,

$$q / (\rho_a C_p) = -\{\alpha + E_h\}\, d\theta / dy \qquad m^\circ C/s \tag{3.21}$$

$$(\tau / \rho_a) = (\nu + E_m)\,(du/dy) \tag{3.22}$$

where

$\alpha = k_a / \rho_a C_p$ = thermal diffusivity of still air (m^2/s)

$\nu = \mu/\rho_a$ = kinematic viscosity or momentum diffusivity (m^2/s)

$$(q / C_p \tau) = - (\alpha + E_h)/ (\nu + E_m) (d\theta / du) \quad (3.23)$$

Reynolds argued that as the eddy components predominate and the eddy diffusivity for heat, *Eh* , must be closely allied to the eddy diffusivity for momentum, *Em*, we may equate those terms, leaving

$$(q / C_p \tau) = - d\theta/du \quad (3.24)$$

Reynolds integrated this equation directly, making the approximation that u remained linear with respect to y across the composite boundary layers as shown in Figure 3.4. However, both Taylor and Prandtl, working independently, later realized that the integration had to be carried out separately for the laminar sublayer and the turbulent boundary layer.

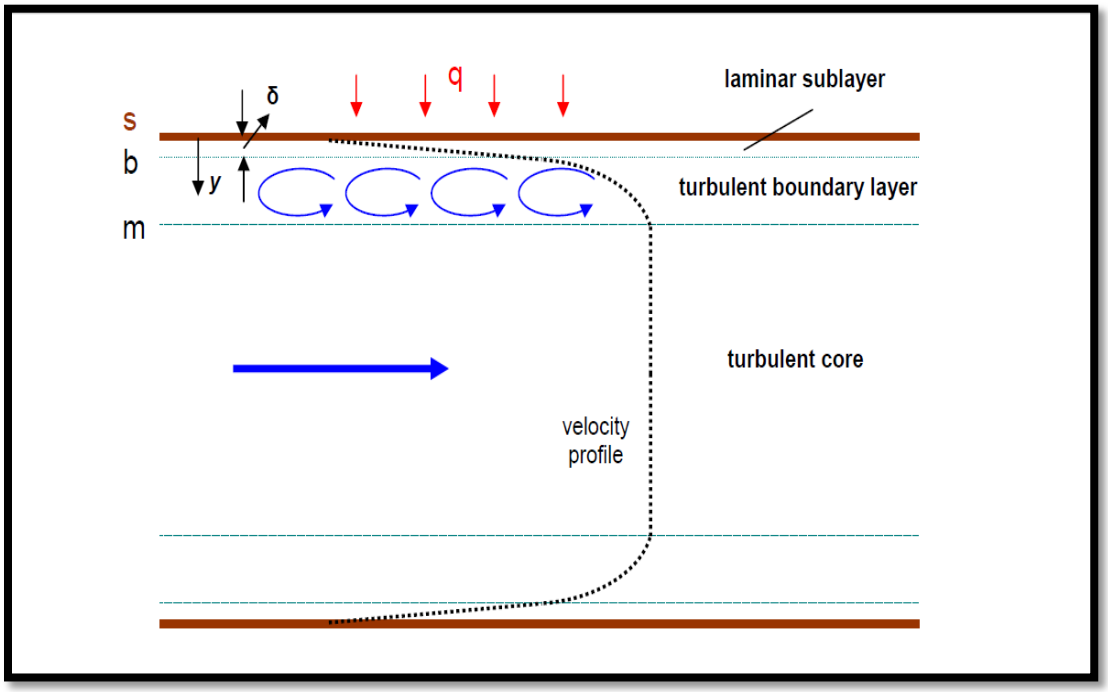

Figure 3.4. Heat is transported by conduction and molecular diffusion across the laminar sublayers, and by eddy diffusion across the turbulent boundary layers

3.10. LAMINAR SUBLAYER

Consider the transfer of heat, q (W/m2) across the boundary layers as shown in Figure 3.4. In the laminar sublayer, there are no cross velocities and Fourier's law of heat conduction applies as shown in Equation 3.25

$$q = - k_a \, d\theta/dy \qquad W/m^2 \tag{3.25}$$

where

k_a = thermal conductivity of air W/(m°C)

θ = fluid temperature (°C) and

y = distance from the wall (m)

So from Equation 3.25

$$q \int_0^{\delta} dy = -ka \int_{\theta s}^{\theta b} d\theta \tag{3.26}$$

$$q \, \delta = k_a \, (\theta_s - \theta_b) \tag{3.27}$$

where

δ = thickness of laminar sublayer (m)

θ_s = temperature at the surface (°C)

θ_b = temperature at the edge of the laminar sublayer (°C)

On the other hand For the laminar sublayer where the flow is viscous, Newton's equation applies:

$$\tau = \mu \, du/dy \tag{3.28}$$

where τ = shear stress transmitted across each lamina of fluid (N/m^2 or Pa)

μ = coefficient of dynamic viscosity Ns/m^2

u = fluid velocity (m/s)

Similarly, integrating equation (3.28) from zero velocity at the wall to u_b at the edge of the laminar sublayer

$$\tau = \mu \, (u_b / \delta) \tag{3.29}$$

Dividing (3.27) by (3.29) gives

$$q / \tau = (k_a / \mu) [(\theta_s - \theta_b) / u_b] \quad (3.30)$$

3.11. TURBULENT BOUNDARY LAYER

In the turbulent boundary layer (and within the mainstream), heat transfer is assisted by eddy action. So we have

$$(q / C_p \tau) = (1 / \{ 1 + (u_b / u_m) [(\mu C_p / k_a) - 1]\}) \ [(\theta_s - \theta_m) / u_m] \quad (3.31)$$

Now the combination $\mu C_p/k_a$ is another dimensionless number known as the Prandtl Number Pr. Furthermore, the shear stress, τ , is related to the coefficient of friction, f, and the mainstream velocity, u_m, by equation

$$\tau = f \ \rho_a u_m^2 / 2 \quad (3.32)$$

Also, we have

$$q = h (\theta_s - \theta_m) \quad (3.33)$$

where

θ_s = temperature of the rock surface (°C)

θ_d = dry bulb temperature in the main airstream (°C) and

h = a heat transfer coefficient (W/ (m^2 °C)) that is a function mainly of the air velocity and the characteristics of the rock surface.

$\theta_m = \theta_d$ = dry bulb temperature of the mainstream

Substituting for τ and q and Pr Number in Equation 3.31

$$[h / C_p \rho_a u_m] = (f / 2) [1 / (1 + (Pr - 1) u_b / u_m)] \quad (3.34)$$

The left hand side of this equation can be separated into three dimensionless groups as following:

1. Nusselt Number (N_u) which is h d / k_a
2. 1 / Reynolds No. (Re) which is μ / ρ_a u_m d and
3. 1 / Prandtl No. (P_r) which is k_a / C_p μ

So the left hand side of this equation is equal to N_u / (Re P_r).

3.12. CONCLUSION OF SECTION

This chapter has drawn on fundamental equations from categories of shock loss, pressure loss, Atkinson's equation, Kirchhoff's law, fan efficiency, Fourier's laws, Gibson's algorithm and laminar and turbulent boundary layers to allow a full understanding of the new material developed in the subsequent chapters. These equations are the fundamental mathematics behind the softwares which have been used in this research. Mine network analysis is generally based on the Hardy Cross method. The Hardy Cross method has followed the application of Kirchhoff's laws. VentFIRE uses a discrete sub-cell transport and node mixing method to simulate moving parcels of heat and gas around a mine.

4. FAN REQUIREMENTS IN THE SECOND 100 YEARS OF A MINE LIFE

4.1. PROBLEM STATEMENT AND OBJECTIVES OF SECTION

The Missouri University of Science and Technology's Experimental Mine is a teaching and research facility which has been excavated in limestone by mining engineering students over almost 100 years. The mine is currently being extended to a second lower level. Available fans for ventilation are two surface fans of 24 kW and two underground booster fans of 12 kW. The design of a ventilation network in conjunction with multi surface fans and booster fans entails a complex procedure.

Ventsim Visual software modeling has been used for network analysis to determine the optimum surface and booster fans locations, blade settings, and speeds. Both natural and mechanical induced ventilation pressures have been taken into account. Three working faces on each level have been designated as target points that minimum air quantities are required. The model has been calibrated against a pressure and quantity survey.

The objectives of this chapter cover the following. The design of ductwork, door/stopping positions and different fans characteristics has been examined. The optimum flow rate at identified working faces has been determined. Efficiency, minimum energy losses and annual network power cost determines the best scenario. Designs have been proposed for the ventilation network for the next 100 years. The optimum flow rate across working faces is the key criterion selected.

4.2. INTRODUCTION

As mining progresses the total resistance of an excavation is increased, the mine characteristic curve becomes steeper, and the operating point moves up the fan curve, reducing the total air quantity and increasing the system pressure. This section is going to describe a study that has been carried out to improve the ventilation system of the Missouri University of Science and Technology (M S&T) Experimental Mine now and into the future based on Ventsim Visual software usage. Numerous parameters such as efficiency, air quantity, total pressure, density and temperature have been considered to

select the most appropriate surface fan taking into account the effects of other fans. Four simulation scenarios have been employed to maximize the networks efficiencies and air flow quantities at three working faces and understand the minimization of annual network power costs. Different locations for surface fans and use of booster fans operating at varying blades angles have been examined in series or parallel connections. Air pressure and quantity surveys have been used to acquire performance specification. The main fan selection has been carried out according to the mine required performance specifications and fans' characteristics. The present ventilation network has been the starting point for ventilation network optimization. The best scenario amongst four one level scenarios has been selected as the basis for investigation of ventilation network on future two-level scenarios. Six working faces have been determined to investigate the airflow in two level scenarios. Four scenarios have been considered to investigate the airflow and efficiency on all six working faces. The highest air quantity scenario amongst 4 two level scenarios has been determined as the future design of mine ventilation network.

4.3. MISSOURI UNIVERSITY OF SCIENCE AND TECHNOLOGY EXPERIMNETAL MINE

4.3.1. Current Ventilation Network. The Experimental Mine is an underground limestone mine located in Rolla, Missouri. The mine is accessed by two adits and has three raises along with two primary ventilation shafts. The 1.2m diameter Joy axial vane fan with 24 kW motor and Alphair 4500 axial vane fan with 24 kW motor have been installed to move approximately 25 m^3/s of airflow at 1,000 Pa static pressure through the underground working faces. Two Spendrup booster fans have been installed underground in series connections to the surface fans. The two main portals have ventilation doors. Each booster fan is driven by a 12 kW three phase 460V motor that loads the circuit by approximately 20A. Booster fans have been mounted on skids to facilitate movement to alternative locations. The location can be altered in order to test the most efficient ventilation networks. A variable frequency drive (VFD) has been installed with each fan. The VFD's have been set up in protective boxes next to the switch boxes (Figure 4.1). Booster fans were designed can operate at different blade angles.

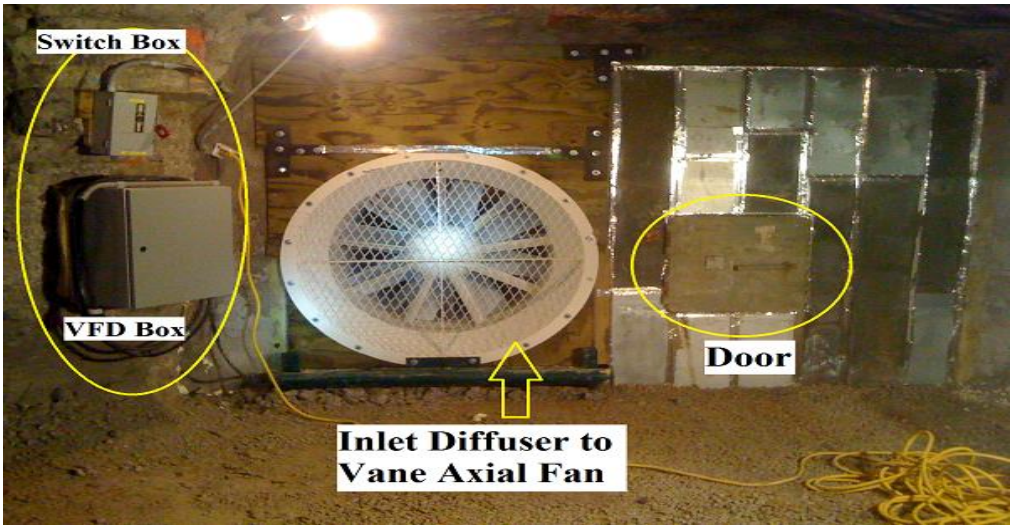

Figure 4.1. Booster fan component

The mine is currently being extended to the second level according to the submitted layout as shown in Figure 4.2. The location of drainage tunnel, closed off headings and new place of booster fan have been illustrated in this figure. The slope of decline has been designed at 1 in 7.

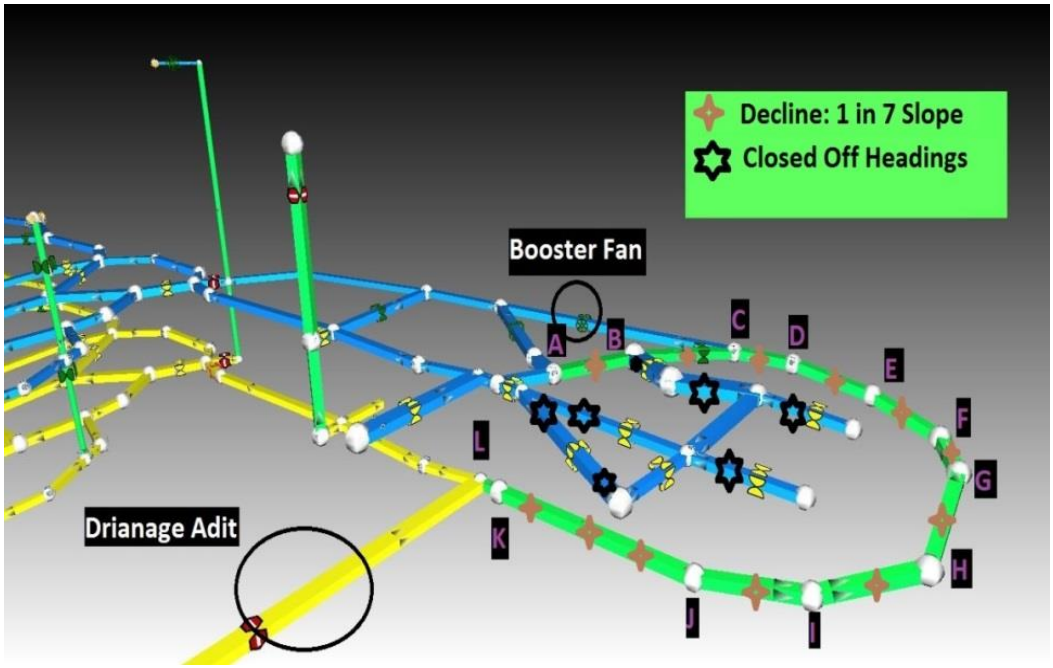

Figure 4.2. Decline position at the east part of the mine

4.4. CHOOSING SURFACE FAN - PRELIMINATRY DESIGN PROCEDURES

Choosing a method to meet projected requirements involves considerations including:

- cost vs. benefit ratio
- reliability
- positional efficiency/flexibility
- installation time
- technology level (Struble, Marks and Brown, 1988)

Mine ventilation main fans are one of the major items of equipment in any underground mine. These run for 24 hours a day as a mine's "breathing" system. They are such an important item for safety that they will be a huge threat to safe production if they do not meet mine production needs for some reason (Wang and Shang, 2009). Before the use of any surface main fan is considered alternative possibilities for optimizing the ventilation network should be considered. To increase airflow various alternative approaches can be considered such as modifications to surface fan, changes to location of surface and booster fans to different parts of the mine, airway widening and reformation on louvers, collar's shaft and mounting the VFD on surface fan. None of them have had an immense impact on air quantity increase at western part of the mine drastically. Procedures for selecting the new surface fan can be divided into three main steps: Location of the main fan, pressure-quantity survey, and fan selection.

4.4.1. Location of Main Fan. Main fans are sited on the surface in the majority of the world's mines. In the case of coal mines this is generally a mandatory requirement. A surface location facilitates installation, testing, access and maintenance while allowing better protection of the fan during an emergency situation. Siting main fans underground may be considered where fan noise is to be avoided on surface or when shafts must be available for hoisting and free of airlocks. In designing the main ventilation infrastructure of a mine, a primary decision is whether to connect the main fans to the upcast shafts such as an exhausting system or, alternatively, to connect the main fans to the downcast shaft in order to provide a pushing or forcing system (McPherson, 1993). The design of

main mine fan installations at underground mines may need to comply with inspectorate requirements. In the United States there is a need to meet mandatory safety standards including that the installation of main mine fans underground in coal mines is prohibited. In the study being described a decision has been made that the location of the main fans will be on the surface. Various systems such as pulling system, pushing system, push-pull system in connection with booster fans have been considered in the design. Ventsim Visual simulation has been used to assist in analysis of models.

4.4.2. Pressure Quantity Surveys. The leapfrog procedure has been employed to determine the mine's characteristics. Pitot tube traverses have been used to measure both static pressure (Ps) and total pressure (Pt) on present within surface fan ducting. Pressure transducers have been utilized to take simultaneous readings at successive stations underground. Vane anemometer has been utilized to measure velocity. The sling hygrometer has been conducted to determine wet and dry bulb temperatures. Numerous specifications such as humidity, dew point and "k" Atkinson factors have been calculated for each airway. Consequently, four different average "k" factors for main airways, sub main airways, shafts and steel ducting have been applied in the scenarios.

4.4.3. Surface Fan Selection. The process of selecting and ordering the fan often commences with the ventilation engineer perusing the catalogues of fan characteristics produced by fan manufacturers (McPherson, 1993). The first consideration is whether to go with centrifugal or axial. Each has been favored in different countries at different times as described by Struble, Marks and Brown, 1988.

Calculated and determined mine airflow quantity and total pressure requirements and detailed information on the design of various fans designs have been used for choosing the most appropriate surface fan. Required total pressure and air quantity of the mine have been calculated at 1000 Pa and 23 m^3/s. The Alphair 4500 Vax 1800 full blade single stage jetstream adjustable pitch vane axial fan with variable blade angles of up to 30 degrees has been chosen as the second surface fan that meets the requirements of the mine.

Fan performance information has been gathered in Table 4.1 from the Alphair fan manufacturer's characteristic curves as shown in in Figure 4.3. Ten different fan total pressures have been determined on 15˚ blade angle line as criteria to calculate other

specifications such as air quantity, fan total efficiency and power. All characteristic of the vane axial fans has been put into the Ventsim Visual program to be employed in the design procedure.

Table 4.1. Performance information, Model: 4500-VAX-1800 full blade single stage jetstream adjustable pitch vane axial fan

Volume (m^3/s)	25
FTP (Pa)	1350
FSP (Pa)	996
Temperature ˚C	21.1
Density (kg/m^3)	1.2
Power (kW)	24
RPM	1780

The optimum fan performance curves have been put into the Ventsim Visual simulator in order to commence designing of the mine's ventilation network as shown in Figure 4.4.

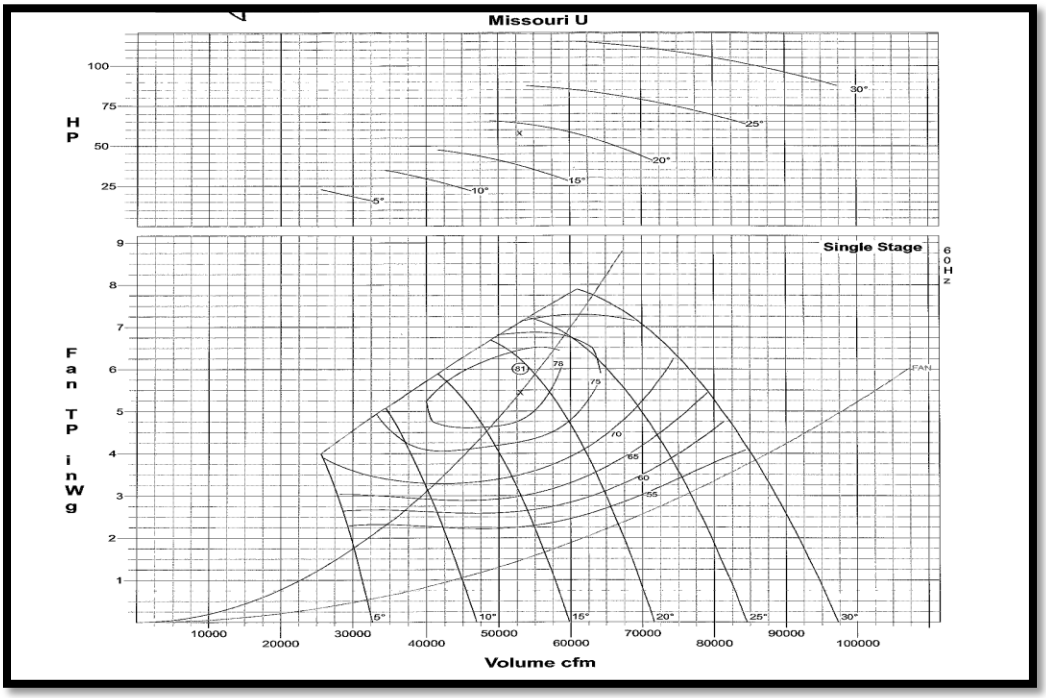

Figure 4.3. Manufacturer's characteristic curve 4500-VAX-1800 Full blade

Figure 4.4. Alphair 4500-VAX-1800-Blade 15 degree

where FSP is fan static pressure, FTP is fan total pressure, EFF is efficiency and PWR is the power.

4.5. VENTSIM VISUAL MODEL

4.5.1. Design Criteria. Three different working faces as shown in Figure 4.5 have been determined as the target points for investigation of various parameters. The total air quantity, network annual power cost, network efficiency and different ventilation systems such as push, pull or push-pull ventilation system have been considered in all target points as an empirical approach to compare four scenarios. All scenarios have been investigated to two different criteria of

- the highest air quantity with the lowest network annual power costs and
- The highest network efficiency with the lowest network annual power costs.

In the study a requirement of three different air quantities (15 m^3/s, 20 m^3/s and 25 m^3/s) has been investigated for all scenarios.

It may be desirable to reverse the airflow in order to provide an escape way or to isolate a fire during a mine fire or other emergency. Also, in colder areas, the airflow may be reversed to prevent ice buildup. Generally, quantity of air is 30 to 65% less when air is in reverse than when operating in the normal forward mode (Rajaram and Thimons, 1985).

In the studies leading up to this paper development a fan reversal factor for pressure and quantity has been adopted of 0.5 for all scenarios.

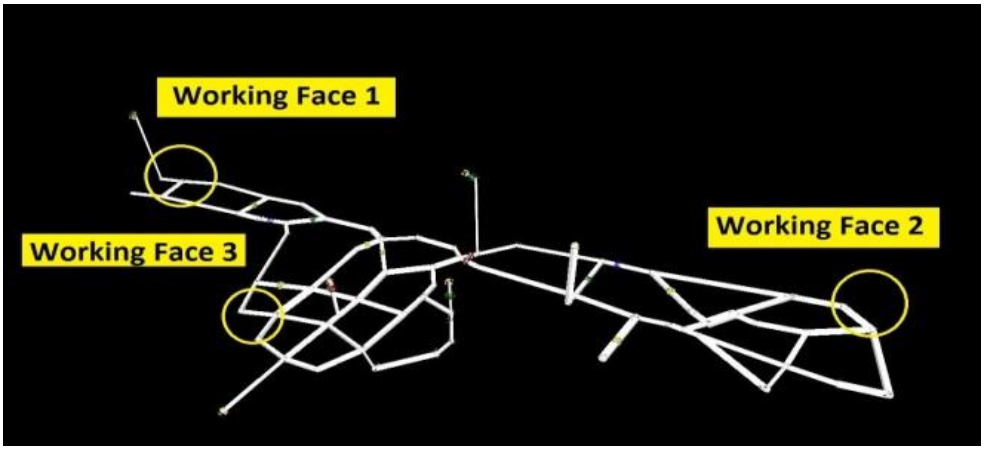

Figure 4.5. Position of determined working faces

4.5.2. Models Simulation. Habibi and Gillies, 2012, stated that the major target of Missouri S&T Experimental Mine ventilation modeling is optimization of ventilation network by improving the airflow circuit at working faces and improving efficiency to reduce annual power cost. Initial results show that with the usage of west booster fan and Joy main fan, the optimum design has been achieved. Total air quantity in these three working faces has been calculated about 54 m^3/s with network annual power cost of $24000 and 21% as efficiency. The location of west and east booster fans, Joy surface fan and the airflow direction is illustrated in Figure 4.6.

A study has been carried out to improve the ventilation network model of the Missouri S&T Experimental Mine based on Ventsim Visual software. Numerous parameters such as efficiency, air quantity, total pressure, density and temperature have been considered to select the most appropriate surface fan taking into account the effects of other fans.

Mine network analysis is generally based on the Hardy Cross method. The Hardy Cross method is a monotonous procedure which applies correction repeatedly to achieve to the sufficient distribution of predetermined accurate flow. This method has followed the application of Kirchhoff's laws. This technique of fluid network analysis involves the making of an initial estimate of flow, q_a, calculating an approximate correction to be applied to each branch flow, Δq and repeating the correction procedure iteratively until an acceptable degree of accuracy has been achieved (El-Nagdy, 2002).

In all simulation scenarios, the selection of operating surface and booster fans with each other and the consideration of reversed ventilation network flow has been considered. A price of electricity in Missouri State of $ 0.10/kWh has been used for the calculation of network annual power costs into the Ventsim Visual program.

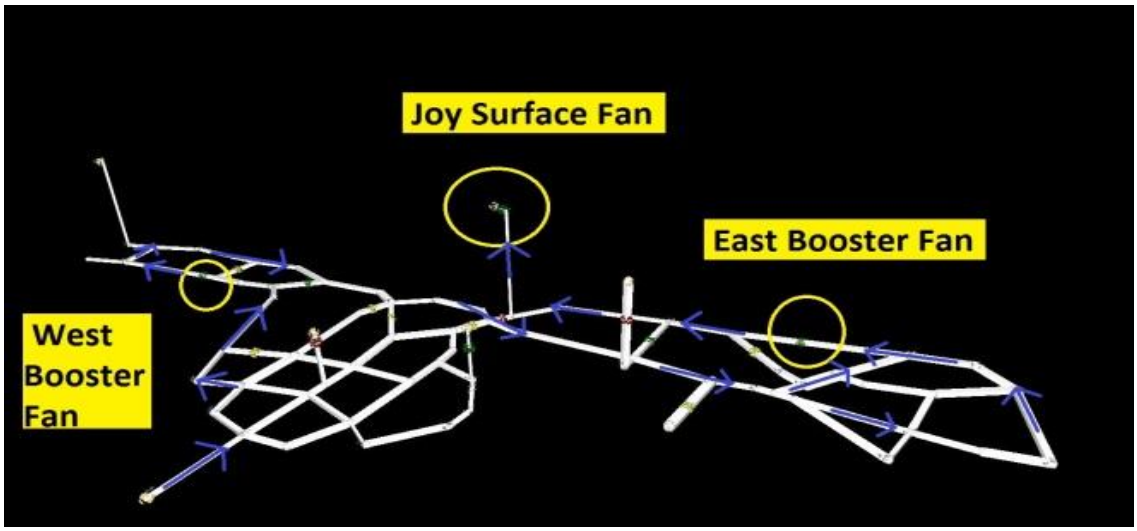

Figure 4.6. Experimental Mine Ventsim Visual model with Joy surface fan and both booster fans

4.6. SCENARIOS

4.6.1. Scenario 1 –Two Surface Fans Positioned in the Same Fan House. The first scenario on Level 1 is shown in Figure 4.7. The Experimental Mine ventilation network has been separated into east and west panels operating independently. A new stopping has been added to the network in order to divide it into two segregated network. The surface fans are both in the same fan house. The result has been shown that total airflow has increased dramatically by adding a new surface fan connected to the western part of the mine.

In this scenario the east booster fan is on and west booster fan has been off. In this scenario the annual power cost has decreased slightly in comparison with the other parameters. The new place for east booster fan with blade angle 25˚ simulated in series connection to the surface fan. By simultaneous usage of west and east booster fans or the

single west booster fan with the other blade angles the efficiency of the mine was decreased. The result of this scenario is shown in Table 4.2.

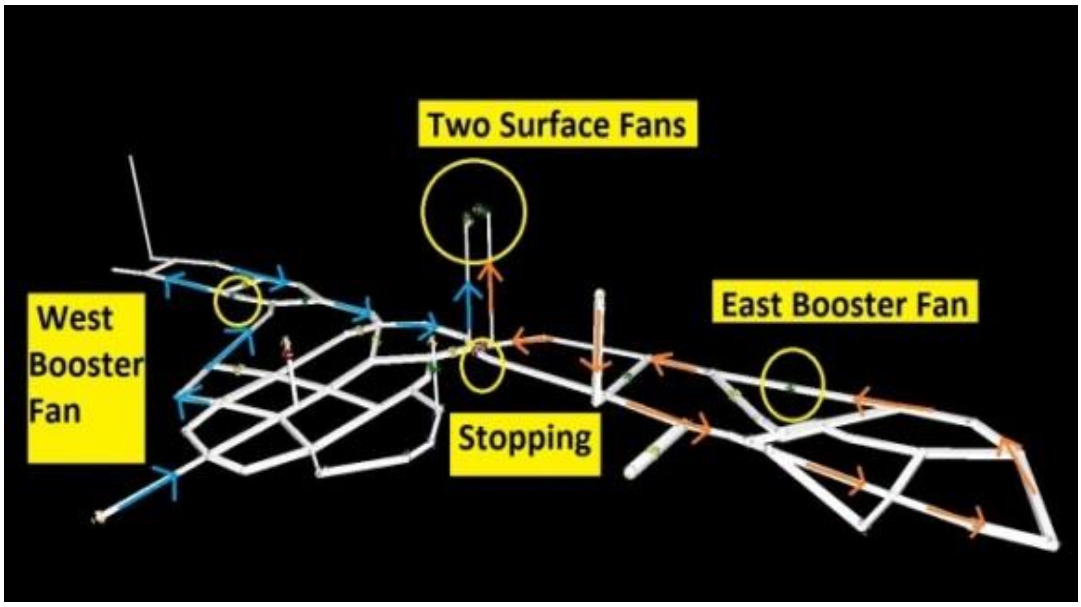

Figure 4.7. Experimental Mine Ventsim Visual, Model- scenario 1

Table 4.2. Ventsim Visual results for scenario 1 Criteria: the highest quantity achievement

Criteria	>15 m^3/s	>20 m^3/s	In Reverse
Q1 m^3/s	25	25	23
Q2 m^3/s	18	25	18
Q3 m^3/s	23	23	21
Total Q m^3/s	66	73	62
Network annual power cost, $ x 1000	24.7	25.6	34.7
Network efficiency, %	41	43	25

In this scenario all working faces do not achieve 25 m^3/s air quantity, the minimum air quantity requirement across all faces. The most efficient situation has been achieved when both east and west booster fans were shut down and the speed of Alphair axial fan has been decreased to 60% of full speed is shown in Table 4.3.

Table 4.3. Ventsim Visual result for scenario 1 Criteria: the highest efficiency

Criteria	Most efficient	Most efficient in reverse
Q1 m^3/s	15	18
Q2 m^3/s	12	18
Q3 m^3/s	14	16
Total Q m^3/s	41	52
Network annual power cost, $ x 1000	7.8	16
Network efficiency, %	53	28

4.6.2. Scenario 2 – Alphair Fan on Central Shaft, Joy Fan at Fan House with West Shaft as Exhaust. The second scenario with location of surface fans has been plotted in Figure 4.8. The furthest northwest shaft has been selected as the inlet or exhaust shaft for the west panel. The network efficiency and total airflow in comparison with the rudimentary ventilation network have been experiencing the sharp increase. On the contrary the network annual power cost has increased slightly. Two Spendrup booster fans with different blade angles in series connection to the surface fans have been investigated for different possibilities of the model. The optimal model has been designed with the activated booster fans with blade angle of 25˚. The optimum design has been chosen to be compared with other scenarios (Table 4.4).

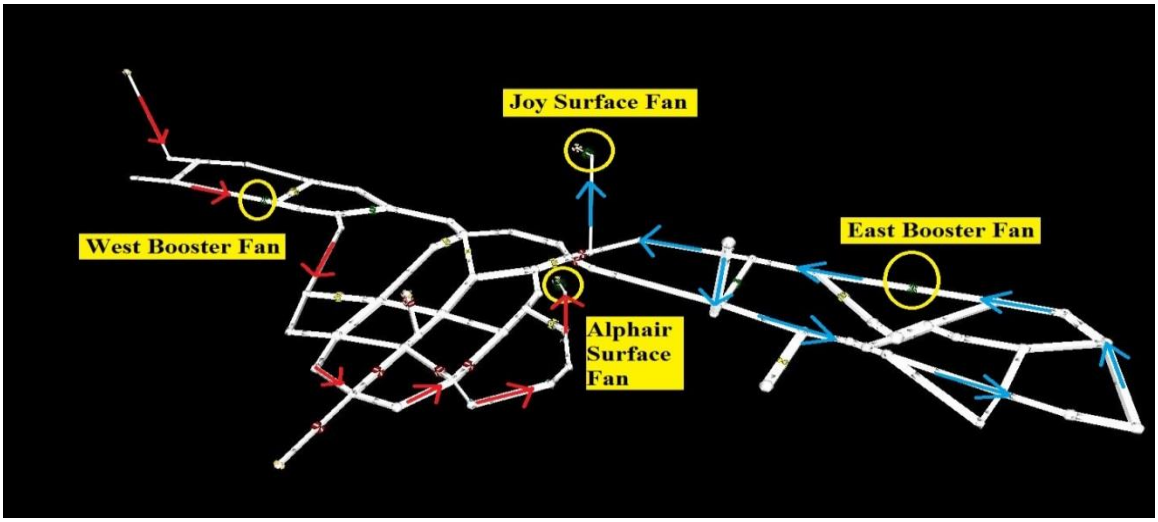

Figure 4.8. Experimental Mine Ventsim Visual, Model- scenario 2

A tight stopping has been added to the ventilation network to meet the minimum requirements. For air quantity 20 m^3/s and above the simulation has been designed successfully with low pressure warnings at both booster fans places.

Table 4.4. Ventsim Visual result for scenario 2 Criteria: the highest quantity achievement

Criteria	> 15 m^3/s	>20 m^3/s	>25 m^3/s	In Reverse
Q1 m^3/s	24	24	25	25
Q2 m^3/s	18	25	25	24
Q3 m^3/s	23	23	25	23
Total Q m^3/s	65	72	75	72
Network annual power cost, $ x 1000	27	27.6	28.2	35.2
Network efficiency, %	49	49	49	32

With 16, 12 and 15 m^3/s in working faces 1, 2 and 3, the highest amount of network efficiency has been achieved. Although, the highest efficiency of the circuit has been achieved by turning the booster fans off in the west and east panels, the minimum air quantity requirements has not been met as shown in Table 4.5.

Table 4.5. Ventsim Visual result for scenario 2 Criteria: the highest efficiency

Criteria	Most efficient	Most efficient in reverse
Q1 m^3/s	16	21
Q2 m^3/s	12	12
Q3 m^3/s	15	18
Total Q m^3/s	43	51
Network annual power cost, $ x 1000	9.8	19.8
Network efficiency, %	54	31

4.6.3. Scenario 3 – Alphair Fan on The Far West Shaft, Joy Fan at Fan House Shaft. In the third scenario the Alphair 4500 vane axial fan has been located at the farthest west point of the mine that as is illustrated in Figure 4.9. The location of booster fans and their blades angles have been varied in order to attain the best design. The changing in surface fans locations have been considered as an option for the model. The optimal design has been selected to be compared to the other scenarios.

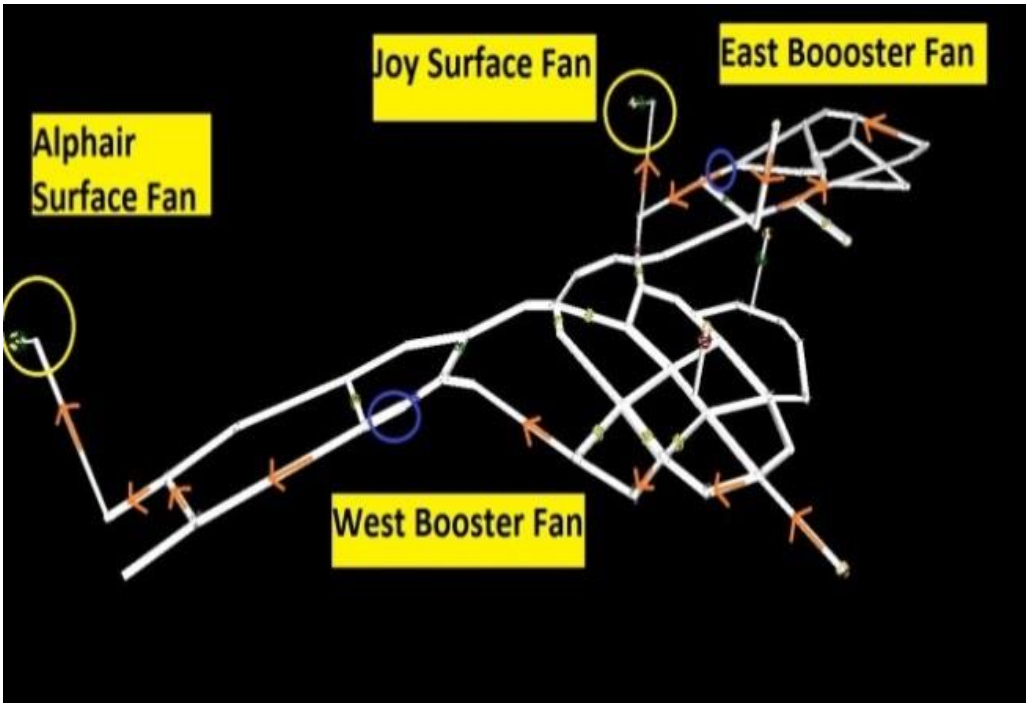

Figure 4.9. Experimental Mine Ventsim Visual, Model- Scenario 3

Minimum air quantity requirement shoud be met at all three determined working faces. The east booster fan can be turned on and the west one can be shut off. If the west booster fan has been added to the network, the program gives a negated fan warning**.** The result is shown in Table 4.6.

The most efficient model has been accomplished by turning two booster fans off, in this scenario, for the most efficient exhausting system booster fans must be turned on though. The result of Ventsim Visual results have been get together in Table 4.7.

Table 4.6. Ventsim Visual result for scenario 3 Criteria: the highest quantity achievement

Criteria	>15 m^3/s	> 20 m^3/s	> 25 m^3/s	In Reverse
Q1 m^3/s	15	21	27	26
Q2 m^3/s	18	22	26	24
Q3 m^3/s	16	21	27	24
Total Q m^3/s	49	64	80	74
Network annual power cost, $ x 1000	8	14.6	26	34
Network efficiency,%	56	50	50	34

Table 4.7. Ventsim Visual result for scenario 3 Criteria: the highest efficiency

Criteria	Most efficient	Most efficient in reverse
Q1 m^3/s	15	18
Q2 m^3/s	12	13
Q3 m^3/s	14	16
Total Q m^3/s	41	47
Network annual power cost, $ x 1000	6	16.6
Network efficiency, %	60	40

4.6.4. Scenario 4 – Alphair Fan on Central Shaft, Joy Fan at Fan House With West Portal as Exhaust. The results have been set down in Table 4.8. Surface fans have been installed on top of east and west shafts as done in scenario number 2. The east booster fan (in series connection to Joy main fan) has been employed in the model to optimize the ventilation network. However, the west Spendrup booster fan has been turned off. The fourth scenario is illustrated in Figure 4.10. In all working faces at least 25 m^3/s has not been achieved.

Table 4.8. Ventsim Visual result for scenario 4 Criteria: the highest quantity achievement

Criteria	>15 m^3/s	>20 m^3/s	In Reverse
Q1 m^3/s	19	21	25
Q2 m^3/s	18	25	24
Q3 m^3/s	18	21	24
Total Q m^3/s	55	67	73
Network annual power cost, $ x 1000	9	20	34
Network efficiency, %	51	44	27

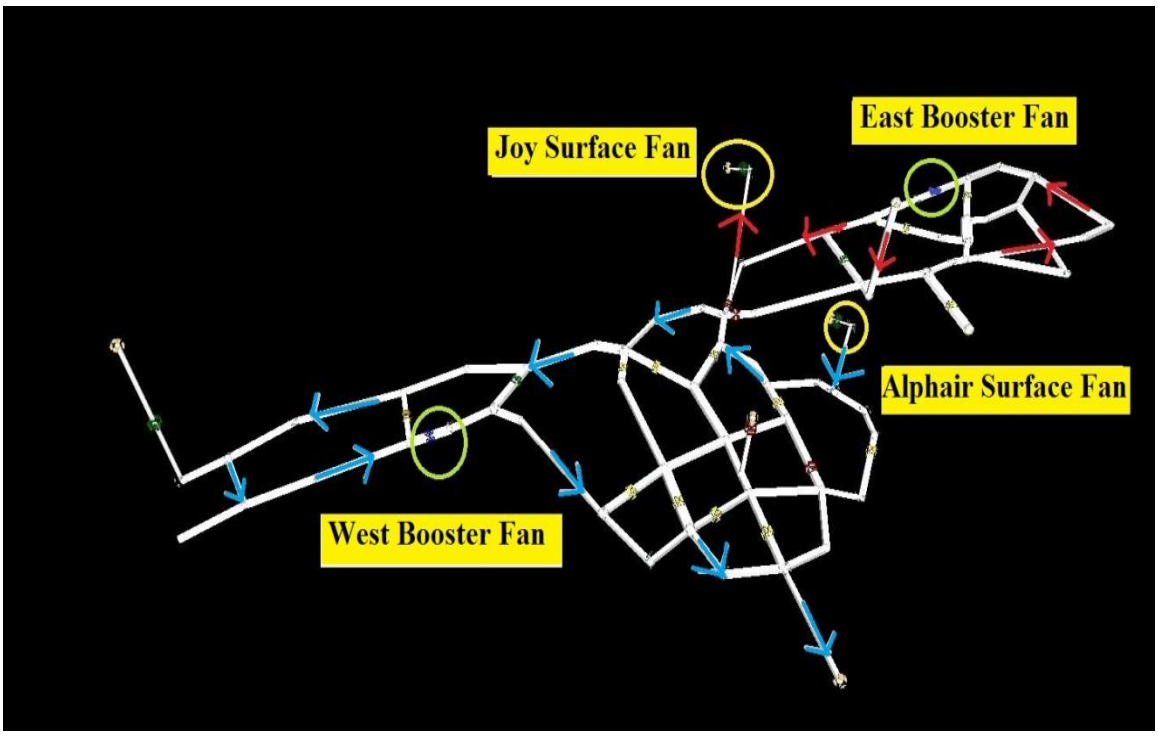

Figure 4.10. Experimental Mine Ventsim Visual, Model- scenario 4

For the highest efficiency achievement in this scenario, west booster fan must be run however the east one should be turned off. The most efficient design and the pulling system are shown in Table 4.9. With considering the most efficient reversed airflow, two booster fans should have been turned on.

Table 4.9. Ventsim Visual result for scenario 4 Criteria: the highest efficiency

Criteria	Most efficient	Most efficient in reverse
Q1 m^3/s	19	19
Q2 m^3/s	12	16
Q3 m^3/s	18	18
Total Q m^3/s	49	53
Network annual power cost, $ x 1000	9	15
Network efficiency, %	52	30

4.7. GENERAL RESULT AND DISCUSSION

Main fans are the heart of the mine's ventilation network and play a key role in supplying required airflow for the mine. A multi-objective study has been undertaken to optimize air flow rate in the Experimental Mine's airways. In this study all possibilities have been considered. By examining different scenarios it can be deduced that 25 m^3/s air quantity in all working faces was not able to be achieved without adding a second surface fan.

Applying the reversed system (pull system) in all scenarios has shown that on account of the reversal loss factor of fans, flow rate and efficiency will be decreasing noticeably. With switching of inlets and outlets of both surface fans, the pushing system has been changed to the pull system without changing the direction of fan blade. So, by this action, we have achieved a pull system without decrease in fan efficiency. By examining the four scenarios it can be concluded that by dividing the experimental mine into two separated ventilation networks each with a main fan, the optimal possibilities will be achieved. In scenarios 1 and 4 the air quantity requirement (at least 25 m^3/s) in all working faces could not be accomplished. Hence, these scenarios cannot be considered as the most befficient designs. Scenarios 2 and 3 have been chosen as the two best scenarios for the experimental mine ventilation network.

After examining network efficiency, air quantity at all working faces, annual network power cost and considering parameters of the pulling system, scenario 3 has

been designated as the most efficient design for the experimental mine ventilation network. With the employment of scenario 3 the network efficiency has been increased by about 35% with 25 m^3/s air quantity at all working faces. In addition network annual power cost has decreased by $ 20,000. The results are plotted in Figures 4.11 and 4.12.

Different blade settings of booster fan have been applied in the design to achieve the best combination of surface fans and booster fans. The best blade angle for booster fans in the most efficient design has been set at 25˚. By the usage of two surface fans and both booster fans, the most efficient and the highest quantity design have been achieved. The network efficiency has been increased by about 35% when the Joy and Alphair surface fans and two booster fans have been utilized. The air quantity has been improved by at least 25 m^3/s at all working faces. By mounting a new surface fan and subdividing the ventilation network into two segregated networks, the feasibility of various designs has been tested. Therefore, pull system has been determined as best for ventilation network.

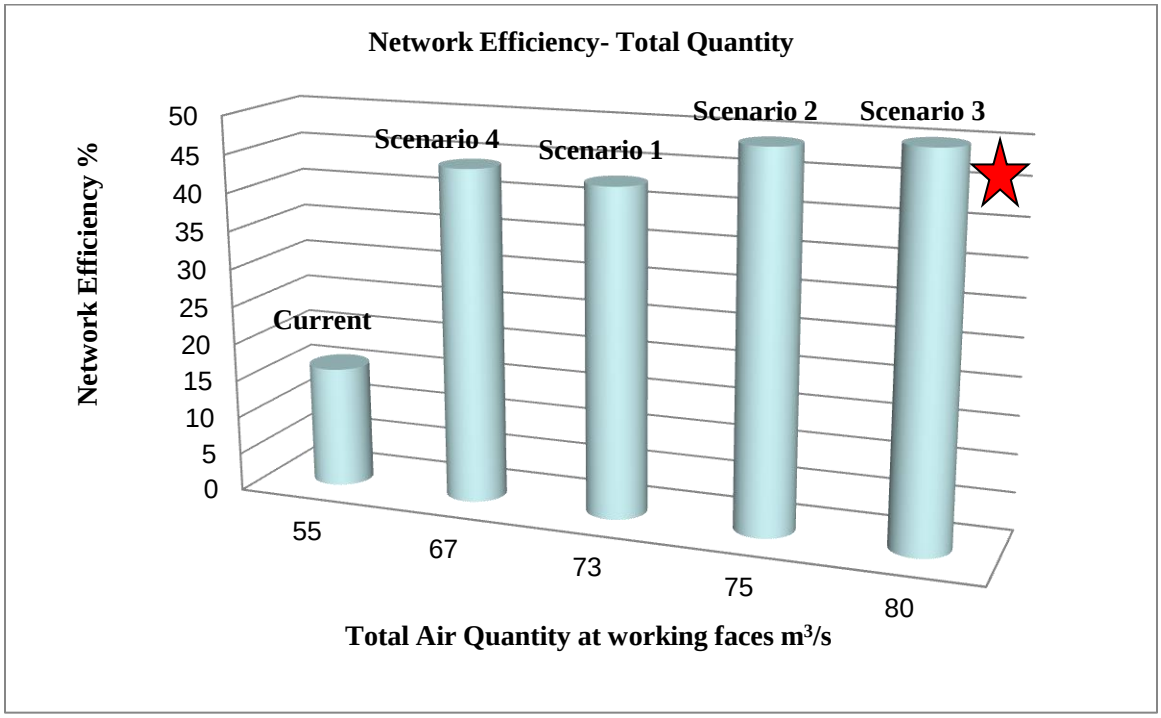

Figure 4.11. Network efficiency- total air quantity bar graph comparison for scenarios

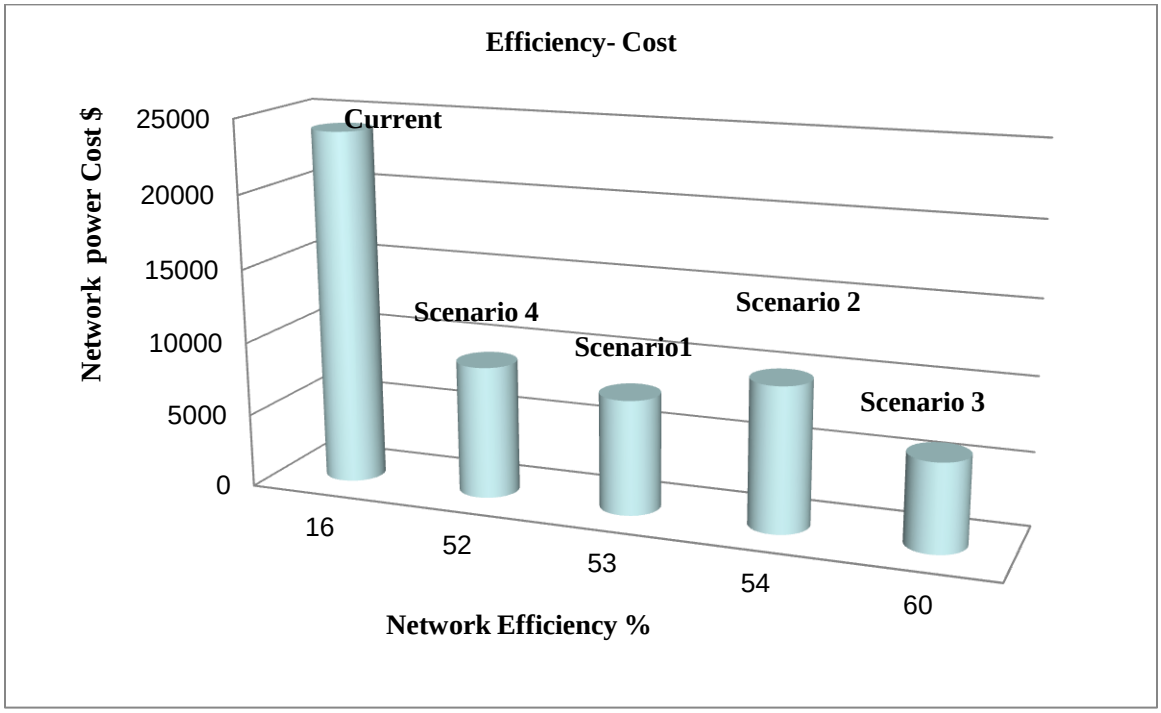

Figure 4.12. Network efficiency- total annual power cost bar graph comparison for scenarios

4.8. NEXT 100 YEARS OF EXPERIMENTAL MINE

The M S&T Experimental Mine ventilation future design has been simulated recognizing planned progress over the next 100 years. The optimum scenario has been selected as the criterion for the designing of mine's future ventilation network. With two levels and three working faces on each, there is a choice of six alternatives for investigation of air quantites at those points as shown in Figure 4.13. Four scenarios have been investigated with varying numbers of surface fans, booster fans and numerous blade settings. In all scenarios, pushing and pulling systems have been examined. Both natural and mechanical induced ventilation pressures have been taken into account.

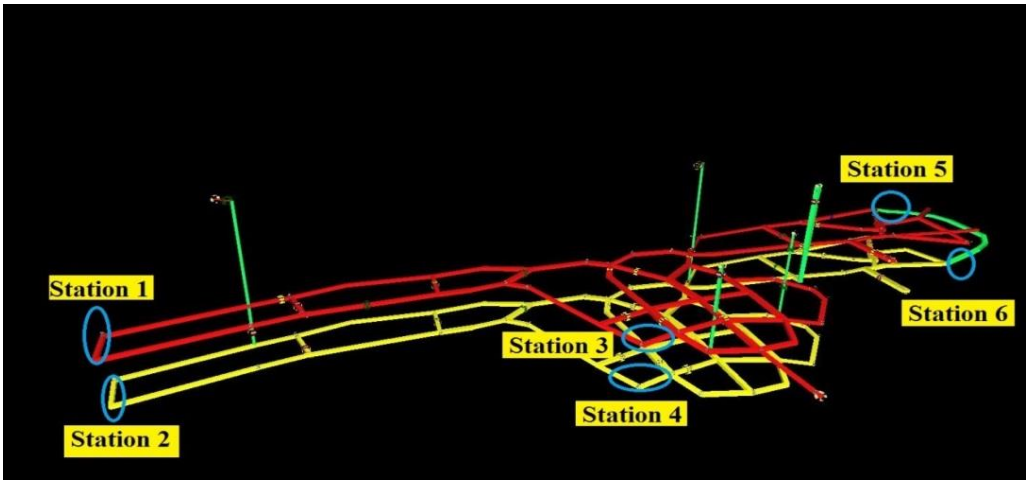

Figure 4.13. The position of working faces (Mine's Future)

4.9. SCENARIOS

4.9.1. Scenario 1 – One Surface Fan. In this scenario the surface Alphair 4500 vane axial fan has been selected as the only surface in the fan house. All other fans have been turned off. The operating point shows that the fan produces the highest quantity of air against very low pressure. Three new tight stoppings have been erected to achieve the highest amount of air at those working faces. The new portal has been designed on the lower level of the mine not only for the drainage of water from the eastern part but also to make an easy access to the bottom level as shown in Figure 4.14. This scenario does not meet the minimum requirements of air quantity on predetermined working faces. The results of forcing and exhausting systems have been shown in Table 4.10.

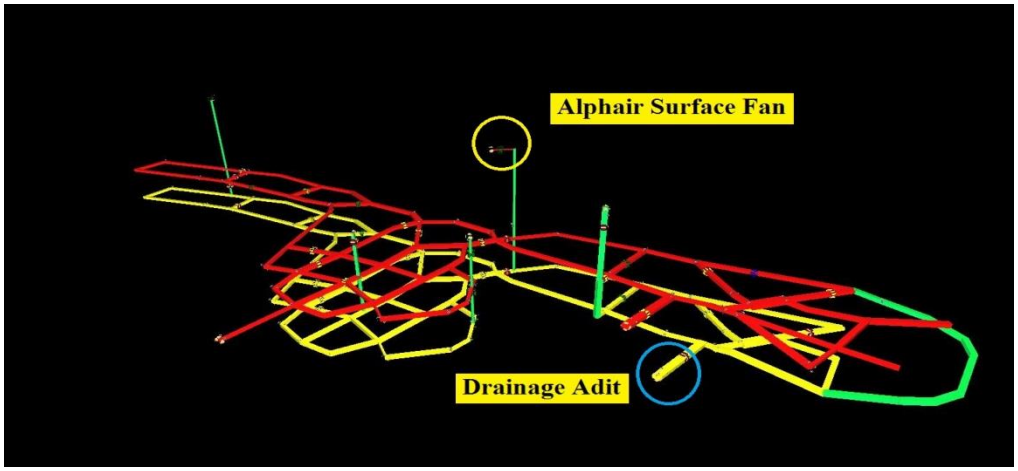

Figure 4.14. Drainage adit location

Table 4.10. Single surface fan results

System	Pushing	Pulling
Network efficiency, %	35	24
Network annual power cost, $ x 1000	21	24.6
Q1 m^3/s	13	12
Q2 m^3/s	11	11
Q3 m^3/s	12	11
Q4 m^3/s	10	9
Q5 m^3/s	22	20
Q6 m^3/s	22	20
Total Q m^3/s	90	83

4.9.2. Scenario 2 –Two Surface Fans. This scenario has been plotted in Figure 4.15. The surface Alphair 4500 Vane axial fan has been simulated on far northwest shaft in the ventilation network and the Joy axial fan has been located on the fan house shaft that is located in the center part of the mine. The fan curves have shown that with a low amount of pressure, a high quantity of air has been achieved. Five new stoppings doors plus two tight steel doors have been added to the network in order to maintain the highest air quantity on all working faces. Two booster fans are not needed under this scenario.

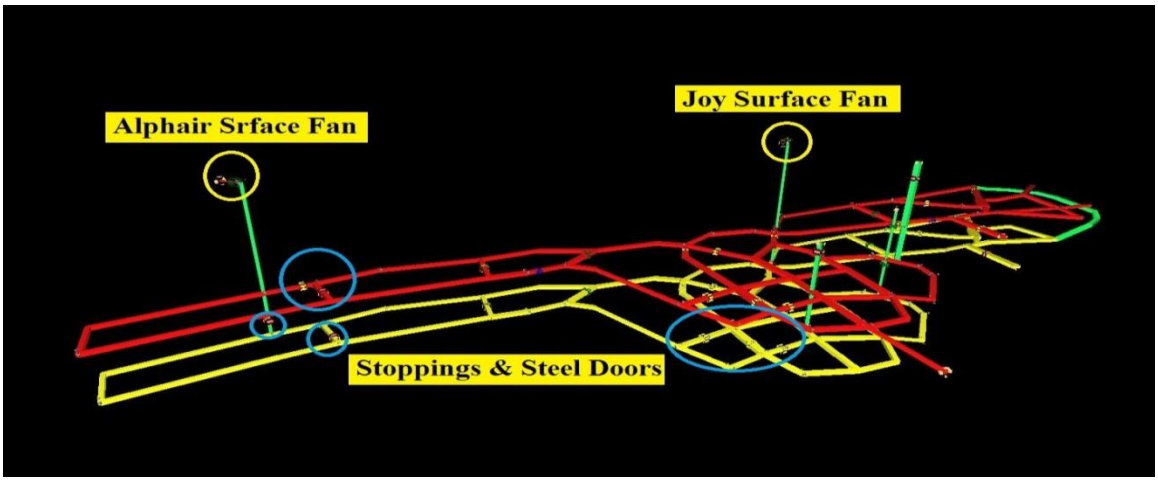

Figure 4.15. Position of surface fans, stoppings and steel doors

The results of pushing and pulling systems have been illustrated in Table 4.11

Table 4.11. Two surface fans results

System	Pushing	Pulling
Network efficiency, %	25	18
Network annual power cost, $ x 1000	46.7	52
Q1 m^3/s	19	17
Q2 m^3/s	21	20
Q3 m^3/s	17	16
Q4 m^3/s	19	18
Q5 m^3/s	21	19
Q6 m^3/s	21	19
Total Q m^3/s	118	109

4.9.3. Scenario 3 –Two Surface Fans and a Booster Fan. In this scenario, two surface fans and one booster fan have been used in the ventilation network. The location of surface fans has been determined as they were selected in the second scenario. All blades angles for booster fans in various airways of the mine and at different speeds of surface fans have been examined to achieve the optimum design as shown in Figure 4.16. The Spendrup booster fan has been located in the west part of the mine on upper level. Blade angle 25˚ has been selected as the most effective blade angle for providing enough air quantity in all working faces.

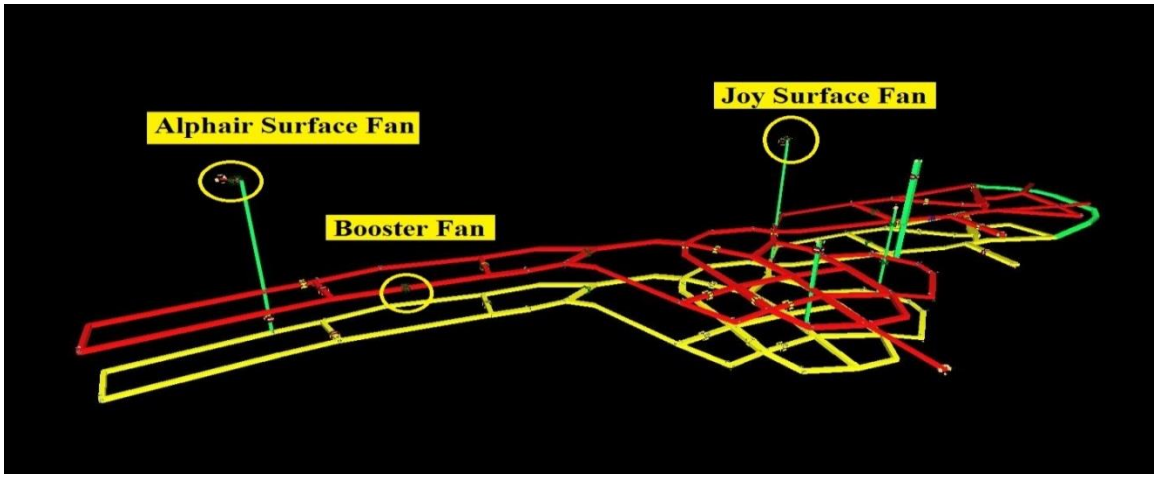

Figure 4.16. Position of Spendrup booster fan and surface fans

The pushing and pushing data have been gathered in Table 4.12.

Table 4.12. Two surface fans and a booster fan results

System	Pushing	Pulling
Network efficiency, %	28	19
Network annual power cost, $ x 1000	47	54
Q1 m^3/s	22	20
Q2 m^3/s	21	19
Q3 m^3/s	19	18
Q4 m^3/s	18	17
Q5 m^3/s	20	19
Q6 m^3/s	20	19
Total Q m^3/s	120	112

4.9.4. Scenario 4 – Two Surface Fans and Two Booster Fans. Two surface fans and two Spendrup booster fans have been utilized in this scenario as shown in Figure 4.17. Different blades of booster fans in various air ways and numerous speeds of surface fans have been taken into account to achieve the optimum design for the network.

All surface fans and booster fans generate high air quantity in low pressure. In this design, the steel door in west shaft has been eliminated from the ventilation network with the intention of meeting the working faces requirements. Different blade angles of booster fans have been investigated with the intention of achieving to the best blade angle. Angle 25˚ has been determined as the optimum blade angle for booster fans.

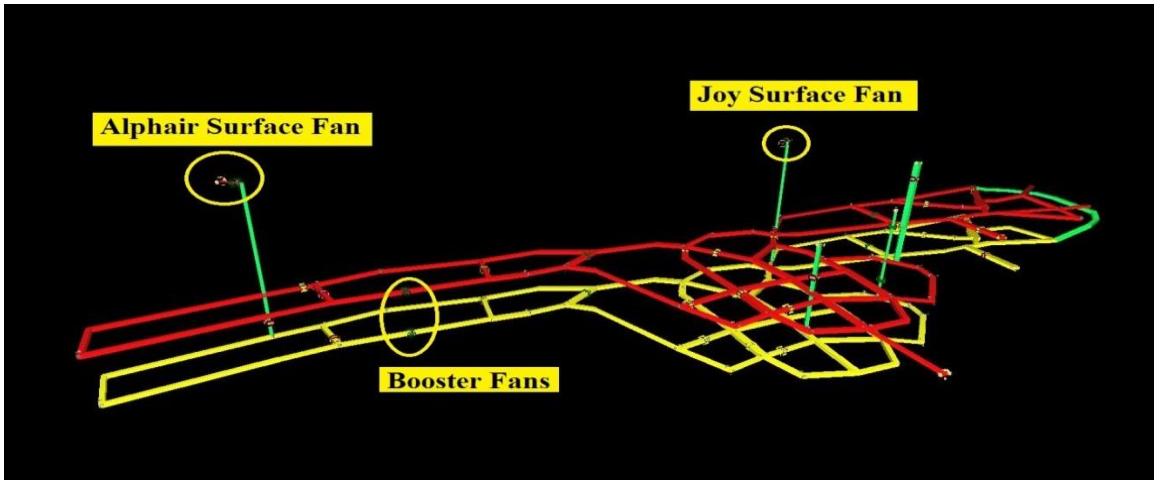

Figure 4.17. The position of two surface fans and two booster fans

The results are illustrated in Table 4.13 with consideration of various systems.

Table 4.13. Two surface fans and two booster fans results

System	Pushing	Pulling
Network efficiency, %	26	20
Network annual power cost, $ x 1000	49	56
Q1 m^3/s	25	25
Q2 m^3/s	25	24
Q3 m^3/s	21	20
Q4 m^3/s	20	20
Q5 m^3/s	25	24
Q6 m^3/s	26	24
Total Q m^3/s	142	137

4.10. CONCLUSION OF SECTION

After examining network efficiency, air quantity at all working faces, annual network power cost and considering parameters of the pulling system, scenario 3 amongst 1 level scenarios has been designated as the most efficient design for the experimental mine ventilation network. With the employment of scenario 3 the network efficiency has been increased by about 35% with 25 m^3/s air quantity at all working faces. In addition network annual power cost has decreased by $ 20,000. Applying the reversed system (pull system) in all scenarios has shown that on account of the reversal loss factor of fans, flow rate and efficiency will be decreasing noticeably. With switching of inlets and outlets of all surface and booster fans, the pushing system has been changed to the pull system without changing the direction of fan blade. So, by this action, we have achieved a pull system without decrease in fan efficiency. By examining the four scenarios it can be concluded that by dividing the experimental mine into two separated ventilation networks each with a main fan, the optimal possibilities will be achieved.

Numerous results from this survey have shown that by adding each fan to the ventilation network in 2 levels scenarios, the amount of air quantity has been improved noticeably. In scenario 1, the minimum requirement (at least 15 m^3/s air quantity in all working faces) has not been met. The target has been established at least 20 m^3/s air

quantity on all six working faces. Although scenarios 2 and 3 meet requirements of at least 15 m^3/s air quantities in working faces, they have not met 20 m^3/s in target points. By adding two booster fans in the ventilation system, the amount of air quantity has been altered dramatically but the network efficiency has not been improved noticeably. The optimum location of booster fans has been determined in line with achieving the optimum layout for ventilation network. The appropriate blade angle for booster fans has been determined 25˚. The Joy surface fan has been mounted on the fan house shaft and Alphair surface fan has been located on far west shaft of the mine with 15˚ bade angle. The new portal has been designed on the lower level of the mine to drain water from the eastern part and also to make an easy access to the bottom level. From reviewing data in tables, it can be seen that network efficiency with use of one booster fan in the circuit in pushing system is higher than utilization of two booster fans. However, it is the reverse in the pulling system. The network annual power cost in scenario 4 in comparison with this issue in other scenarios doesn't have a significant changes, the amount of air quantity has a noticeable aberration though. So, the amount of air quantity, network efficiency and the network annual power cost determined that the fourth scenario as the most efficient design for the ventilation network for the next 100 years.

5. FIRE BEHAVIOR ANALYSIS ON FUTURE PLAN OF THE MINE

5.1. PROBLEM STATEMENT AND OBJECTIVES OF SECTION

No underground peril has greater potential for large loss of life than a mine fire or explosion. A study has been carried out on Missouri University of Science and Technology's Experimental Mine in order to better understand fire behavior in unpredicted incidents. Ventsim Visual software modeling has been used to investigate fire behavior through the airways on future plan of mine ventilation network. Both natural and mechanical induced ventilation pressures have been taken into account.

Three different scenarios have been determined in different parts of the mine. In all scenarios fire source has been set to the Bobcat vehicle burning. Two different kinds of tire have been considered in all scenarios. Four main events as fire commencement, fire increases, fire maximum and fire termination have been fixed for dynamic simulation through determined period of the time in all simulations. Numerous parameters such as amount of CO, CO_2 and Psychrometric behavior, visibility and airflow direction have been investigated during the time. Four stations have been chosen as the target points to monitor predetermined factors. Various options have been considered to quench the produced fire in the mine. The effect of tires on an unpredicted fire event has been considered as one of the most important factor for fire control. The most perilous part of the mine has been distinguished. The least monitored amount of CO, CO_2 and dry bulb temperature and high visibility has been selected as the key parameters to determine an approach to control the fire. The needful procedures to control the fire from outside of the mine have been proposed in three main parts of the mine.

5.2. INTRODUCTION

The smoke and gases produced by such an event in a confined space quickly creates a lethal atmosphere for any underground workers exposed to the event. For this reason, there is great interest in being able to predict the effects of underground fires and utilize the results to establish emergency response procedures and systems to ensure the safety of people working underground (Ventsim manual). A study has been carried out to

simulate a fire event on the MS&T Experimental Mine future layout based on Ventsim Visual software usage in order to investigate produced noxious gases and enclose the fastest and safest design to mitigate the percentage of hazard in that mine. Heat simulation and dynamic simulation has been calibrated for fire simulation commencement. All psychrometric data has been put in to the simulator according to the latest field survey. Three scenarios have been considered to investigate numerous parameters such as CO, CO_2, airflow and dry bulb temperature at stations. Four different stations have been determined as the target points to monitor heat and fire behavior. All scenarios have been run through four hours. Fire event in all scenarios has been set to 20% diesel and 80% rubber in four main steps.

Natural and mechanical ventilation pressures have been considered in all scenarios. The direction of airflow has been investigated through each scenario. Surface fans have been turned off or left on according to the least amount of hazard accomplishment. Three minutes have been set for both booster fans to be turned off according to the distance to the fire situation. Various options have been considered to reduce the amount of dangerous gases at monitored stations in all scenarios. Tires selection has been considered in all simulations. Confining the fire in a limited area and the least monitored amount of CO, CO_2 and dry bulb temperature and the high amount of O_2 at determined stations have been determined as the key criterion amongst all scenarios for selecting the optimal scheme in emergency situations. The ideal long distance control of fire for mitigation of hazards, temperature and toxic gases has been selected as the most advantageous plan in each scenario.

5.3. VENTFIRE SIMULATION

VentFIRE is a module that uses dynamic simulation techniques (time based) to simultaneously model heat, gas and airflow changes on a mine environment over a period of time. VentFIRE allows a ventilation model to be dynamically modified during simulation (for example doors may be opened or closed, or fans may be turned on or off at certain times). The result is that a complete scenario may be modelled over a period of

time, and the atmospheric changes observed at different points in the mine as described in Ventsim Visual manual.

VentFIRE uses a discrete sub-cell transport and node mixing method to simulate moving parcels of heat and gas around a mine. To dynamically model mine ventilation and accurately take into account continual changes in atmospheric concentrations of gases and heat including recirculation, VentFIRE breaks the model into small independent 'cells' which move freely around a model, mixing with other cells at junctions. heat transfer to and from each cell from rock strata is calculated by the radial heat transfer method, but with strata heat transfer modified by the assumption of exposed rock boundary temperatures at a long term aged average, coupled with a very short time Gibson's algorithm constant to accelerate heat transfer to and from the immediate rock boundaries during the fire simulation as described in Ventsim Manual.

5.3.1. VentFIRE Limitations. A number of limitations need to be recognized when using VentFIRE:

5.3.1.1 Fire effect simulation, not fire chemistry simulation. Fire chemistry is not simulated (apart from oxygen deficiency). Simulated results are only as good as assumptions entered into the program. Gas levels are highly dependent on assumed yield rates of combustible materials and should not be generally used to indicated 'safe' gas level and 'dangerous' gas levels. Any abnormal gas level simulated by VentFIRE should be considered potentially hazardous.

5.3.1.2 Rollback. VentFIRE does not currently consider 'rollback' where heat and fumes can travel along the roof in the opposite direction to the airflow for some distance back from the fire. Rollback distances are highly variable and depend on fire intensity, the slope of the airway, and the velocity of the opposing airflow.

5.3.1.3 Chocking limitation. The initial expansion phase of the fire will produce a 'non' mass balanced model where the mass flow of cold air exiting an airway may be greater than the mass flow (of hotter air) entering the same airway. In other words, for a limited time the lower mass-flow of hotter air pushes out a higher mass-flow of cold air. Because airflow simulation in VentFIRE is based on a mass balanced Hardy Cross algorithm, even though this takes into account the greater pressure losses and choking effects of airways produced from higher volume flows of hot air, it does not take into

account the short term periods were greater masses of cold air are being pushed out. The 'net' effect is that VentFIRE may temporarily underestimate the choking effect of the fire as explained in Ventsim Manual.

5.4. SCENARIOS

Fire simulations have been designed according to the designed air simulation of experimental mine future ventilation network. In all scenarios main surface fans have been set to the pull system. Heat and dynamic simulation as prerequisite of fire simulation have been designed appropriately. Dynamic increment has been set to 0.5 seconds for all simulations. Total simulation time after which the simulation will halt has been set to 4 hours. Both natural and mechanical induced ventilation pressures have been taken into account in all scenarios. Three different scenarios have been considered to investigate airflow behavior and numerous characteristics in all parts of the mine. Rock type has been set to limestone in all scenarios with 1.3 W/m ˚C thermal conductivity, 1.2 m^2/s 10-6 Thermal diffusivity, 840 j/kg ˚C Specific heat and 1.290 kg/m^3 as density. In all simulation 25˚ C has been assigned to the rock temperature. According to the latest pressure and quantity survey 18.5˚ C and 22˚ C have been put in simulation for surface wet bulb and dry bulb temperature. 20% diesel and 80% rubber have been put into the program as the fuel type for burning. Four main events with different start and end time period and initial and ending burning rates have been set as the dynamic events for the creation of fire simulation. Dynamic events data for the design of bobcat burning have been shown in Table 5.1. Smoothing factor for simulation result has been set to 500. Four monitors as shown in Figure 5.1 have been established to investigate different airflow parameters at those stations. For all scenarios the amounts of CO_2, CO and O_2, Psychrometric properties, visibility and airflow have been monitored at four predetermined stations. Numerous procedures have been investigated to control produced fire at selected working face. An optimum way has been proposed to reduce hazard in perilous situations at three main spots of the mine. In all scenarios the threshold limit values (TLV) for CO and CO_2 has been considered 25 ppm and 0.5% respectively.

Table 5.1. Bob cat with EarthForce compact tires burning event information through 4 hours

Events	Time Range (sec)		Fuel	Burn Rate (Kg/hour)	
Name	Start of period	End of period	Fuel type	Initial rate	Ending rate
Fire starts	0	1800	Diesel and Rubber	0	200
Fire escalates	1800	3600	Diesel and Rubber	200	480
Fire maximum	3600	13800	Diesel and Rubber	480	480
Fire ends	13800	14400	Diesel and Rubber	480	0

It has been assumed that the first 30 minutes is the initiating step of the fire. Twenty percent diesel and eighty percent rubber have been assigned to be burnt. During the first 30 minutes, 2500 kW energy has been produced by burning of that fuel. The second step of the fire event is when it escalates. The period of this step has been set to 1 hour. The amount of energy has been increased to 6000 kW.

During the third step of fire event (fire maximum) 6000 kW has been produced by the fire. The period of this step has been set to two hours and 50 minutes. During the fire termination step, 6000 kW has reduced to zero in the last 10 minutes.

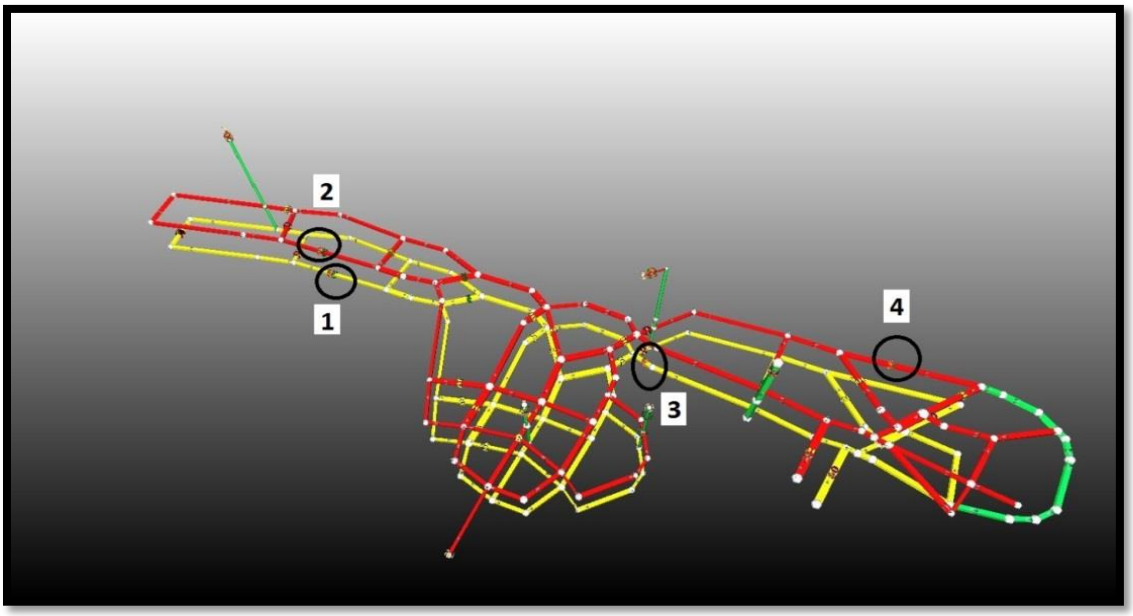

Figure 5.1. Monitors position through airways

5.4.1. Tires Specifications in the Mine. Bobcats in MS&T Experimental Mine have been using two different types of solid tires. All Scenarios have been simulated according to the EarthForce solid press-on tire. The use of standard duty pneumatic tires has been compared to the EarthForce solid tires too.

5.4.1.1 EarthForce solid press-on tires. These kinds of tires with their sidewalls are designed to prevent cuts and cracks in aggressive terrain, EarthForce solid press-on tires offer performance and driver comfort with a partially pneumatic tire design. They are made of heavy duty rubber compounds for increased service life.

• Deep lug treads provide traction in an assortment of terrains

• Great shock absorption for machine longevity and operator comfort

• Super smooth tires also feature air-cushioned design

The use of this tire in the Experimental Mine is shown in Figure 5.2.

Figure 5.2. EarthForce Solid Press-on tire

By the use of this kind of tire, the money spent due to flat tires has been eliminated and the longer tire life time has been achieved. Specification of this kind of tire has been shown in Table 5.2.

Table 5.2. EarthForce Solid Press-on Tire Specifications in Experimental Mine

Style	Outside Dia. (mm)	Tire Width (mm)	Rim Dia. (mm)	Tread Depth (mm)	Weight (kg)
Dirt Terrain with Rim	838	305	406	51	113

5.4.1.2 Standard duty pneumatic tires. These tires are created for long wear during normal machine-hour applications as shown in Figure 5.3.

Figure 5.3. Standard Duty Pneumatic tires

The special rim guard and thick sidewalls provide protection against punctures. They're constructed with natural and synthetic rubber. Specification of Standard Duty Tires is shown in Table 5.3.

Table 5.3. Standard Duty Pneumatic Tire Specifications

Model	Style	Outside Dia. (mm)	Tire Width (mm)	Rim Dia. (mm)	Tread Depth (mm)	Weight (kg)
Skid-Steer Loader	Standard	787	254	419	14	36

5.4.2. Scenario 1, Fire at the West Working Face (Down Level). In this scenario fire has been set at the west working face on the lower level. The pull system of surface fans has been considered to investigate the behavior of fire and different characteristics through the airways in four hours real time. Fire event has been set to act as shown in Table 5.1. Six minutes after fire event commencement east surface fan has been set off. Three minutes after initiate time of fire event booster fans in lower and upper levels have been turned off. Two blocked raises at center and east part of network and two closed adits at the east panel of Experimental Mine as shown in Figure 5.4 have been opened after ten minutes in simulation. West portal has been closed 10 minutes after the fire initiation time. All times for this scenario have been selected according to the distance and the action of the mine's work force. The distribution of fire through the airways after 1 hour is shown in Figure 5.5.

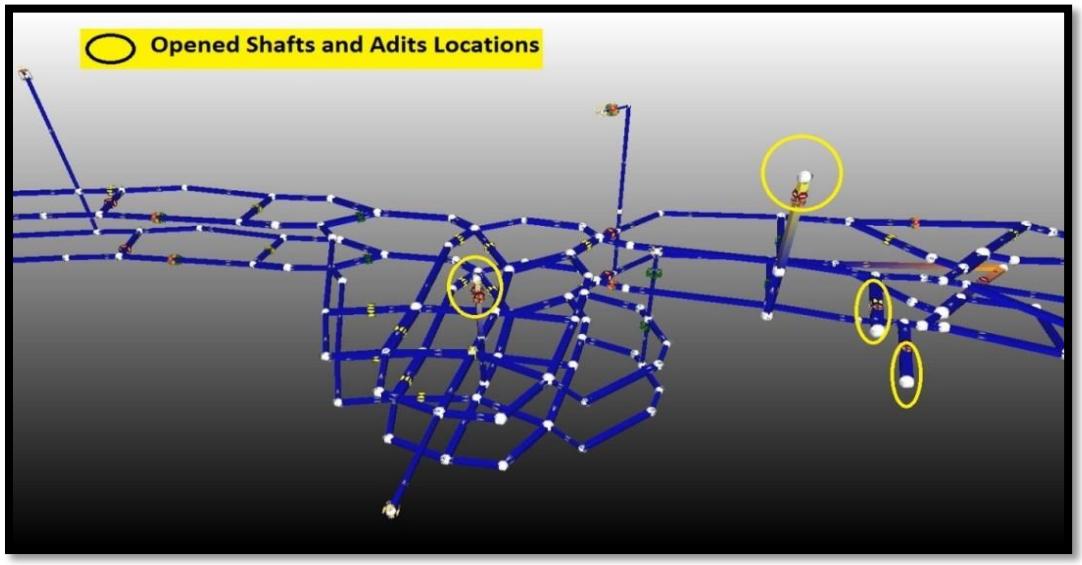

Figure 5.4. Opened adits and shafts 10 minutes after fire starts

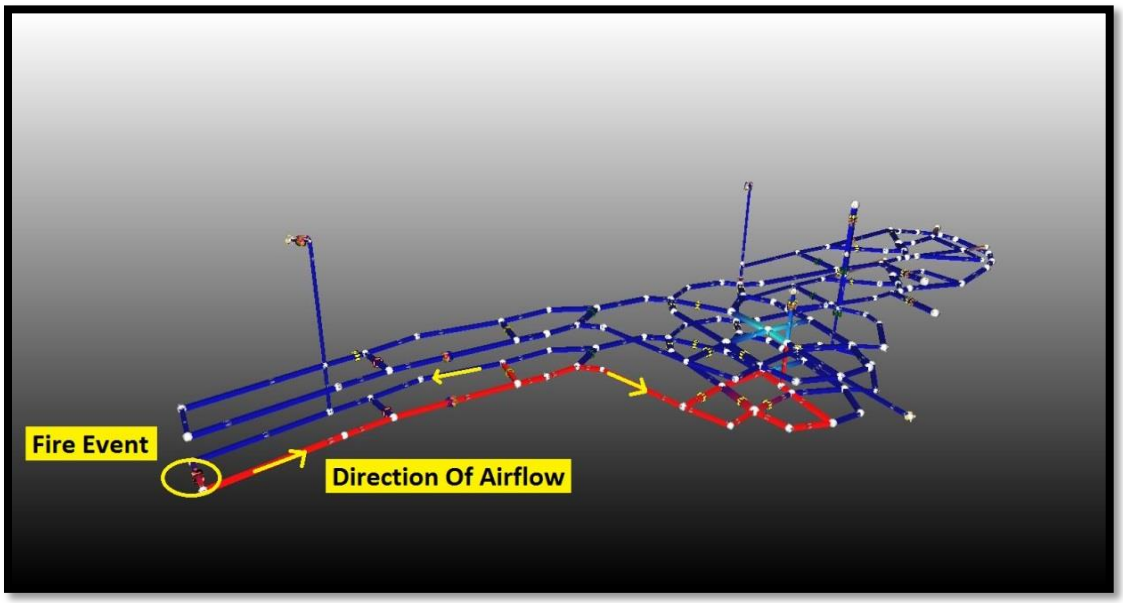

Figure 5.5. Fire distribution, 1 hour after fire initiation (pull system)

5.4.2.1 Airflow and O_2 behavior at stations. On account of natural ventilation Pressure and opened adits and shafts and fire effect the direction of airflow at all stations have been changed. The airflow direction has been changed at station 1 about 1 hour after fire event initial time. The airflow result at station 1 during whole burning time is shown in Figure 5.6.

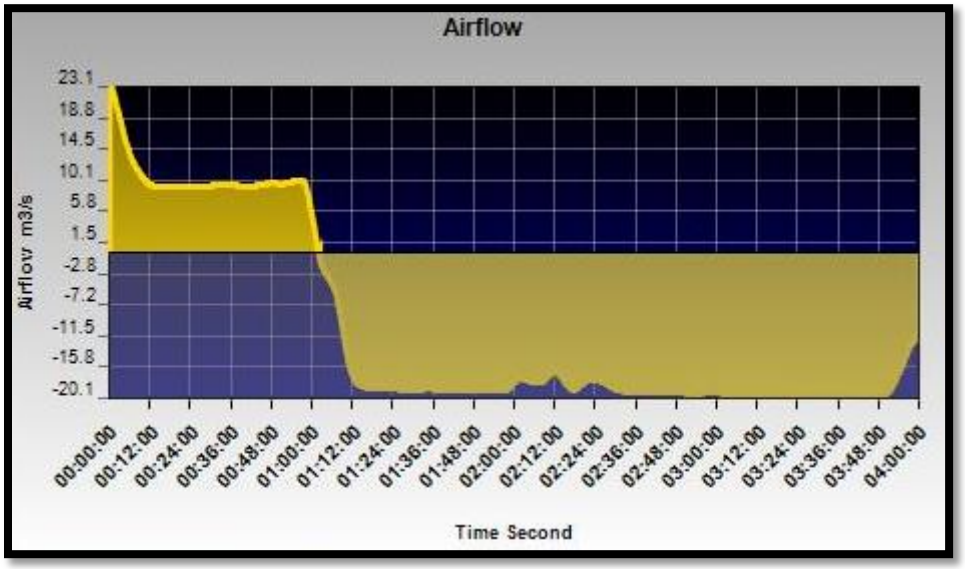

Figure 5.6. Air flow behavior at station 1

It is evident from Figure 5.6 that maximum amount of airflow at station 1 in the reversed direction was 20.1 m^3/s. As it can been seen in this figure the graph is experiencing sharp drop during the first 12 minutes when booster fans and east surface fan have been turned off and the adits and raises have been opened completely at 10 minutes and then remained constant up to 1 hour. The airflow has been decreased dramatically at that time because airflow has been reversed and it almost leveled off up to the last 10 minutes. The last drop happened in the last 10 minutes of fire event. The graph under the zero line is showing the reversed direction of airflow at that station through the time. When the fire got close to be finished the airflow has been decreased.

Airflow at stations 3 and 4 has behaved the same. The least amount of airflow has been recorded at 8.1 m^3/s at station four in the reversed direction. Airflow diagram at station 4 is plotted in Figure 5.7. At 10 minutes the airflow direction at station 4 has been changed and then increased marginally to 8.1 m^3/s up to the end of 1 hour and almost remained constant up to the end of simulation. Minimum and maximum amount of airflow at station 3 has been recorded at 26.3 and 26.7 m^3/s.

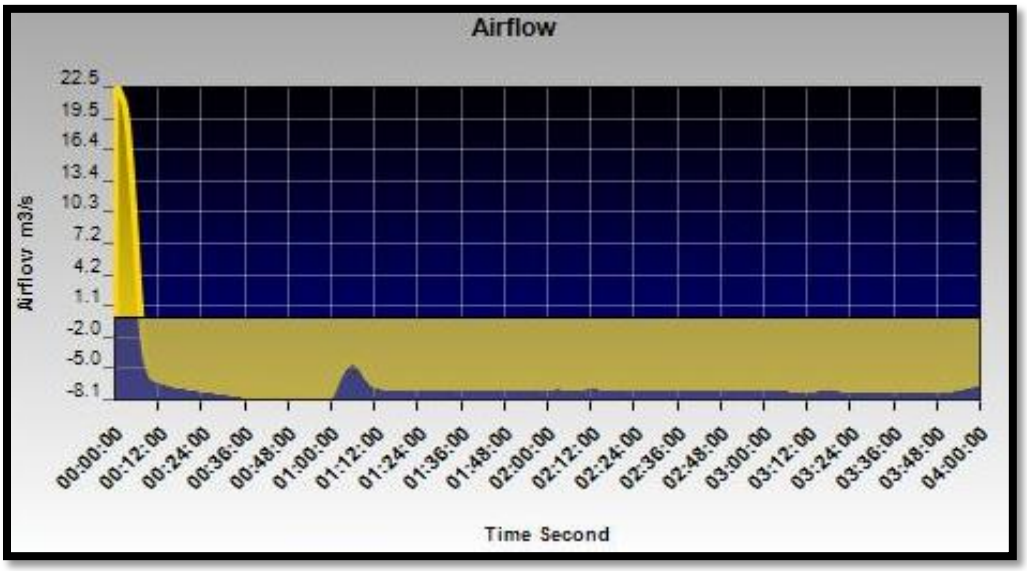

Figure 5.7. Airflow distribution in 4 hours at station 4

According to the airflow data at station number 2, it is evident that airflow graph has decreased with turning the fans off. Then the airflow has increased conspicuously

from 10 minutes to 1 hour to 22.4 m^3/s. Because of the fire behavior the direction has been changed again at 1 hour after fire initiation and reached to 5.5 m^3/s and remained constant up to the end of event. The results is illustrated in Figure 5.8

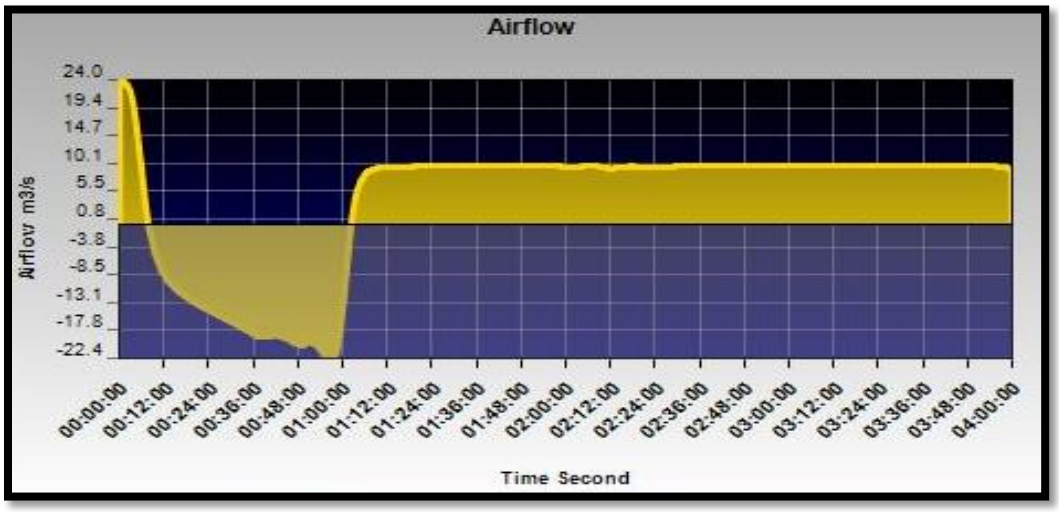

Figure 5.8. Airflow distribution at station 2

It is evident from above figures that natural ventilation pressure, effects of opened adits and shaft and fire effect has had great impression on the direction of airflow at all part of the mine. The effect of natural ventilation pressure on the direction of airflow is shown in Figure 5.9.

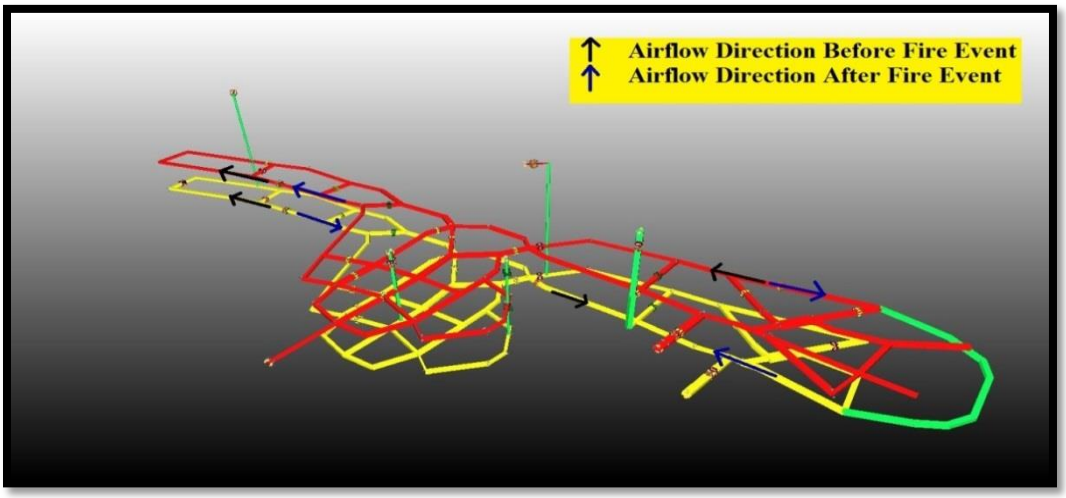

Figure 5.9. Direction of airflow before and after fire event

Before the fire event the amount of O_2 range has been recorded 21.1% to 21.7% in all scenarios. The least amount of O_2 has been monitored 18.8% at closest station to the fire when the fire has been simulated in 4 hours. As it can be seen in Figure 5.9 the closest station to the fire was station 1. The range of O_2 in all stations is shown in Table 5.4.

Table 5.4. Oxygen percentage in all stations through 4 hours

Station	Min O_2 %	Max O_2 %
1	18.8	21.3
2	20.5	21.4
3	21.6	21.7
4	21.0	21.1

5.4.2.2 CO and CO_2 behavior at stations. In all stations the amount of CO and CO_2 has been recorded in order to get better understanding of fire behavior through the airways. At station 1 amount of CO has increased dramatically and approached to 2200 ppm as the peak point after 1 hour and then it remained constant up to the last 10 minutes. The graph is experiencing sharp decrease in fire termination period. The amount of CO at the end of fire event after 4 hours has been recorded 700 ppm approximately.

By briefly glancing at CO_2 graph in this station it is evident that this is behaving as CO behaved in the period of the fire. The highest amount of CO_2 at this station has been recorded 1.86 % and at the end of 4 hours this amount has been diminished to 0.220 % conspicuously. The highest amount of CO and CO_2 has been monitored in this station.

The amount of CO has escalated dramatically in the first 1 hour and 12 minutes of the event at station number 2. The peak point has been calculated 1427 ppm and then it decreased sharply to 714 ppm. A direction change has been determined as the main reason for the great change in amount of CO between 1 hour and 1:12. After 1 hour and 12 minutes the amount of CO has decreased sharply to 714 and then almost leveled off up to the last 10 minutes. The sharp decrease happened during the last 10 minutes. The amount of CO at the end of 4 hours has been monitored 350 ppm. The results have been gathered in Figure 5.10.

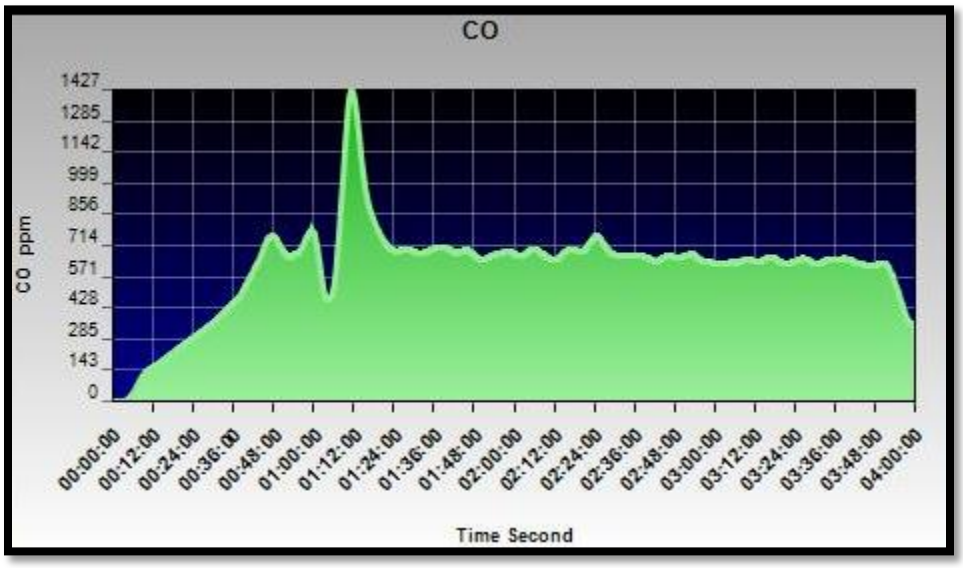

Figure 5.10. Amount of CO at station 2

When the CO_2 graph at this station has been studied it has been discerned that the behavior of CO_2 was the same as CO behavior at this station. Maximum amount of CO_2 at station 2 has been recorded 0.438% as shown in Figure 5.11.

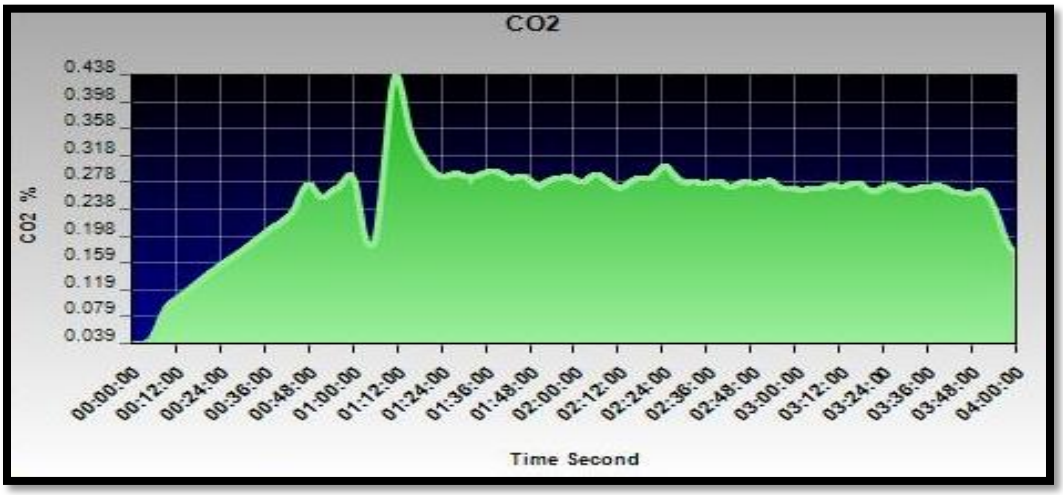

Figure 5.11. CO_2 behavior at station 2

It is clear that with the addition of distance proportion to the fire event location the amount of CO and CO_2 has decreased sharply. The furthest station has had the least

amount of toxic gases rather than the other stations. So on a count of distance the least amount has been recorded at station 4. Monitored amount of CO and CO_2 at the east part of the mine was not considerable. Stations 3 and 4 have been determined the safest place amongst all determined stations in this scenario. At these stations the amount of CO and CO_2 has been kept less than TLV. As has been seen in previous stations the graph behavior of CO and CO_2 has been monitored as same as each other at both 3 and 4 stations. The result of CO and CO_2 at stations 3 and 4 has been shown in Table 5.5.

Table 5.5. CO and CO_2 results at stations 3 and 4

Station	3	4
Min CO (ppm)	0	0
Max CO (ppm)	7	4
Min CO_2 %	0.039	0.038
Max CO_2 %	0.063	0.054

5.4.2.3 Psychrometric behavior at stations. In this study all dry and wet bulb temperatures and rock temperature have been investigated at all stations. The highest amount of temperature has been monitored at station 1. Temperature changes during 4 hours fire event at stations 3 and 4 were not considerable. During the first 1 hour the dry bulb temperature graph remained at the lowest amount of itself. During the next 12 minutes temperature has reached to the pinnacle point at 201˚ C at station 1. Then it reduced to 183.4 ˚C and it reached plateaus up to the last 10 minutes of simulation. During the last 10 minutes the graph has descended noticeably to 78˚ C at the end of 4 hours simulation. The result of dry bulb temperature at station 1 has been manifested in Figure 5.12. Wet bulb temperature behavior has been recognized as same as the dry bulb temperature behavior. Minimum and maximum amount of wet bulb temperature has been monitored at 19.8˚ and 52.7˚ C.

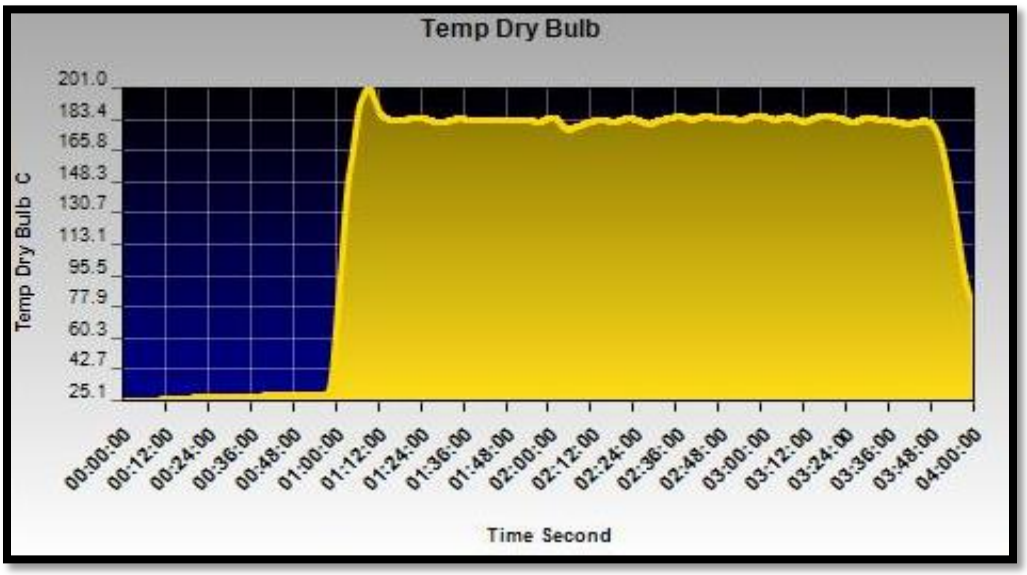

Figure 5.12. Dry bulb temperature graph at station 1 in 4 hours fire event

Rock temperature has increased from the beginning of fire event up to the end. The highest amount of rock temperature amongst all stations has been recorded at 67.4˚ C at station 1. The result of rock temperature at station 1 has been shown in Figure 5.13.

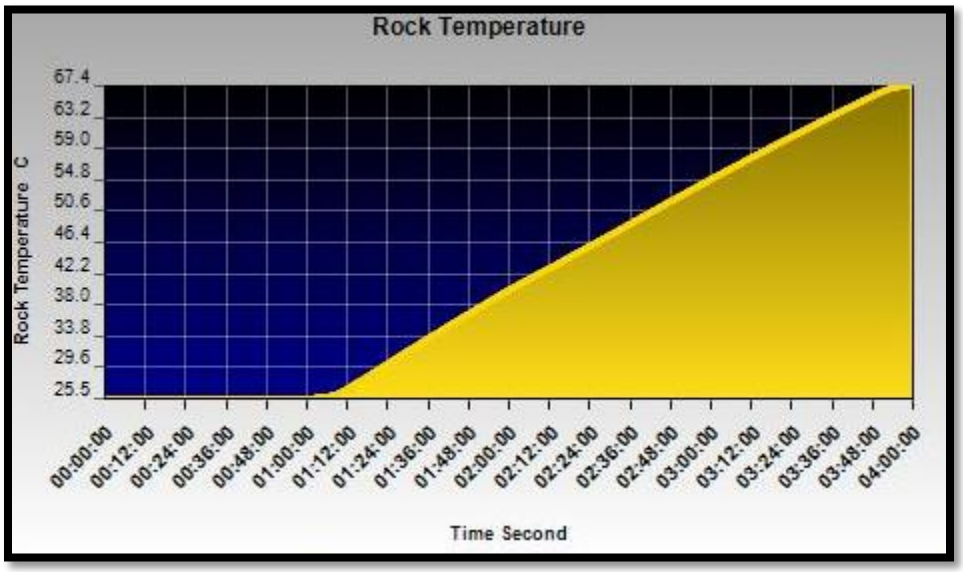

Figure 5.13. Rock temperature changes at station 1

The range of psychrometric behavior at the other stations has been recorded and is illustrated in Table 5.6.

Table 5.6. various temperature result at stations 2, 3 and 4

station	2	3	4
Min DB Temp ˚C	24.8	25.1	24.5
Max DB Temp ˚C	77.2	28.8	26.1
Min WB Temp ˚C	19.6	19.9	19.6
Max WB Temp ˚C	34.8	20.0	20.6
Min Rock Temp ˚C	25.1	21.5	24.6
Max Rock Temp ˚C	28.4	25.2	24.6

It is evident from Table 5.6 that fire has not had a significant impact on temperature changes at eastern part of the mine.

5.4.2.4 Visibility at stations. With the exception of stations 1 and 2 all stations visibility has not been affected by the fire. This is evident that east part of the mine was devoid smoke. Visibility at station 1 has been decreased from 25 m to 0.1 m during the first 1 hour and then it remained the same up to the last 10 minutes. During the final step of the fire the visibility at that station has increased to 2.6 m. Visibility graph has been plotted in Figure 5.14.

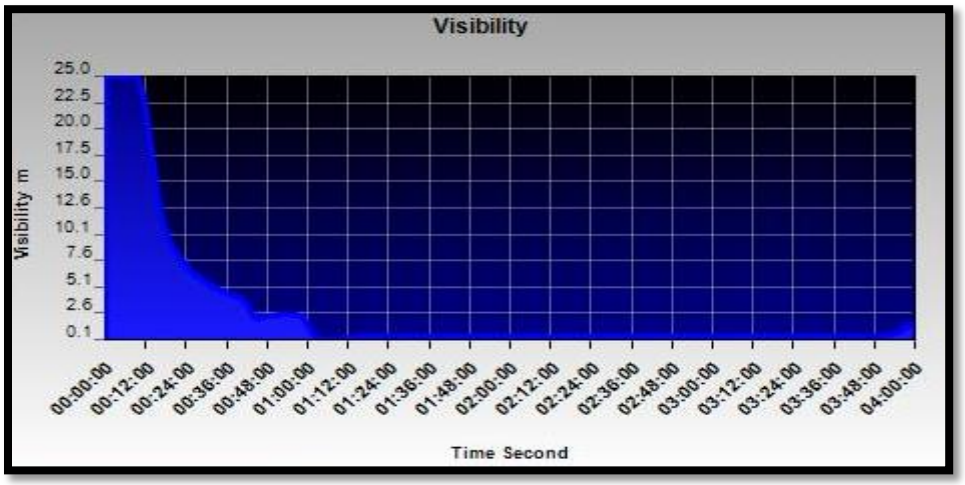

Figure 5.14. Visibility graph at station 1

The behavior of visibility graph at station 2 has been recorded the same as station 1. Before the fire event visibility was 25 m while after the fire it decreased spectacularly to 0.6 m and remained constant up to the last 10 minutes. At the fire termination step visibility increased to 3 m.

5.4.2.5 Heat behavior study at stations. During the first 6 minutes amount of heat at station 2 has decreased when the fans have been turned off and the natural ventilation pressure and opened adits and shafts have changed airflow direction and then has increased conspicuously. The maximum amount of heat has been recorded 76 kW at that station. The sharp increase trend continues up to last 1 hour of fire event and then descended noticeably during the next 6 minutes and remained almost constant up to the end of event. Recorded amount of heat at 4 hours has been monitored 4.5 kW as shown in Figure 5.15. The amount of heat above and under zero line is showing the different direction of airflow through the time. Because of direction changes in airflow between 1:00 to 1:06 the sharp drop happened. The highest amount of heat has been recorded at this station.

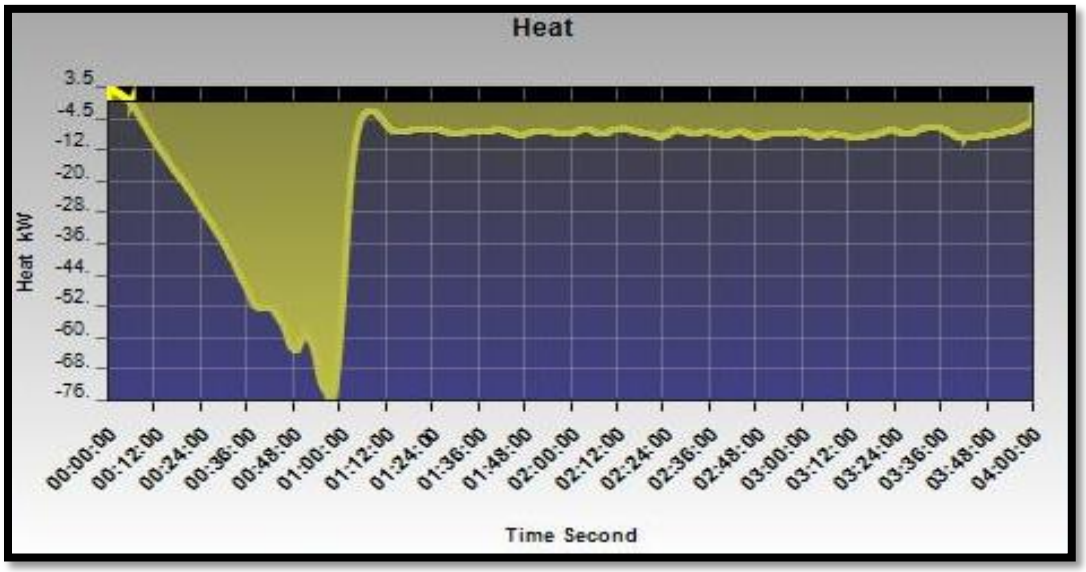

Figure 5.15. Heat behavior at station 2

The amount of heat at other stations has been illustrated in Table 5.7. It is evident from Figure 5.15 that the direction of heat has been determined the same as their airflow direction.

Table 5.7. Heat amount at stations 1, 3 and 4

station	Min heat kW	Max heat kW
1	4.2	28
3	0.1	2
4	0.3	1.1

In summary it is noteworthy that the fire has been controlled in the west part of the mine by opening the specified adits and shafts. This action half of the mine has been saved from noxious gases. The other options have been examined in order to get the safest atmosphere through the mine. It is not recommended the situation when all fans have been turned off. The amount of toxic gases has been recorded too high. The following procedure has been determined as the best approach to diminish the hazard level in emergency situations at that working face:

(a) East surface fan has been set off.

(b) Booster fans in lower and upper levels have been turned off.

(c) Two blocked raises at center and east part of network and two closed adits at the east panel have been opened.

(d) West portal has been closed.

This approach has been determined as the optimum reaction to decrease the hazards of the fire at the bottom west panel in an emergency situation.

By the change of EarthForce compact tires to standard duty pneumatic tires in simulation the amount of burning has decreased and also hazards have decreased respectively. Result is shown in Table 5.8.

Table 5.8. Average CO and DB temperature according to 2 different tires at all stations

Tire Kind	Property	Station 1	Station 2	Station 3	Station 4
EarthForce	Average CO (ppm)	1100	350	3.5	2
Standard Duty	Average CO (ppm)	308	174	1	0.5
EarthForce	Average DB Temp ^{o}C	113	51	27	25.3
Standard Duty	Average DB Temp ^{o}C	48	40	25.7	24.6

5.4.3. Scenario 2, Fire at the West Working Face (Surface Level). In this scenario fire has been set at the west working face on the surface level. Pull system of surface fans has been considered to investigate the behavior of fire and different characteristics through the airways in four hour real time. Fire event has been set as same as previous scenario as shown in Table 5.1. Six minutes after fire event commencement east surface fans has been set to be off while west surface fan is left on. Three minutes after initiation time of fire event booster fans in surface and down levels have been deactivated. Ten minutes after fire start time, the central shaft has been opened. All times for this scenario has been selected according to the distance and react of mine's working forces. The distribution of fire 1 hour after fire initiation through the airways is shown in Figure 5.16. EarthForce Solid Press-on tires has been selected as the Bobcat tires in fire simulation.

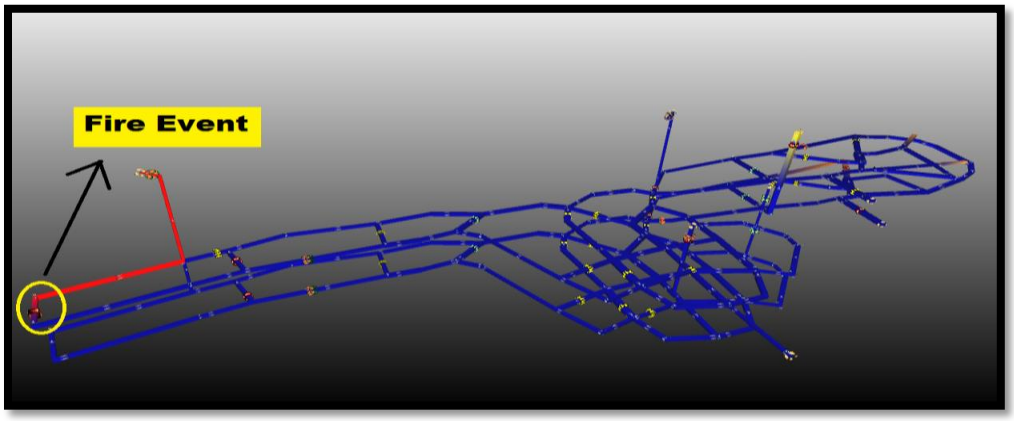

Figure 5.16. Fire distribution through the airways after 1 hour

5.4.3.1 Airflow and O_2 behavior at stations. On account of off booster fans and East surface fan airflow direction has been changed in stations number 3 and 4. However when the fire event has been set at down level, the direction of airflow at all stations was changed. The maximum airflow changes in the period of fire event have been monitored at station 3. The airflow result in four hour at station 3 is shown in Figure 5.17. By turning the fans off in the mine the amount of airflow has been decreased noticeably to zero m^3/s at station number 3 during the first six minutes and then the airflow direction reversed and leveled off to 4 m^3/s up to the end of event. The graph is experiencing sharp

decrease during the first 6 minutes and then has increased to 4 m^3/s. The airflow graph is experiencing no fluctuation after 10 minutes up to the end of fire event.

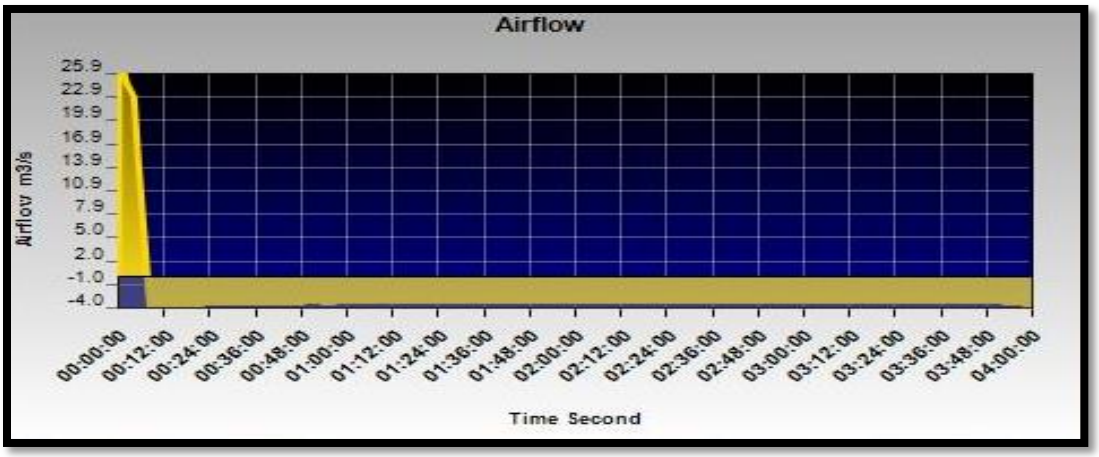

Figure 5.17. Airflow distribution at station 3

Airflow at station 4 has experienced the same behavior with different range. The general amount of airflow at that station has been monitored at 3.6 m^3/s as shown in Figure 5.18. The airflow direction at other stations has not been changed. Consistent with data from airflow graph it is perceived that the direction of airflow at the east part of the mine has been changed while airflow direction at west remained the same. The result of airflow at statins 1, 2 and 4 is shown in Table 5.9.

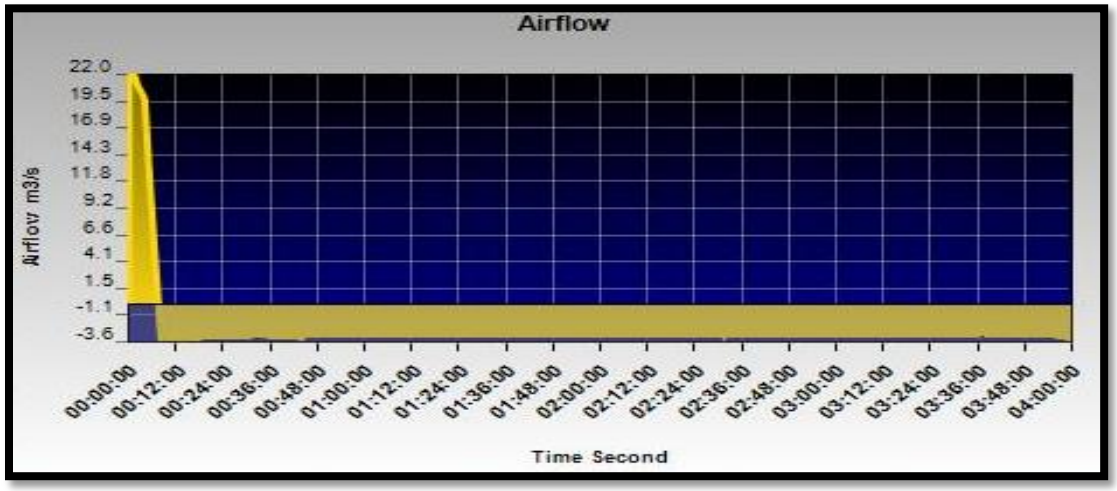

Figure 5.18. Airflow behavior at station 4

During the first six minutes the airflow has reduced spectacularly to the minimum amount and then remained constant up to the end of event.

Table 5.9. Amount of airflow at stations 1, 2 and 4

station	1	2	4
Min airflow m^3/s	3.7	6.7	3.6
Max airflow m^3/s	23.2	23.2	22

Before fire event the amount of O_2 range has been recorded 21.1% - 22.1% in all scenarios. The highest drop has been monitored 0.7% at closest station to the fire when the fire has been simulated in 4 hours. As it can be seen in Figure 13 the closest station to the fire was station 2. The range of O_2 in all stations is shown in Table 5.10. It is evident from Table 5.10 that the amount TLV has not been reached at all stations.

Table 5.10. Oxygen percentage in all stations through 4 hour

Station	Min O_2 %	Max O_2 %
1	21.3	21.4
2	21.4	22.1
3	21.6	21.7
4	21.1	21.1

When the fans have been turned off the amount of airflow has been decreased dramatically. However the rate of O_2 has not impinged from the minimum rate of O_2 in underground mines.

5.4.3.2 CO and CO_2 behavior at stations in scenario 2. In all stations the amount of CO and CO_2 has been recorded in order to determine the toxic atmosphere and fire behavior through the airways. At station number one and two with the passage of time the amount of CO has not increased. The amount of CO at those stations has been recorded at zero. The highest amount of CO has been recorded at 3 ppm at stations 3 and 4 while after 6 minutes this amount has reduced to zero. The range of CO at all stations has been shown in Table 5.11. By managing the ventilation network the amount of CO has been saved in the safe area and TLV has not been reached at all stations.

Table 5.11. CO amount at stations

Station	Min CO (ppm)	Max CO (ppm)
1	0	0
2	0	0
3	0	3
4	0	3

When all fans were turned off, the amount of CO at stations has increased dramatically. The amount of CO at station 2 had reached to 6000 ppm approximately. The amount of CO at the other station has been recorded too high. The average amount of CO at all stations is shown in Table 5.12.

Table 5.12. Average CO at stations when all fans are off

Station	1	2	3	4
Average CO (ppm)	170	3000	300	300

If we take a closer look at CO_2 graph at all stations it is evident that the graphs are behaving as CO behaved in the period of the fire event. The highest level of CO_2 at this station has been recorded at 410 ppm. After a period of 4 hours this amount has diminished to 390 ppm. It is clear that the percentage of CO_2 has not reached the TLV. The level of CO_2 at station 3 has been shown in Figure 5.19. If all fans have been turned off, the CO_2 percentage has increased to 1.4% which is in excess of the TLV.

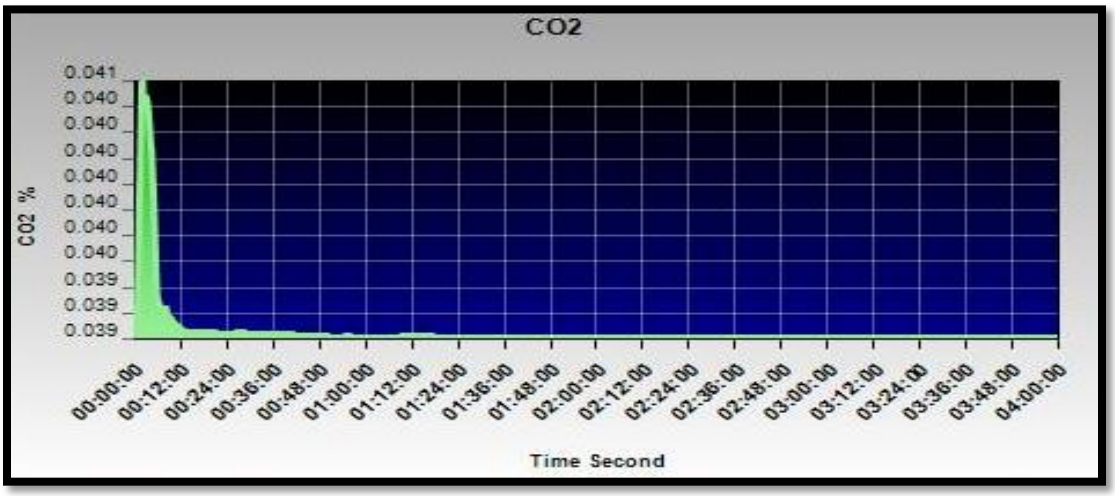

Figure 5.19. The amount of Co_2 at station 3

The result of CO and CO_2 is illustrated in Table 5.13. This study has shown that by turning the fans off the amount of CO and CO_2 has increased sharply at stations.

Table 5.13. CO and CO_2 results at stations 1, 2 and 4

Scenarios	1	2	4
Min CO (ppm)	0	0	0
Max CO (ppm)	0	0	3
Min CO_2 %	0.038	0.039	0.038
Max CO_2 %	0.039	0.040	0.040

5.4.3.3 Psychrometric behavior at stations. In this study all dry and wet bulb temperatures and rock temperature have been investigated at all stations. The highest amount of temperature has been monitored at station 1. Temperature changes during 4 hours fire event at all stations in the mine were not considerable. After 12 minutes minutes the dry bulb temperature graph has reached to the highest point at all stations and then it stabilized up to the end of 4 hours simulation approximately. The result of dry bulb temperature at station 3 is shown in Figure 5.20.

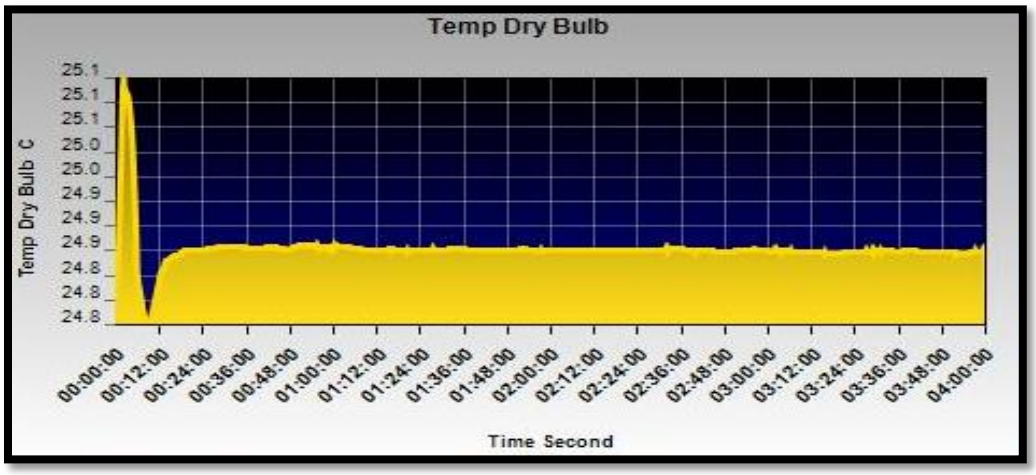

Figure 5.20. Dry bulb temperature behavior at station 3

Wet bulb temperature behavior has been recognized as same as the dry bulb temperature behavior as foregoing scenario. Minimum and maximum amount of wet bulb temperature has been monitored at 19.9˚ and 20.1˚ C at station 3. The highest amount of rock temperature amongst all stations has been recorded at 24.5˚ C at station 4.

Fire has not had any impression on the rock temperature at all stations. The result of temperature at other stations is illustrated in Table 5.14.

Table 5.14. Various temperature result at stations1, 2 and 4

station	1	2	4
Min DB Temp ˚C	25.1	24.7	24.3
Max DB Temp ˚C	25.3	24.9	24.6
Min WB Temp ˚C	19.8	19.5	19.7
Max WB Temp ˚C	20	19.6	19.9
Min Rock Temp ˚C	25.3	25.1	24.5
Max Rock Temp ˚C	25.4	25.1	24.6

According to the data from Table 5.14 it is understood that the fire has not had great impression on stations' temperature differences drastically. However dry bulb temperature at station 2 has been reached to 107˚ C when the fans have been deactivated.

5.4.3.4 Heat behavior study at stations. Heat behavior in this scenario at all stations was not considerable. Minimum and maximum amount of heat has been gathered in Table 5.15 for all stations. At the beginning of the event the amount of heat was at the maximum amount of itself at all stations. After 6 minutes heat at all stations has decreased to the minimum amount and then remained constant up to the fire termination step.

Table 5.15. Amount of heat at all stations

Scenario	Min heat kW	Max heat kW
1	0.1	4.1
2	0.2	4.1
3	0.1	0.2
4	0.1	1.5

All in all fire has been controlled in all part of the mine by turning the west surface fan on. So by this action all parts of the mine have been saved from noxious gases and a balance has been made in all part of that. The other options like opening closed shafts and adits have been examined in order to achieve the safest atmosphere through the mine. This approach has been determined as the accepted reaction to decrease the hazards of the fire at the all levels in an emergency situation. When all surface and booster fans have been turned off the amount of toxic gases and temperature have increased dramatically. The amount of burning has descended conspicuously and also hazards have decreased respectively by the change of EarthForce solid tires to standard duty pneumatic tires in simulation. The amount of rubber differences caused to this result. Average amount of carbon monoxide and dry bulb temperature results are shown in Table 5.16 when all fans have been turned off.

Table 5.16. Average CO and DB temperature according to 2 different tires at all stations

Tire Kind	Property	Station 1	Station 2	Station 3	Station 4
EarthForce	Average CO (ppm)	170	3000	300	300
Standard Duty	Average CO (ppm)	80	1500	50	70
EarthForce	Average DB Temp ^{o}C	25.2	76.3	25.1	25.2
Standard Duty	Average DB Temp ^{o}C	25	53	24.9	24.8

The following procedure has been determined as the best approach to diminish the amount of hazard in emergency situation at that working face:

(a) East surface fan off.

(b) West surface fan left on.

(c) Booster fans in surface and down levels off.

(d) The central shaft has been opened.

The visibility has not been affected by the fire in this scenario. Because the fire has been led to the exhaust shaft, there are not any changes in visibility at all stations.

5.4.4. Scenario 3, Fire at the East Working Face. Fire has been set at the ramp on the east part of the mine. Surface fans pulling air has been considered to investigate the behavior of fire and different characteristics through the airways in four hour real time. Six minutes after fire event commencement west surface fan has been set to be off while east surface fan hasn't been turned off. Booster fans on surface and lower levels have not been deactivated during the whole time of fire event. All two shafts at central part of network have been opened 10 minutes after fire event. East adit and drainage adit and shaft have been opened 10 minutes after fire initiation time too. All times for this scenario has been selected according to the distance and react of mine's working forces. The distribution of fire and determined adits and shafts for pull system of surface fans through the airways is shown in Figure 5.21.

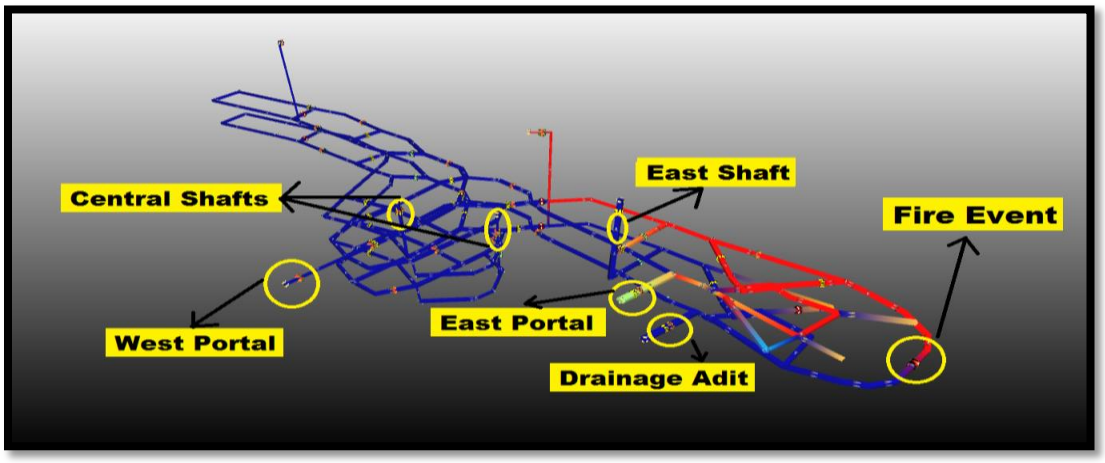

Figure 5.21. Fire distribution and effective mine's component on airflow direction

5.4.4.1 Airflow and O_2 behavior at stations. Because of east surface fan and two booster fans pressure, natural ventilation pressure has not influenced airflow direction at all stations. The maximum airflow changes in the period of fire event have been monitored at station 3. The airflow result in four hours at station 3 is shown in Figure 5.22. The amount of airflow through the west part of the mine has decreased by turning the west surface fan off. The amount of airflow at the east part of the mine has increased noticeably and then it remained constant. Maximum amount of airflow at station 3 has been recorded at 40.5 m^3/s. The amount of airflow has been constant between 15 minutes up to the end step of fire event.

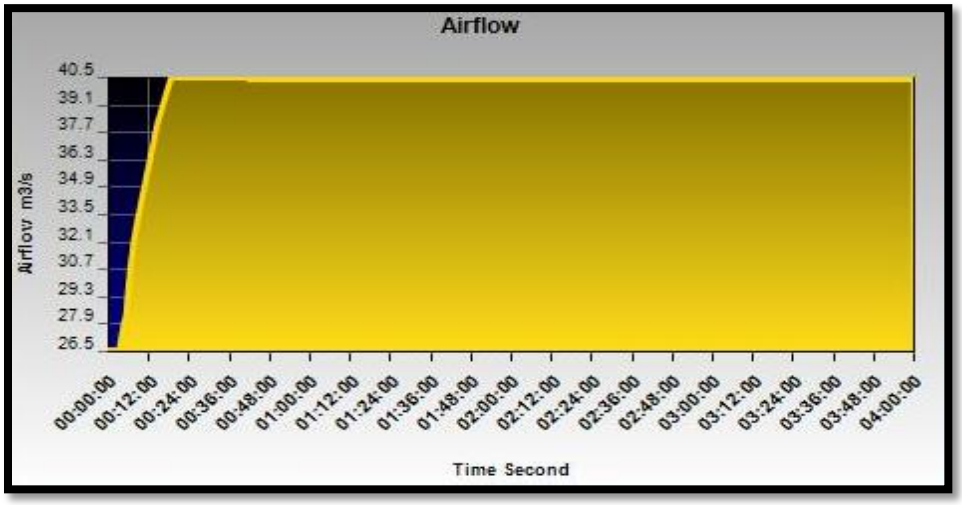

Figure 5.22. Airflow distribution at station 3

The direction of airflow at stations 1 and 2 has not changed. During the first 6 minutes the amount of airflow has been decreased to 20.0 m^3/s and then started to be increased to 21.7 m^3/s sharply up to 15 minutes and then it leveled off up to the end of event. The behavior of airflow is plotted in Figure 5.23. It is evident from airflow diagrams at all stations that the behavior of airflow at the two stations in the west part of the mine and two stations in the east part of the mine are the same.

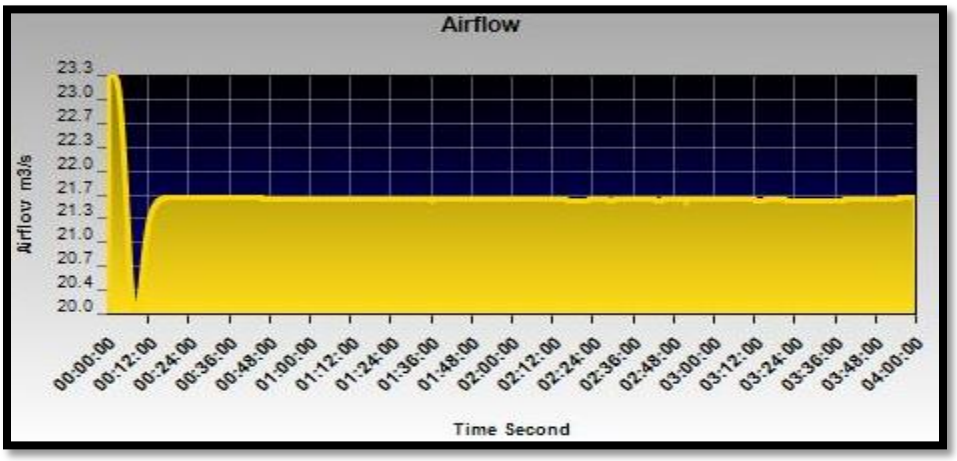

Figure 5.23. Airflow behavior at station 1

Before fire event the amount of O_2 range has been recorded 21.1% - 21.6% in all scenarios. The highest change has been monitored at 1% at station 4. The percentage of O_2 at other stations has not been changed considerably. The range of O_2 in all stations is shown in Table 5.17. The amount of O_2 has decreased conspicuously at the closest station to the fire however the TLV has not been reached as illustrated in Figure 5.24.

Table 5.17. Oxygen percentage at all stations

Station	Min O_2 %	Max O_2 %
1	20.9	21.3
2	21	21.4
3	21.1	21.6
4	20.1	21.1

When the west surface fan has been turned off the amount of airflow has decreased. The level of O_2 has not gone below the O_2 TLV.

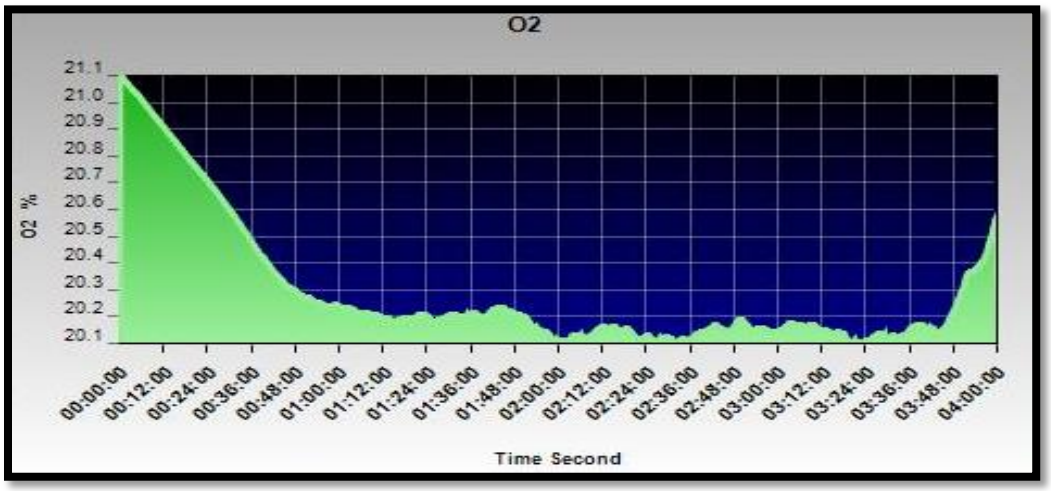

Figure 5.24. O_2 percentage at station 4 during the fire event

The direction of airflow has been changed when all fans have been turned off. The direction of airflow when the fans have been turned off is plotted in Figure 5.25.

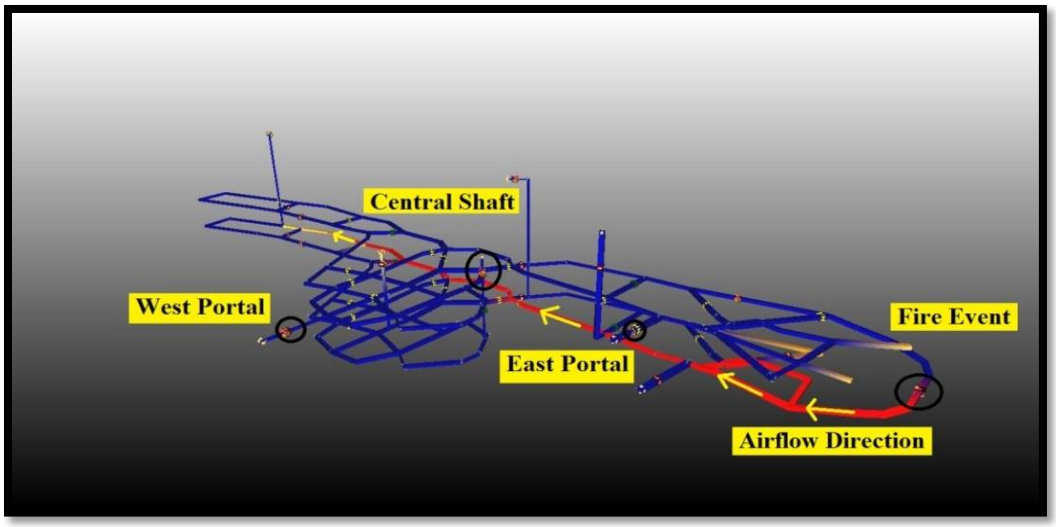

Figure 5.25. Direction of airflow when all fans are off

5.4.4.2 CO and CO_2 behavior at stations in scenario 3. In all stations the amount of CO and CO_2 has been recorded in order to determine the toxic atmosphere and fire behavior through the airways. At station 4 the amount of CO has increased to 809 ppm dramatically when the west surface fan has been turned off. The graph has reached to the highest point at 2 hours and then has remained almost constant up to the 3:50 hours and dropped to 490 ppm during the last 10 minutes. If all surface and booster

fans have been turned off, the amount of CO has increased in the mine and also the direction of fire has been changed. The monitored result for CO at station 4 is shown in Figure 5.26. Maximum amount of CO has been recorded at station 4. When the amount of CO is high at station 4 the amount of CO at the other parts of the mine has been monitored zero.

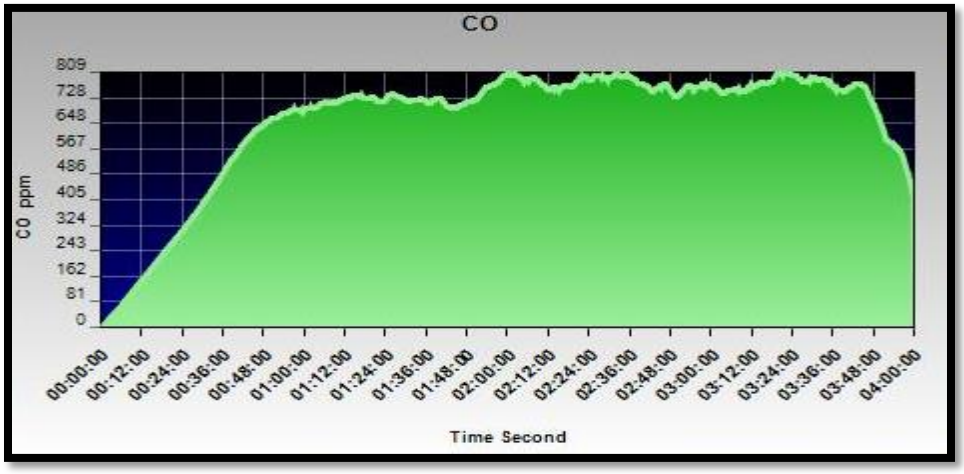

Figure 5.26. CO distribution at station 4

By this action fire has been controlled at the east part of the mine without any hazardous effect on the other parts of the mine.

If we take a closer look at CO_2 graphs in all stations it is evident that this is behaving as CO behaved in the period of the fire event. The highest amount of CO_2 has been recorded as 0.36 % at station 4.The highest amount of CO and CO_2 has been monitored at that station. The result of CO and CO_2 at stations is shown in Table 5.18.

Table 5.18. CO and CO_2 results at all stations

Scenarios	1	2	3	4
Min CO (ppm)	0	0	0	0
Max CO (ppm)	1	1	1	809
Min CO_2 %	0.038	0.038	0.039	0.038
Max CO_2 %	0.039	0.039	0.040	0.359

Consistent with the data in the Table 5.18, it is seen that the TLV for CO_2 and CO at the central and eastern part of the mine has not been reached. Hence those parts of the mine have been selected as the safe parts in an emergency situation. The result of CO_2 at station 4 is shown in Figure 5.27.

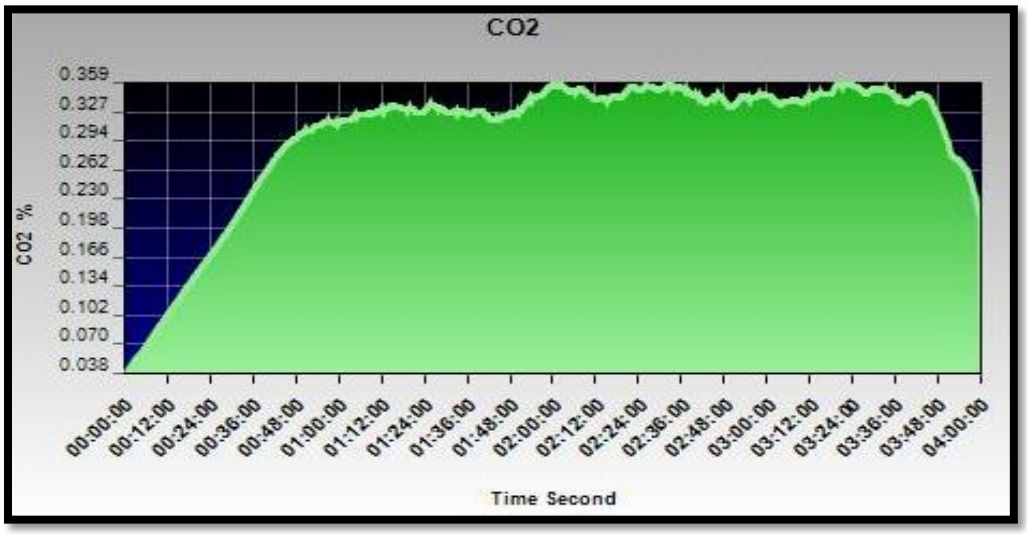

Figure 5.27. CO_2 distribution at station 4

When all fans have been turned off, the amount of CO at station 4 has increased dramatically. The amount of CO at that station had reached to 5500 ppm approximately. The amount of CO at the other stations has been recorded too low. The average amount of CO at all stations is shown in Table 5.19.

Table 5.19. CO amount at stations when all fans are off

Station	Average DB ˚C	Visibility (m)	Average CO_2 (%)	Average CO (ppm)
4	120	0.3	1.2	2750

5.4.4.3 Psychometric behavior at stations. In this study all dry and wet bulb temperatures and rock temperature have been investigated at all stations. Obviously, the highest temperature has been monitored at station 4. Temperature changes during the 4 hours fire event at other stations were not considerable. After 2 hours dry bulb temperature has reached to the peak point at 112.3˚ C at station 4 and then it remained

constant during the next 1 hour and 50 minutes. The graph is experiencing sharp decrease between 3:48 to 4:00 hours. The result of dry bulb temperature at station 4 is shown in Figure 5.28.

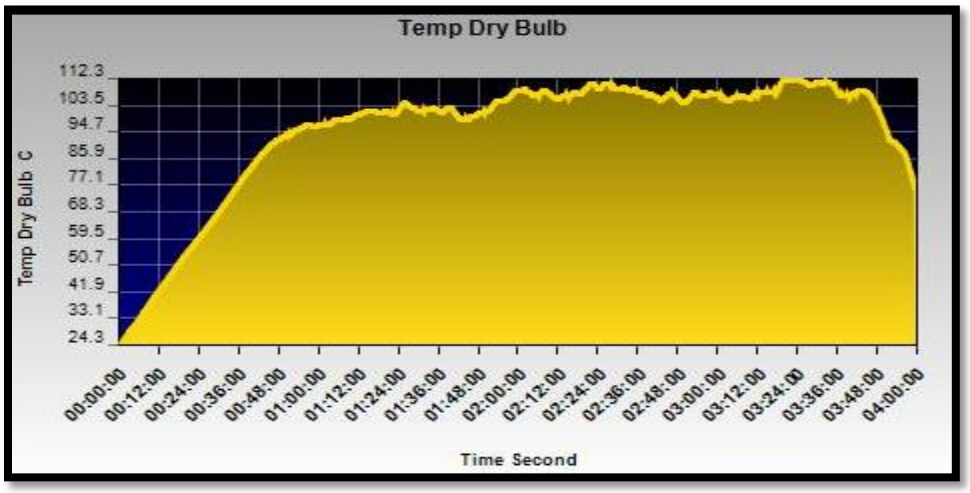

Figure 5.28. Dry bulb temperature at station 4

Wet bulb temperature behavior has been recognized as same as the dry bulb temperature behavior as previous scenarios at all stations. Minimum and maximum amount of wet bulb temperature at station 4 has been recorded at 19.9˚ and 39.8˚ C. The highest rock temperature amongst all stations has been recorded 38.5 ˚C at that station. The rock temperature at station 4 is illustrated in Figure 5.29. Rock temperature has increased dramatically up to the termination time of simulation.

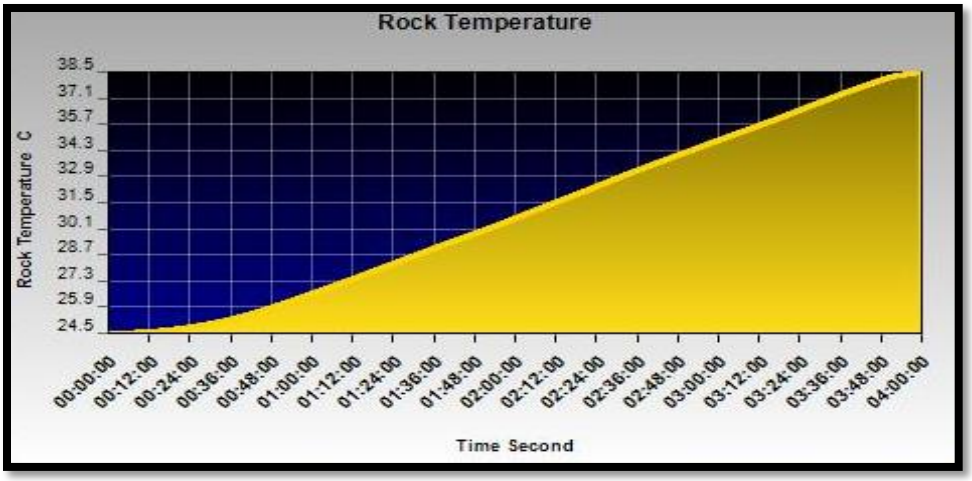

Figure 5.29. Rock temperature behavior at station 4

Dry bulb and wet bulb temperatures have not been experiencing any important changes at stations 1, 2 and 3. Fire has not had any impression on the rock temperature at those stations too. The result of temperature at other stations is illustrated in Table 5.20.

Table 5.20. Various monitored temperatures at stations 1, 2 and 3

Station ˚C	1	2	3
Min DB	25.2	24.8	24.8
Max DB	25.4	25	24.9
Min WB	19.9	19.6	19.9
Max WB	20	19.7	20.1
Min Rock	25.4	25	24.8
Max Rock	25.4	25.1	25.1

From Table 5.20 data it can be seen that the fire has not changed temperatures at stations significantly.

5.4.4.4 Heat behavior study at stations. Heat at stations 1, 2 and 3 has not been changed drastically. During the first 6 minutes, heat at stations 1 and 2 has increased to 5.7 kW when the west surface fan has been turned off and then has decreased sharply to 4.3 kW. The heat behavior at those stations is illustrated in Figure 5.30.

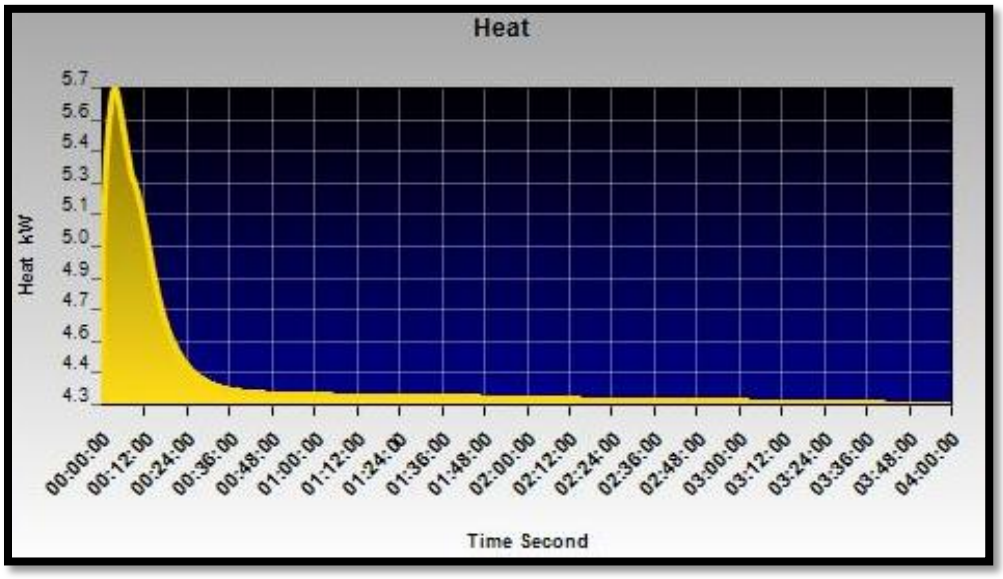

Figure 5.30. Heat diagram at stations 1 and 2

The maximum amount of heat has been recorded at station 4 when the fire was close to the maximum step and it remained constant at 46 kW in 20 minutes and then it experienced marginal decrease and remained constant up to the last 10 minutes. When the fire got close to the terminate point, the amount of heat has decreased respectively. The amount of heat above and under zero line is showing the different direction of airflow through the time. Heat result at station 4 over four hours is shown in Figure 5.31.

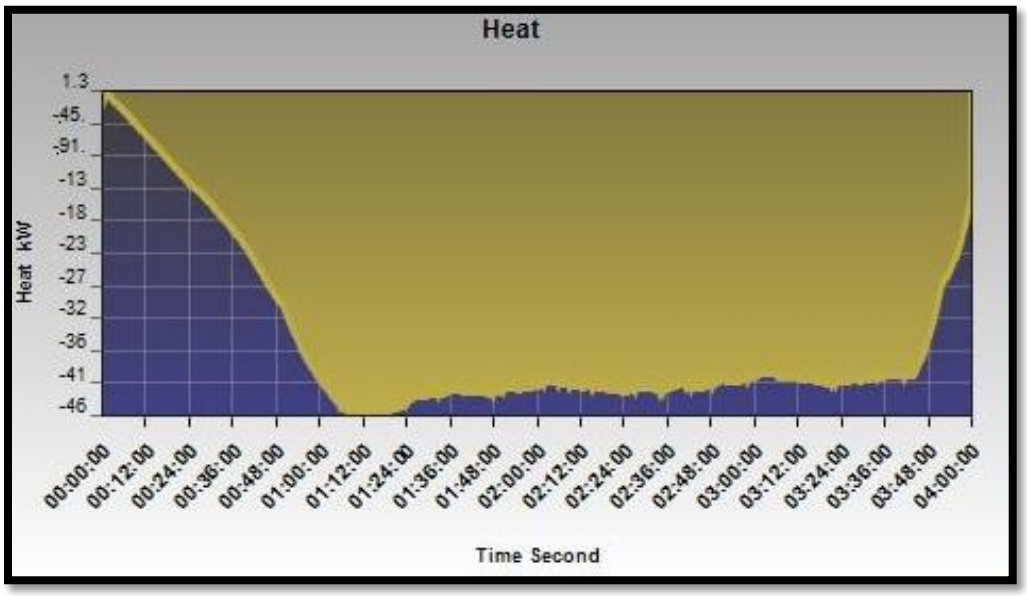

Figure 5.31. Heat diagram at station 4

The amount of heat at other stations is illustrated in Table 5.21. The direction of heat has been determined as same as their airflow direction.

Table 5.21. Heat amount at stations 1, 2 and 3

station	Min heat kW	Max heat kW
1	4.3	5.7
2	4.3	5.7
3	1.3	46

5.4.4.5 Visibility at stations. With the exception of station 4 all stations' visibility has not been affected by the fire. Visibility at station 4 has been decreased from 25 m to 1 m during the first 30 minutes and then it remained the same up to the last 10 minutes. During the final step of the fire the visibility at that station has increased to 3.4 m. Visibility graph is plotted in Figure 5.32.

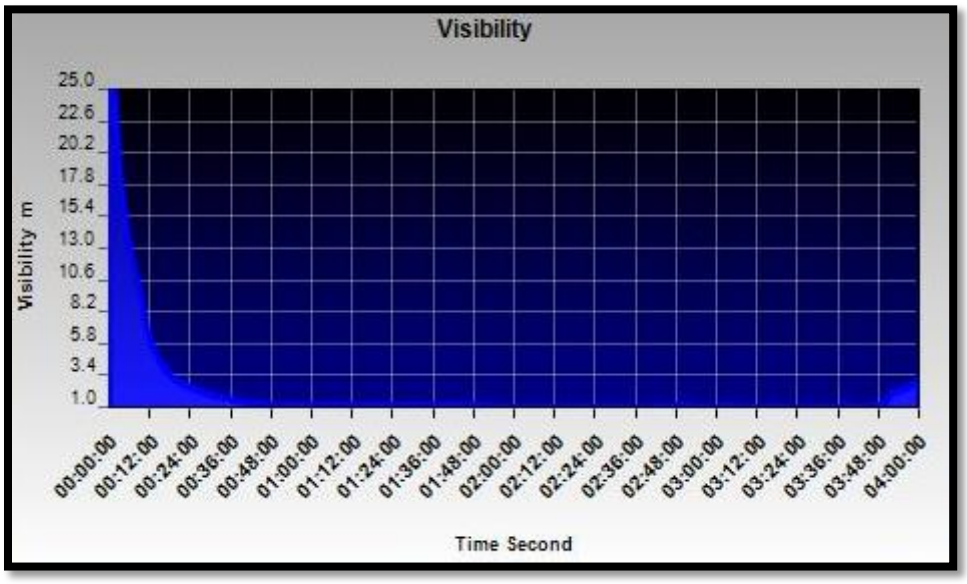

Figure 5.32. Visibility graph at station 4

The amount of burning has descended and also hazards have decreased respectively by the change of EarthForce compact solid tires to standard duty pneumatic tires in simulation. Results are shown in Table 5.22.

Table 5.22. Average CO and DB temperature according to 2 different tires at all stations

Tire Kind	Property	Station 1	Station 2	Station 3	Station 4
EarthForce	Average CO (ppm)	0	0	0	400
Standard Duty	Average CO (ppm)	0	0	0	170
EarthForce	Average DB Temp ^{o}C	25.3	24.9	24.85	68.3
Standard Duty	Average DB Temp ^{o}C	25	53	24.9	45.2

All in all fire has been controlled by turning the west surface fan on. Although by this action east and central parts of the mine have been saved from noxious gases, cannot be ignored the effect of opened adits and shafts in emergency situations. The other

options like opening closed shafts and adits or turning the east surface fan off have been examined in order to get the safest atmosphere through the mine. If all fans have been turned off, the direction of fire has not been changed and the amount of toxic gases and temperature has increased considerably in all parts of the mine. The following procedure should be considered for mitigation of hazards when the fire happens at the decline in emergency situation:

(a) West surface fan should be off.

(b) East surface fan and booster fans should be turned on.

(c) All adits and shafts should be opened.

5.5. CONCLUSION OF SECTION

It is noteworthy that distance and airflow direction have played key role in the amount of CO and CO_2 and temperature changes. Unfortunately, the anticipation of fires before the event is extremely difficult, not only the location (which to some degree may be predicted using risk assessment techniques on possible combustible sources), but also to the nature, size and behavior of the fire. This study has been carried out for better understanding of airflow behavior and fire behavior when a Bobcat vehicle started to be burnt at working faces. The highest amount of toxic CO gas has been monitored 3000 ppm at the closest station to the fire when all fans have been turned off.

West working face at the down level has been determined as the most perilous part of the mine for executing more safety issues. It is very hard to control the fire when it happens at that part of the mine. By turning all fans off, noxious gases have been trapped in the mine. So turning all surface and booster fans off wasn't selected as the ideal approach to control the fire. Maximum temperature has been monitored at 200˚ C at station 1 in scenario 1. The behavior of CO and CO_2 at each station has been recognized as same as each other. Numerous applications such as closing or opening different doors and shafts and the turning on or off of different fans have been investigated to achieve the optimum procedure for controlling the fire. However the best approach has been achieved in each scenario by following the proposed procedures. The amount of O_2 in all scenarios

has not decreased under the minimum amount according to the MSHA regulations in the safe parts of the mine. This study has shown that tires of vehicles are one of the most important factors in burning event. However the least consideration has been employed for choosing the tires of vehicles in the mines. The life time of tires always pulled focus of purchasers in industry while burning hazards were neglected. Standard duty pneumatic tires have been selected as the Experimental Mine Bobcats' tires for working in underground. The reversed direction of surface fans has been considered in this study while in real mines is very hard to employ this application. In addition mismanagement and lack of emergency layout in emergency situations can cause to a malignant consequences for a mine. This study has been carried out to show that the emergency plan ahead of any emergency is needed for every mine.

6. BEHAVIOR OF FLOW THROUGH MINE DUCTING

6.1. PROBLEM STATEMENT AND OBJECTIVES OF SECTION

Main mine fans are often connected to underground workings through bends or elbows. These connections may include damper controls or louvers. An investigation has been undertaken of the main surface fan system at a mine and their associated elbows and louver. Leakage and shock losses in different parts of mine airways are of major concern. Comprehensive analyses has been undertaken of these ventilation shock losses experimentally, numerically and computationally to increase understanding and optimize air flow through the mine. Pressure and air flow velocity across different parts of elbows and louver set at different angles have been measured experimentally. Two precision pressure transducers have been used simultaneously to measure pressure drops across the louver and the inlet and outlet of the elbow. Vane anemometers have been utilized to measure velocity in ducting before elbows and throughout the mine.

Losses considering various elbows' angles and louver angles have been calculated numerically by using Bernoulli's equation for incompressible fluid. Calculations have been compared with measured K loss factors for different angles and air power losses across the louver. The experimental results of the mine's elbow and louver have been compared to the computational and numerical results. Pressure losses in the fan ducting elbow and louver have been investigated by computational fluid dynamics (CFD). The CFD exercises have been conducted to gain understanding of flow behavior at various louver blade angles and elbow design after comparison with measurement results. Ansys Fluent 14 has been applied in order to investigate pressure drops across the louver and the elbow. The velocity inlet boundary condition has been applied at the shaft inlet. The pressure outlet boundary condition has been applied at the outflow faces and walls specified for a non-slip condition. Research has been undertaken to achieve the lowest shock loss elbow model and louver angles. The computational and numerical results have been used to analyze various feasible designs. Numerous models have been compared with each other in order to achieve the optimal model. The model has been used to predict possible locations and leakage flow rates for numerous boundary conditions and geometries over the elbow and inlet shaft. A series of simulations has been performed for

ideal design of main fan ductwork by reducing shock loss in that air way. The minimum shock loss and maximum velocity in the inlet shaft has been determined as the best scenario for the ventilation network. Surface fan locations have been selected.

6.2. INTRODUCTION

As air progresses through the ducts produced pressure by main mine fan is dropped, the velocity is decreased and needful air quantity problem at working faces will emerge. A comprehensive study has been carried out to improve ducting systems at the MS&T Experimental Mine by experimental, numerical and computational approaches. Two 765-16B Paroscientific pressure transducers with claimed accuracy of ±8 Pa have been used simultaneously to measure pressure drops across the louver, the inlet and outlet of elbows. Vane anemometers and Pitot tubes have been utilized to measure velocity in ducting before elbows and throughout the mine.

Pressure drop across the louver set at different angles and a 90˚ elbow has been measured. Shock loss factors across the elbow have been calculated using various dimensions and angles in order to achieve an acceptable design numerically. Two approaches have been used to determine shock loss factor across the elbow numerically.

Atkinson's friction factor "k" for the mine elbow has been determined. The Bernoulli Equation has been used to calculate pressure loss across the louver at two discrete angles. An approach has been used to determine 60˚ and 0˚ loss factors (K factors) across the louver numerically. Computational Fluid Dynamics (CFD) exercises have been conducted to gain understanding of flow behavior at various louver blade angles and elbow design. Different parameters such as velocity inlet and outlet pressure drops have been determined and ideal elbow and louver designs have been selected according by use of three approaches. Experimental design has been compared to the computational and numerical designs. Differences in values derived from various simulations and approaches have been found. The optimum position of main mine fan has been determined from results of this study.

6.3. CURRENT VENTILATION NETWORK

A study has been done at an underground limestone mine located in Rolla, Missouri. The MS&T Experimental Mine is accessed by two adits, three raises and two primary ventilation shafts. The mine has a 1.2 m diameter Joy axial vane fan with a 24 kW motor and an Alphair 4,500 axial vane fan with a 24 kW motor installed to move approximately 25 m^3/s of airflow at 1 kPa pressure through the underground working faces. Two 12 kW Spendrup booster fans have also been installed underground in series with the surface fans. The Joy axial surface main fan with two different speeds is connected to the 1.0 m diameter mine shaft inlet with a 90˚ elbow. The Alphair surface fan is installed vertically. Dimensions through the ducting system have been measured in order to be used in numerical, experimental and computational designs. The mine's elbow is constructed of 1 mm thickness steel. Ducting with curved bend has a width of 0.98 m as shown in Figure 6.1.

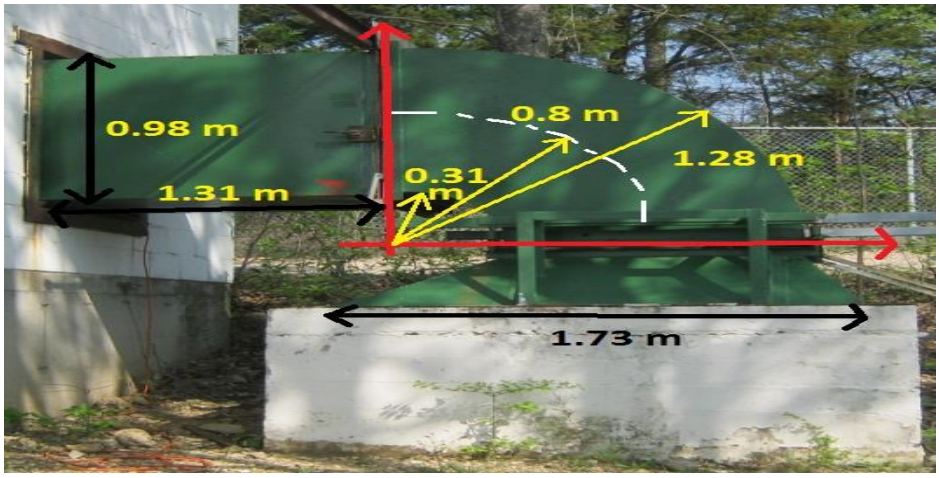

Figure 6.1. Dimensions of the 90˚ elbow

The louver controls airflow through the ducting attached to the Joy fan. Dimensions of louver blades have been measured and are shown in Figure 6.2. Louver blades thickness and each blade's internal angle have been measured at 2 mm and 120˚ respectively. The louver blades are controlled by a hydraulic pump in order to protect the surface fan from moisture or to use in emergency situations.

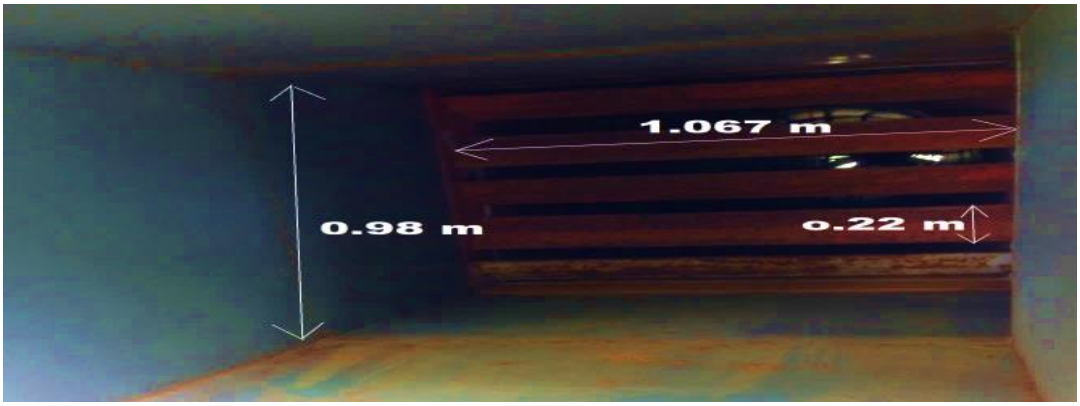

Figure 6.2. Dimensions of louver blades

6.4. EXPERIMENTAL DESIGN

Although CFD has many advantages, it does not completely eliminate the need for experiments which are still needed to validate numerical solutions. For this reason, data collected during actual mine tests and CFD simulations are compared. This comparison allows a better understanding of the flow phenomena. Moreover, once the numerical solutions have been validated, CFD can be used with better confidence to predict the effect of changes in ductwork configurations on energy losses. CFD reduces the number and cost of tedious experiments, while enabling a broader scope of design comparisons (Wala, Yingling, Zhang, and Ray, 1993).

Pressure and air flow velocity across different parts of the elbow and louver set at different angles have been measured experimentally in MS&T Experimental Mine. Five different stations were established along the duct. There is one within the surface atmosphere. In addition there is one underground, station 7 within the rock lined shaft of the mine as shown in Figure 6.3. Points 1, 2, 3, 4, 5, 6 and 7 were used for pressure measurements. Readings have been repeated four times at each of the seven stations.

Two Precision Paroscientific pressure transducers with Pitot tubes have been used simultaneously to measure pressure drops across the louver and at the inlet and outlet of the elbow as illustrated in Figure 6.4. A hydraulic motor has been used to change louver blade angles automatically.

Louver blade angles of 60˚ and 0˚ to the horizontal have been set for measurements. Percentage of pressure drop across the louver and the elbow has been determined. Pressure at the surface and underground has been measured by transducers.

Because of lack of access through the duct only one station was used before the elbow. Vane anemometers were considered to be appropriate for velocity measurement in a curved bend duct.

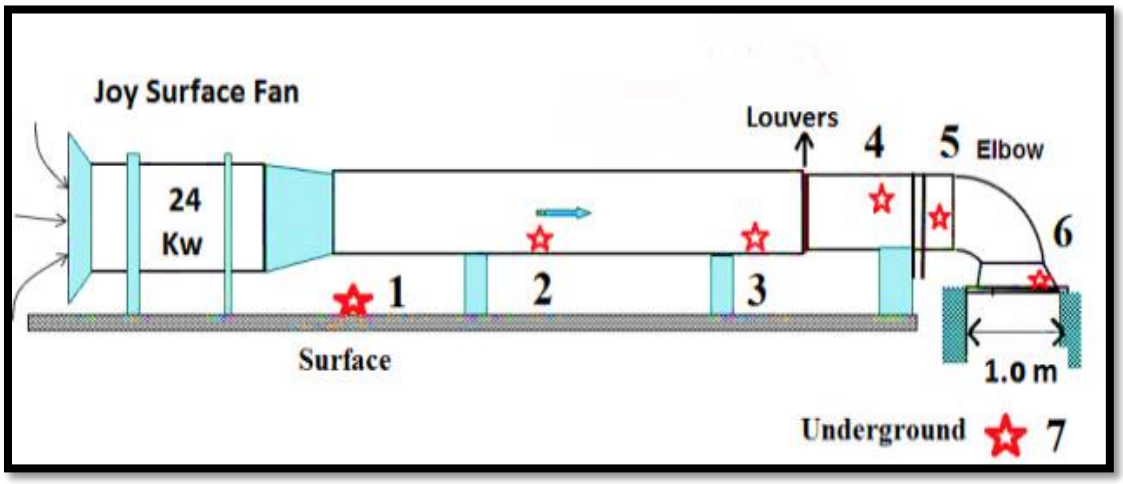

Figure 6.3. Joy surface fan and the position of stations

Figure 6.4. Transducers usage through the ducting

6.4.1. Louver with a 60˚ Blade Angle. In this experiment the Joy axial surface fan has been set at its higher speed to produce an expected 1,000 Pa total pressure. The blade angle of the louver has been fixed at 60˚ to the horizontal as shown in Figure 6.5. Measurements have been taken in each station four times with four different lengths of Pitot tube (152 mm, 254 mm, 406 mm, and 560 mm) in the ducting in order to achieve accurate results from all parts of a section. The average total pressure and also the

percentage of pressure drop across the elbow and the louver has been calculated and plotted as shown in Table 6.1. With the exception of the surface and underground pressure readings all values are total pressure and take into account elevation and fan pressure. In this experiment velocity at the elbow's inlet has been measured as 12.3 m/s.

Figure 6.5. 60˚ Louver blades angle position

Table 6.1. Pressure drop at different stations with 60˚ louvers

Number	Location	P (kPa)	ΔP (Pa)	loss (%)
1	Surface (absolute)	97.35	-	-
2	After fan	98.342	-	-
3	Before Louver	98.338	845	85
4	After Louver	97.493		
5	Before Elbow	97.476	101	10
6	After Elbow	97.375		
7	Underground (absolute)	97.534	-	-

The results from this experiment have shown that The Joy axial fan can only deliver 992 Pa due to wear and tear. Through the louver system a pressure drop of 85% of 992 Pa has occurred. In addition a second main pressure drop of 10 % has occurred across the elbow. The pressure gradient of this experiment is plotted in Figure 6.6.

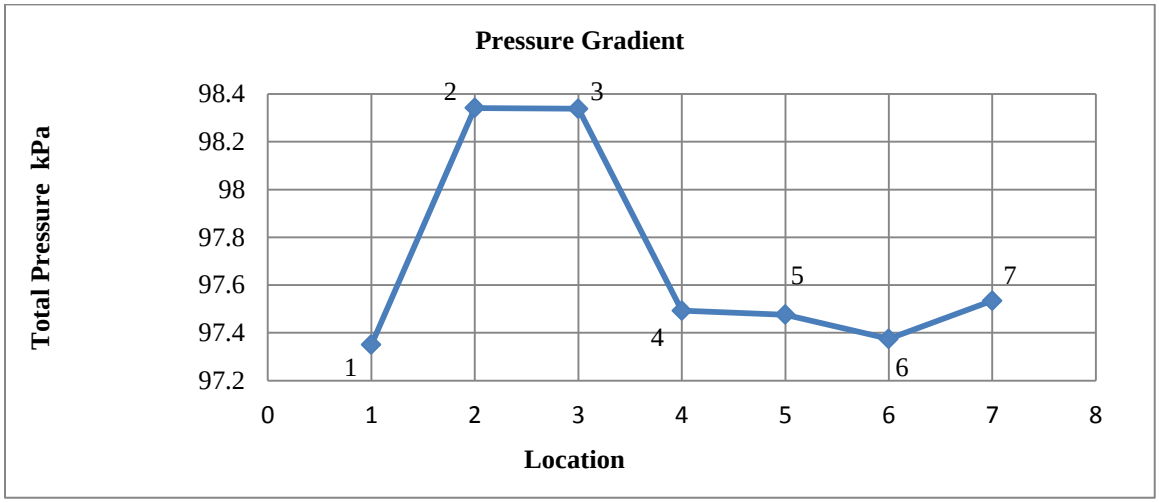

Figure 6.6. Pressure gradient across the ducting with 60˚ louver

6.4.2. Louver with a 0˚ Blade Angle. As with the previous experiment the Joy axial surface fan has been set at its higher speed to produce an expected 1,000 Pa pressure. The blade angle of the louver has been fixed parallel to ducting walls as shown in Figure 6.7. Measurements have been repeated four times (the same as in the previous experiment) with four different lengths of Pitot tube at each station. The results have been plotted in Table 6.2. Inlet velocity upstream of the elbow has been measured at 18.9 m/s.

Figure 6.7. Louver blades at 0˚ angle position

Table 6.2. Pressure drop at different stations with 0˚ louver

Number	Location	P (Kpa)	ΔP (Pa)	Loss (%)
1	Surface (absolute)	97.35	-	-
2	After fan	98.342	-	-
3	Before Louver	98.335	69	7
4	After Louver	98.266		
5	Before Elbow	98.242	237	23.8
6	After Elbow	98.005		
7	Underground (absolute)	97.534	-	-

It is evident from the above table that the pressure produced by the Joy axial surface fan was the same as the previous experiment. According to the data shown in Table 6.2, the pressure drop across the louver has been decreased dramatically by the blade angles change from 60˚ to 0˚. Pressure drop across 0˚ angle of the louver has been measured at 69 Pa of the Joy axial fan total pressure. However the pressure drop across the elbow increased noticeably (about 24% of total pressure; the highest pressure drop measured in this experiment). The pressure gradient of this experiment has been illustrated in Figure 6.8.

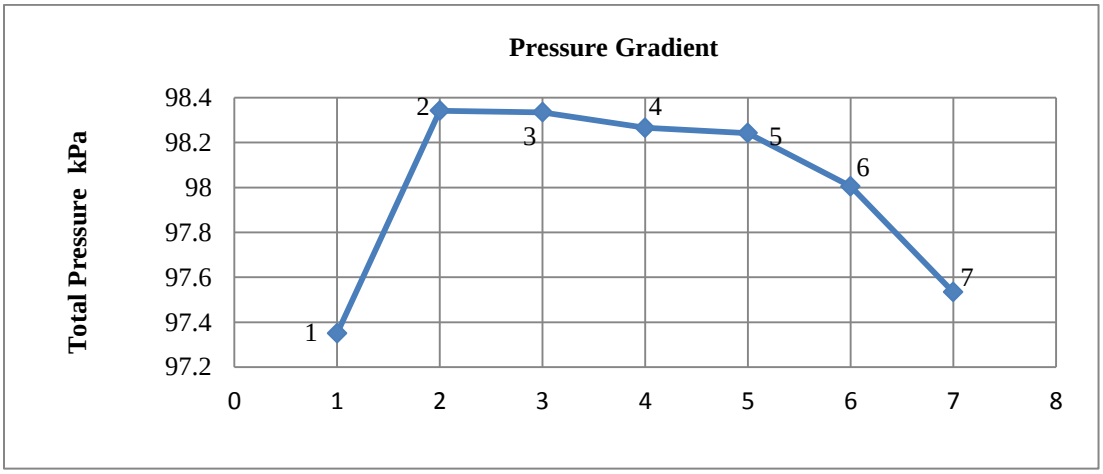

Figure 6.8. Pressure gradient across the ducting with 0˚ louver

In summary, it is noteworthy that with the changes of the louver blade angles from 60˚ to 0˚, the total pressure loss in the duct has decreased significantly. Louvers

play a key role as airflow modulators. They do this by increasing or decreasing the pressure loss through the louvers. It is self-evident that if the angle of the louver is changed, the pressure loss will be changed as will the airflow. Fan power is wasted due to air shock loss in passage through the louvers. Fans may stall when a louver blade angle is set to give a high obstruction. With the reduction in pressure drop across the louver, the pressure drop across the elbow has proportionally increased. Available air quantity and pressure underground has been improved 64% by these experimental actions.

6.5. NUMERICAL DESIGN

In this study different airflow parameters such as pressure drop, shock loss factor, equivalent Atkinson resistance, rational resistance with consideration of various blade angles and dimensions of the louver and elbow have been calculated. Loss factors (K factors) across louvers caused by different blade angles have also been calculated. The lowest pressure drops across elbows and louver from all scenarios have been selected as the ideal numerical design.

6.5.1. Pressure Drop Across Elbow. Shock loss (X) factors may be defined by the number of distinct points of velocity pressure loss due to turbulence at any bend, variation in cross-sectional area, or any other cause of a change in the direction of airflow (McPherson, 1993).

Equation 6.1 has been utilized to calculate P_{shock} across an elbow with different angles and dimensions.

$$P_{shock} = X\,(\rho/2)\,(Q^2/A^2) = R_{shock}\,Q^2\ Pa \qquad (6.1)$$

The relation between shock loss factor and equivalent Atkinson resistance has been defined by Equation 6.2.

$$R_{shock} = X\,(\rho/\,(2A^2))\ \ Ns^2/m^8 \qquad (6.2)$$

Equation 6.2 and rational resistance equation (Equation 6.3) have been used in order to compare various scenarios.

$$R_{t,shock} = (X/(2A^2))\ \ m^{-4} \qquad (6.3)$$

where ρ is the density of air (kg/m^3), Q is the air quantity (m^3/s) and A is the area (m^2)of cross section (McPherson, 1993).

Shock loss factor for right angled bends of circular and rectangular cross sections for θ= 90˚are dependent on the height, width and radius of the bend as shown in Figure 6.9.

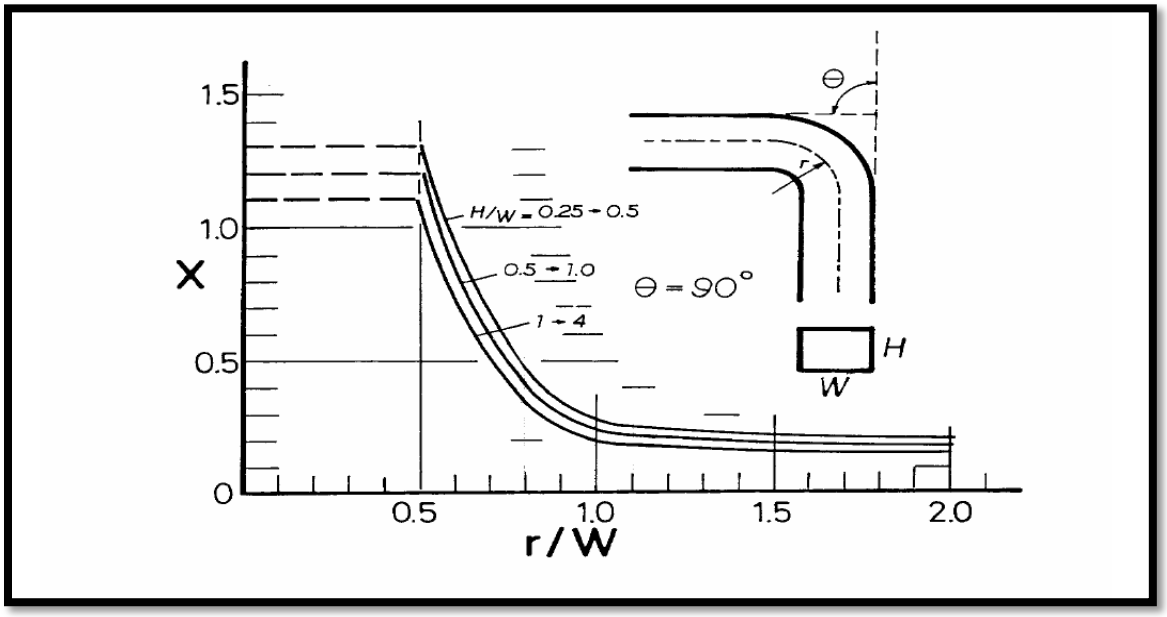

Figure 6.9. Shock loss factor for right angled bends of rectangular cross section (after McPherson, 1993).

Correction factors for all shock loss factors other than 90^o have been considered in the calculations. The ratio of H/W and r/W for potential mine elbows of 60˚ and 45˚ have been calculated as 1.0 and 0.8 in the same way as the actual mine elbow ratios which have been calculated for the real mine elbow. In Figure 6.9 it can be seen that an acceptable X factor for a 90˚ bend with r/W ratio approaches close to 2.0. A lower shock loss can be achieved for a bend by changing cross sectional dimensions. In the mine under study the height of cross section at the bottom of the shaft was measured to be 1.5 m and the width is 0.64 m. The ratios of H/W and r/W for an alternative elbow have been calculated at 2.3 and 2. These changes improve the shock loss with reference to Figure

6.9 from 0.35 to 0.15. In all calculations air density of 1.23 kg/m^3 and air velocity of 18.9 m/s have been used. Calculated results of various conceivable situations are shown in Table 6.3 relying on information from McPherson, 1993 for circular and rectangular cross sections.

Table 6.3. Calculated results for elbows with different angles

Scenarios	X	$R_{t,shock}$ (m^{-4})	R_{shock} Ns^2/m^8	P_{shock} (Pa)
Actual Mine Elbow 90˚ Rectangular	0.4	0.190	0.233	76.7
Elbow 90˚ Circular	0.3	0.264	0.323	65.59
Elbow 60˚ Rectangular	0.3	0.152	0.186	61.23
Elbow 45˚ Rectangular	0.2	0.114	0.140	46.1
Elbow 90˚ Rectangular (new size)	0.2	0.080	0.098	32.26

It is apparent that the best design is the rectangular option. The pressure drop experiences only a moderate decrease with the change of cross section from rectangular to circular as is evident in Table 6.3. A related consideration is that circular pipes can withstand large pressure differences between the inside and the outside without undergoing any significant distortion, but noncircular pipes may not (Çengel, 2006).

Noncircular pipes are used in situations such as in major surface fans. Also instance every surface centrifugal fan has a circular to rectangular transition. The data in Table 6.3 shows that with a decreasing trend in bend angle of elbow from 90˚ to 45˚ the pressure drop is reduced while the minimum pressure drop design has not been achieved. The minimum pressure drop has been achieved by the change of width and height of a smooth curved 90^o elbow.

Analytical dependence of the local loss coefficient on the geometric parameters of the fitting was found as follows:

$$\xi = C_1 (R/B)^{-1} + C_2 \exp (C_3 (R/B)^{-1}) \quad (6.4)$$

where

$$C_1 = (A/B) (- 0.069 - 3.458 (A/B)^2)^{-1} \quad (6.5)$$

$$C_2 = 0.092\ (A/B)^{-1} + 0.046 \quad (6.6)$$

$$C_3 = 1.247 + 0.177 \ln (A/B) \quad (6.7)$$

The radius of the inner and outer edges is characterized by the ratio R/B. The local pressure loss coefficient ξ is also affected by the ratio of the duct high and width A/B (Zmrhal and Schwarzer, 2009). For mine elbow the ratios of R/B and A/B have been calculated 0.82 and 1. So the local pressure loss coefficient and P_{shock} have been calculates 0.29 and 63.46 Pa.

The loss factor for 90° bends varies considerably with Reynold's number as can be seen in Figure 6.10 (Miller, 1990). Loss coefficients from standard performance charts have been modified by the application of Reynold's number correction factors.

.

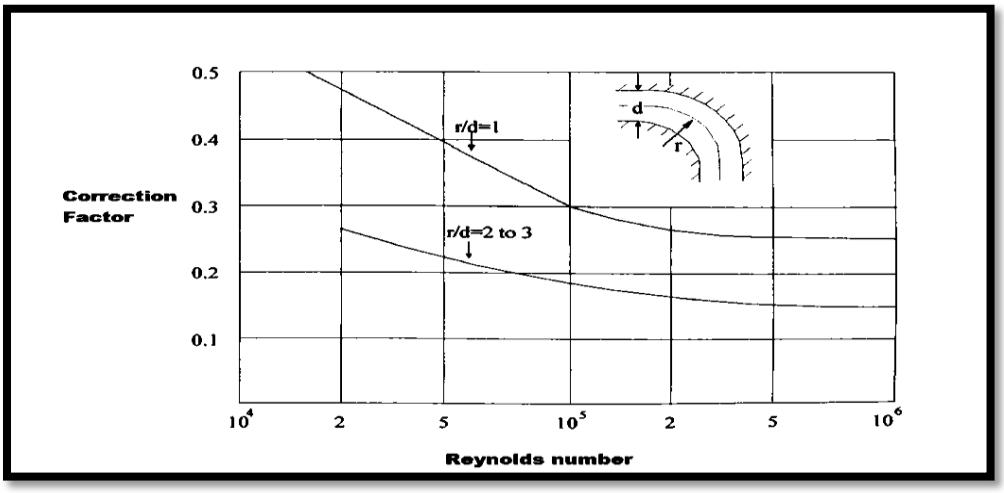

Figure 6.10. Effect of Reynold's number on 90˚ bend loss coefficients graphs

6.5.2. Friction Pressure Loss Across the Louver. Bernoulli's equation (6.8) for incompressible fluid was used.

$$(P_1) + \rho(V_1^2/2) + \rho g z_1 = (P_2) + \rho(V_2^2/2) + \rho g z_2 + P_f \quad (6.8)$$

where ρ is the density of the fluid at all points in the fluid, V is the fluid flow speed at a point on a streamline, P is the pressure at the chosen point and g is the acceleration due to gravity.

Friction loss (P_f) across a louver with two different angles used in experiments has been calculated with the use of the Bernoulli equation for incompressible fluid flow. All measured data from Table 6.4 were used to calculate P_f across the louver. 1.225 kg/m^3 has been used in the calculation as the density of air for 15˚ C.

Table 6.4. Input data for louver pressure drop calculation

Scenario	V No.3 (m/s)	V No.4 (m/s)	P_{abs} No.3 kPa	P_{abs} No.4 kPa
6o˚ louver	18.9	12.3	98.34	97.49
0˚ louver	18.9	18.9	98.34	98.27

Friction pressure loss for 60˚ and 0˚ of the louver has been calculated as 961 Pa and 72 Pa respectively. In summary, it is noteworthy that a 60˚ blade angle has played a role as an impediment against airflow in the duct. The least pressure drop across the louver has been achieved with the change of blade angle to 0˚. The pressure drop up to the elbow's inlet has been improved to 89.6% numerically by changing the blade angle of the louver to 0˚.

In practice, it is convenient to express the pressure loss for all types of fully developed internal fluid flows (laminar or turbulent flows, circular or noncircular pipes, smooth or rough surfaces, horizontal or inclined pipes) in the form of Atkinson's equation

$$\Delta P_L = f\,(L/D)(\rho\, V^2_{avg}/2) \qquad (6.9)$$

where $\rho V^2_{avg}/2$ is the dynamic pressure and f is the Chezy Darcy friction factor (Çengel, 2006).

The hydraulic diameter (D_h) and relative roughness of the mine's louver duct have been calculated as 1.006 and 9.94 x10^{-4}.

$$D_h = 4\,A/P \qquad (6.10)$$

where A is the area and P is the perimeter of cross section.

With a velocity of 18.9 m/s and air kinematic viscosity of 15.11 x10^{-6} m^2/s a Reynolds number has been calculated as 1,225,810. Chezy Darcy friction factor, *f*, for circular cross section has been found to be 0.019 from a Moody chart. Unlike the dimensionless Chezy Darcy coefficient, *f*, Atkinson's friction factor is a function of air density and, indeed, has the dimensions of density (McPherson, 1993).

$$f = 4\,f \tag{6.11}$$

$$k = f\,(\rho/2) \quad kg/m^3 \tag{6.12}$$

where f is the Fanning factor which is related to the shear stress at the wall.

Atkinson's "k" friction factor across the louver's duct has been calculated as 0.0029 kg/m^3. Pressure loss across this 1.0 m length of duct according to the Equation 8 has been determined as 4.1 Pa. Consistent with the calculated pressure loss according to the equation 6.9 it is concluded that the amount of loss through a duct without any louver blade presence is inconsequential.

The louver loss factor (K factor) is a dimensionless value that indicates the aerodynamic resistance to airflow. This value describes the link between the airflow through the louver and the pressure drop over it. During the experiments the static pressure difference was measured across a louver as calculated at distances in the upstream and downstream flow. The resulting K factor can be calculated using:

$$K = (\Delta P_t / P_k) \tag{6.13}$$

where ΔP_t, is the total pressure difference across the duct fitting and P_k is the dynamic pressure in the duct calculated by using:

$$P_k = \rho\, V^2/2 \tag{6.14}$$

where ρ is the air density (i.e. 1.2 kg/m^3 at STP) and V is the mean air velocity in the duct. Where the duct cross-sectional area is constant, the total pressure difference ΔP_t is given as the static pressure difference ΔP_s, because the mean air velocity remains constant (Smith, 1998).

Dynamic pressure and total pressure differences for two different blade angles of the louver have been calculated and K factor has been determined. Results are shown in Table 6.5.

Table 6.5. Calculated pressure drop and K factors across the louver

Scenarios	60˚ louver	0˚ louver
Total pressure difference (Pa)	845	69
Dynamic pressure (Pa)	149.06	218.79
K factor	5.67	0.32

6.6. COMPUTATIONAL DESIGN

6.6.1. Governing Equation and Solution Procedure

6.6.1.1 CFD simulation (solving process). The mesh files imported and the CFD simulation carried out using FLUENT. Before starting the CFD simulation the solver type must be chosen. There are two types of solver available in Fluent: (i) pressure based and (ii) density based. The air flow inside the ducting was incompressible and the pressure based solver, suitable for these types of flow conditions. The transient simulation option has been selected to determine time-dependent results. The governing equations and boundary conditions have been assigned. The accuracy of the CFD simulation is dependent on the proper selection of governing equations and boundary conditions (ANSYS, Inc., 2009).

6.6.1.2 Governing equations. The simulation involved fluid flow inside the computational domain so the 3D Navier-Stokes equations and continuity equation have been selected. The governing equations of Navier-Stokes have been listed as below:
Continuity Equation:

$$\frac{\partial \rho}{\partial t} + \frac{\partial \left(\rho \overline{u_i}\right)}{\partial x_i} = 0 \qquad (6.15)$$

Momentum Equation:

$$\frac{\partial\left(\rho\overline{u_i}\right)}{\partial t}+\frac{\partial}{\partial x_j}\left(\rho\overline{u_i}\,\overline{u_j}\right)=-\frac{\partial p}{\partial x_i}+\frac{\partial}{\partial x_j}\left[\mu\left(\frac{\partial\overline{u_i}}{\partial x_j}+\frac{\partial\overline{u_j}}{\partial x_i}\right)\right]+\frac{\partial}{\partial x_j}\left(-\rho\overline{u_i'u'}_j\right) \tag{6.16}$$

where

u_i' = velocity fluctuation;

$\overline{u_i}$ = avarage velocity in x direction;

$\overline{u_j}$ = average velocity in y direction;

Turbulence Equation:

***k*-equation**

$$\frac{\partial(\rho k)}{\partial t}+\frac{\partial}{\partial x_i}\left(\rho k\overline{u_i}\right)=\frac{\partial}{\partial x_j}\left[\left(\mu+\frac{\mu_t}{\sigma_k}\right)\frac{\partial k}{\partial x_j}\right]+G_k-\rho\varepsilon \tag{6.17}$$

where:

ρ = density;

k = turbulent kinetic energy;

ε = turbulent dissipation;

G_k = generation of turbulent kinetic energy;

μ_t =turbulence viscosity;

***ε*-equation**

$$\frac{\partial(\rho\varepsilon)}{\partial t}+\frac{\partial}{\partial x_i}\left(\rho\varepsilon\overline{u_i}\right)=\frac{\partial}{\partial x_j}\left[\left(\mu+\frac{\mu_t}{\sigma_\varepsilon}\right)\frac{\partial\varepsilon}{\partial x_j}\right]+C_{1\varepsilon}\frac{\varepsilon}{k}G_k-C_{2\varepsilon}\rho\frac{\varepsilon^2}{k} \tag{6.18}$$

where:

$$\mu_t=\rho C_\mu\frac{k^2}{\varepsilon} \tag{6.19}$$

$$G_k=-\rho\overline{u_i'u_j'}\frac{\partial\overline{u_j}}{\partial x_i} \tag{6.20}$$

$$-\rho\overline{u_i'u_j'} = \mu_t\left(\frac{\partial\overline{u_i}}{\partial x_j}+\frac{\partial\overline{u_j}}{\partial x_i}\right)-\frac{2}{3}\rho k\delta_{ij} \tag{6.21}$$

Model constants appearing in the governing equations

$C_{1\varepsilon}=1.44,\ C_{2\varepsilon}=1.44,\ C_{\mu}=0.09,\ \sigma_k=1.0,\ \sigma_{\varepsilon}=1.3$

Wall functions are a set of semi-empirical formulas and functions that in effect "bridge" or "link" the solution variables at the near-wall cells and the corresponding quantities on the wall. The wall functions comprise

- Laws-of-the-wall for the mean velocity and temperature (or other scalars)
- Formulae for the near-wall turbulent quantities

Depending on the choice of turbulent model, ANSYS FLUENT offers three to four choices of wall-function approaches:

- Standard Wall Functions
- Non-Equilibrium Wall Functions
- Enhanced Wall Functions (as a part of EWT)
- User-Defined Wall Functions

The standard wall functions in ANSYS FLUENT are based on the work of Launder and Spalding, and have been most widely used in industrial flows. They are provided as a default option in ANSYS FLUENT (ANSYS, 2009). This approach has been used to solve this problem. Time-averaged Navier-Stokes Equations have been gathered in Figure 6.11.

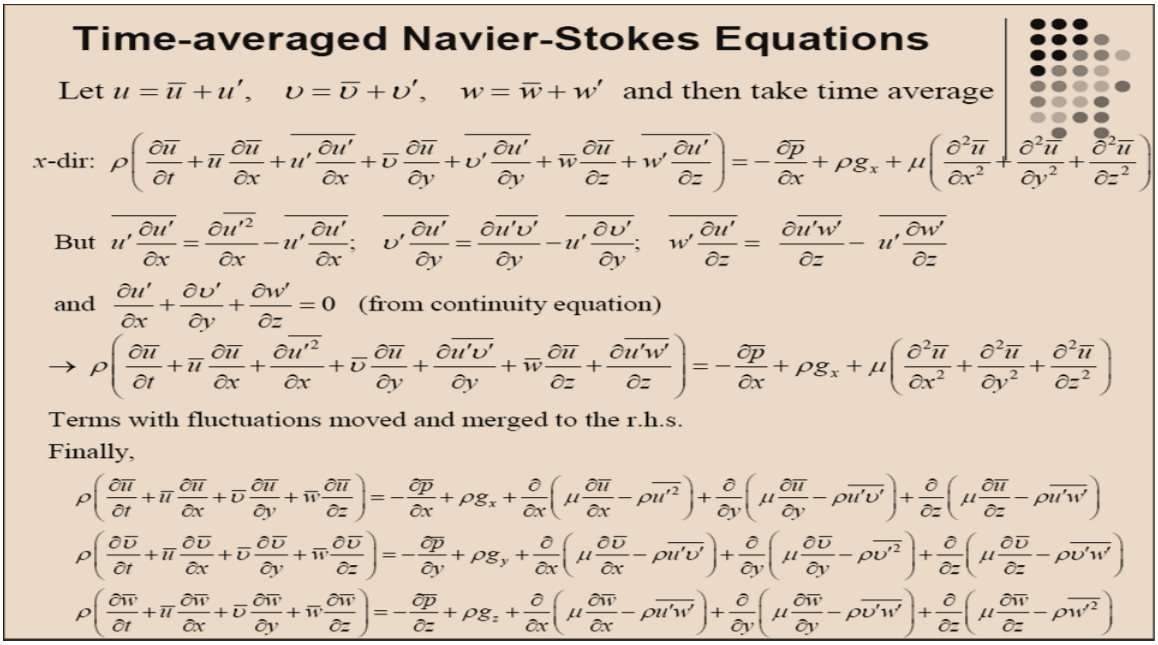

Figure 6.11. Time- averaged Navier-Stokes Equations

6.6.2. CFD Model. Fluid mechanics can be mathematically complex and there are no general analytical schemes for solving nonlinear partial differential equations contained in the governing equations for available fluid flow models. To resolve engineering problems, one approach is to simplify the governing equations and boundary conditions. Another approach is to use numerical methods and algorithms, with the help of a computer, to get the approximate solutions(Zheng, 2011; Habibi and Gillies, 2012).

The Experimental Mine elbow and louver geometric CFD model has been built using AutoCAD 2012 software. The geometric model for various bend angles of elbow and louver blade angles was created. The geometry models have been imported to Ansys Workbench to investigate the fluid flow in them. The geometry of elbow and louver has been designed according to the measured dimensions.

The numerical solution of Navier–Stokes equations in CFD usually implies a discretization method. This means that the partial differential equations are approximated by algebraic expressions which can be alternatively obtained by means of the finite-difference or the finite-element methods. Because the governing equations are non-linear, several iterations of the solution loop must be performed before a converged solution is obtained (Habibi and Gillies, 2012).

Numerical modeling has been run using FLUENT, the CFD module of ANSYS Workbench 14.0 software. The field measurement results have been used to set up and initialize the simulation. The velocity inlet boundary condition has been applied at the elbow and louver inlet. The pressure outlet boundary condition has been applied at the outflow faces of elbow and louver. The blades of the louver are symmetrical. These have been assigned as symmetry boundary condition. All the other surfaces have been treated using a no-slip boundary condition. The backflow turbulent intensity has been assumed to be 3% and the hydraulic diameter for every boundary condition has been calculated.

6.6.2.1 Elbow's scenarios. Four different scenarios have been simulated to investigate airflow distribution through the elbow and compare the predicted pressure drop and velocity. The three dimensional continuity equations and time averaged Navier-Stokes along with the boundary conditions were solved using finite volume method. The geometries have been simulated by AutoCAD 2012 and imported to the Ansys fluent 14. The mesh has been generated and discretized with fluent mesh using approximately 64,000 to 77,000 tetrahedral control volumes as shown in Figure 6.12. The viscous model is set using standard k-ε realizable model with standard wall functions for near wall treatment. The physical properties of air are treated as constants with the density of 1.225 kg/m^3 and viscosity of 1.7894e-05 kg/m-s. 18.9 m/s air velocity has been applied to the velocity inlet as boundary condition and no slip boundary conditions are applied to all the wall boundaries and pressure outlet boundary condition is imposed at the elbow outlet.

Thickness of the wall has been set to 1 mm. 15.11 $x10^{-6}$ m^2/s has been used as the kinematic viscosity for Reynolds number calculation. The hydraulic diameter and Reynolds number have been calculated for each scenario and 3% turbulent intensity has been embedded in to the program. The SIMPLE algorithm was used as the solution method for the pressure-velocity coupling.

The momentum was discretized using second order. The convergence criterion was set at10e-05 for continuity, kinetic energy (k) and turbulent dissipation (ε) equations. The calculation has been run with 250 iterations. A plate has been inserted before elbow's outlet to plot and investigate the velocity contour at those parts of the elbow.

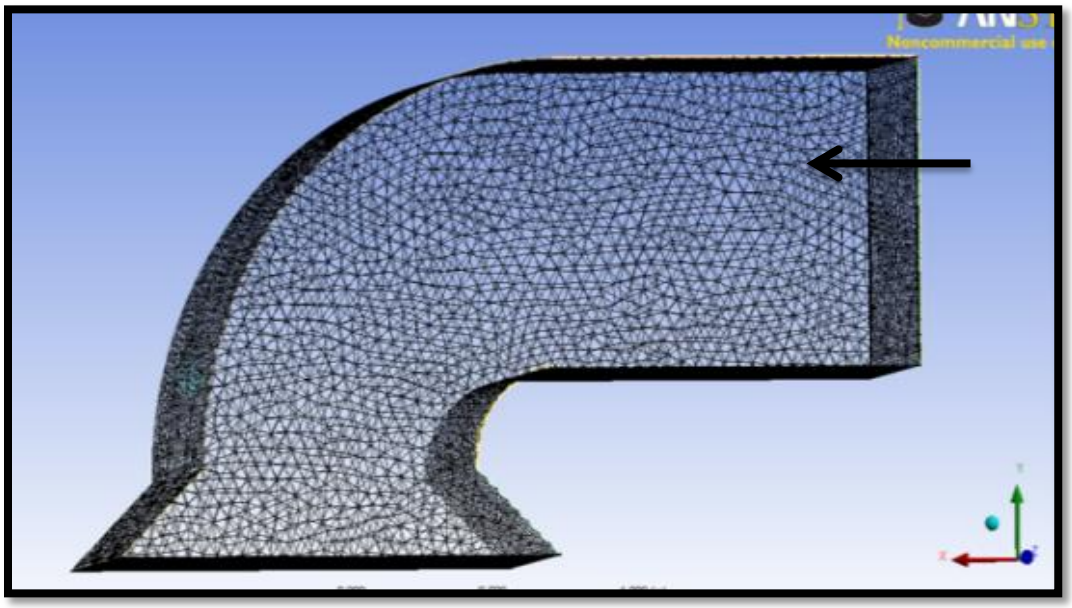

Figure 6.12. The meshed geometric mine's elbow model with airflow direction

6.6.2.1.1 Scenario1, mine elbow. This scenario was allocated to investigate airflow behavior through the original Experimental Mine elbow. An attempt was made to simulate the airflow distribution inside the mine elbow. Two different inlet velocities have been measured at the elbow inlet. Different air velocities have been established by varying the louver blade angles. The velocities measured at the inlet were 18.9 and 12.3 m/s. The hydraulic diameter has been calculated as 0.98.

Air entering the inlet duct is fully developed with Re numbers of 1,225,810 and 797,749 for two different velocities. In this scenario the mesh generated approximately 77,000 tetrahedral control volumes. Two plates before and after bend as shown in Figure 6.13 has been used to illustrate pressure counter through the elbow's bend.

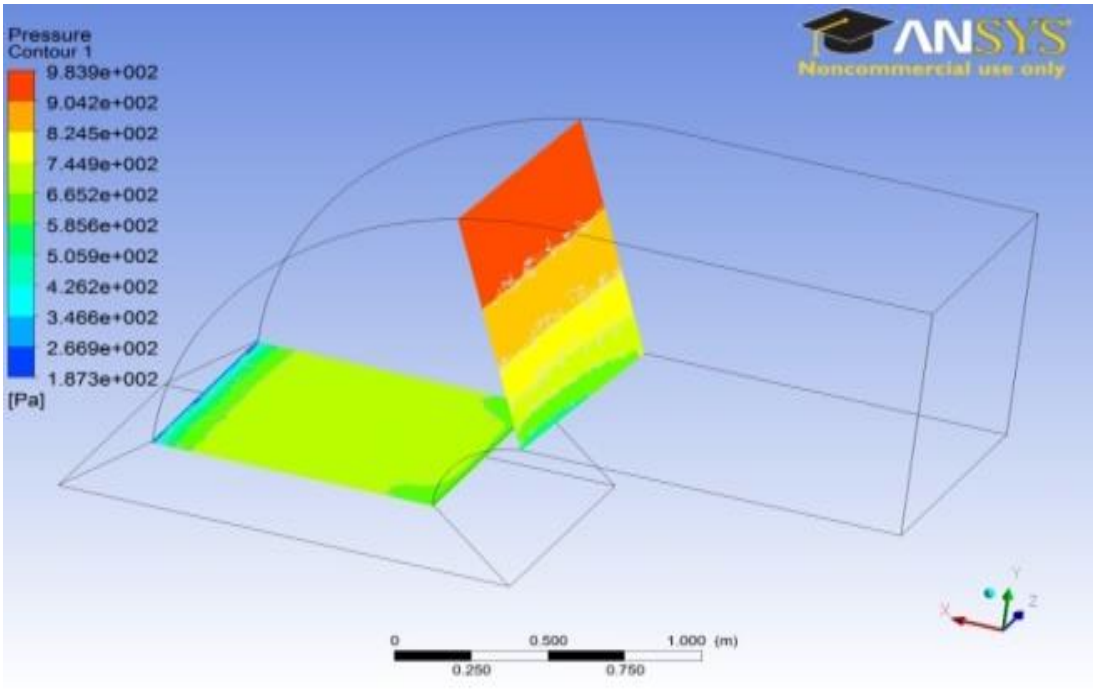

Figure 6.13. Pressure contours before and after the bend

The result of this scenario with two different inlet velocities in comparison with experimental results is shown in Table 6.6**.**

Table 6.6. Correlation of experimental and CFD results across mine elbow with 90˚ bend angle

Scenario	V_{Inlet} m/s	V_{outlet} m/s	ΔV m/s	P_{Drop} (Pa)
1A Computational	18.9	14.3	4.6	217
1A Experimental	18.9	Inaccessible	-	237
1B Computational	12.3	9.3	3	90.3
1B Experimental	12.3	Inaccessible	-	101

Simulated result for the pressure distributions are shown in Figure 6.14 for 18.7 m/s inlet velocity and blade angle of a 90˚.

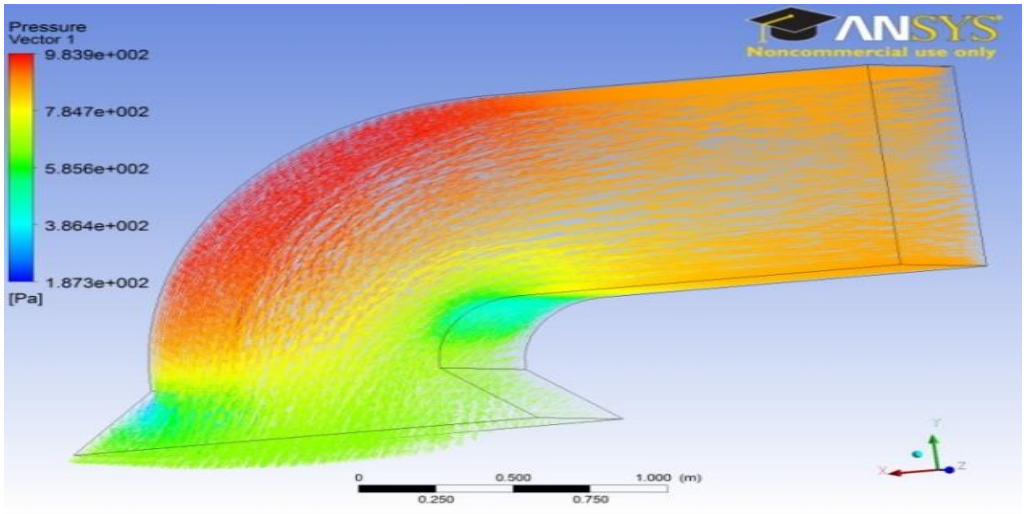

Figure 6.14. Pressure vectors through the mine elbow

6.6.2.1.2 <u>Scenario 2, 60˚ elbow.</u> In this scenario an attempt is made to simulate the airflow distribution inside the 60˚ elbow and the same dimensions were used as were used in the first scenario. Inlet velocity has been set at 18.9 m/s. The mesh has been discretized for approximately 74,000 tetrahedral control volumes. The hydraulic diameter has been calculated as 0.98. Air entering the inlet duct is fully developed with Reynolds number of 1,225,810. Pressure distributions have been simulated and are illustrated in Figure 6.15.

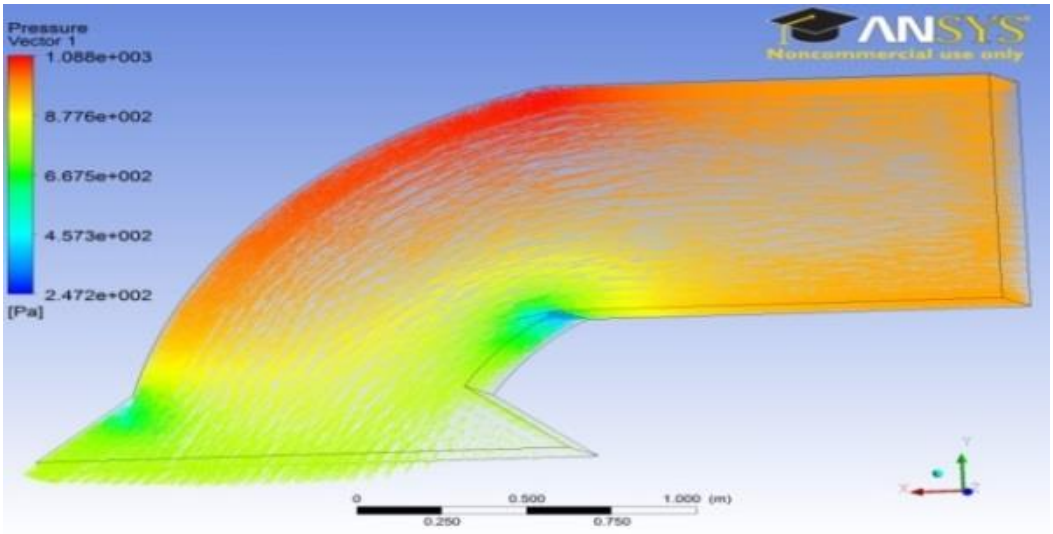

Figure 6.15. Pressure vectors through 60˚ elbow

With the change of bend angle to 60˚ the outlet velocity increased to 15.3 m/s. the amount of pressure drop in comparison with 90˚ elbow decreased as shown in Table 6.7.

Table 6.7. 60˚ elbow CFD results

Scenario	2
Velocity Inlet (m/s)	18.9
Velocity outlet (m/s)	15.3
Velocity Difference (m/s)	3.6
Pressure Drop (Pa)	181

The pressure contour has been plotted in Figure 6.16.

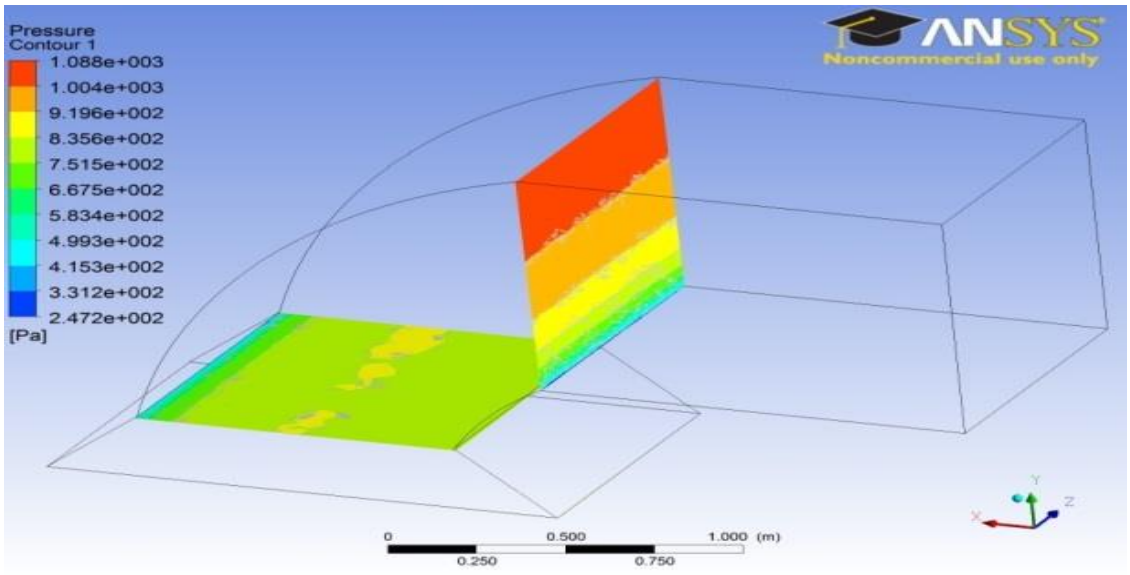

Figure 6.16. Pressure contours before and after the bend

6.6.2.1.3 <u>Scenario 3, 45˚ elbow.</u> In this scenario the geometry of the elbow has been designed with a 45˚ bend. The inlet velocity has been embedded 18.9 m/s. The hydraulic diameter has been calculated as 0.98.

The mesh generated approximately 73,000 tetrahedral control volumes. Air entering the inlet duct was fully developed with Reynolds number of 1,225,810. Pressure distributions have been simulated and are illustrated in Figure 6.17.

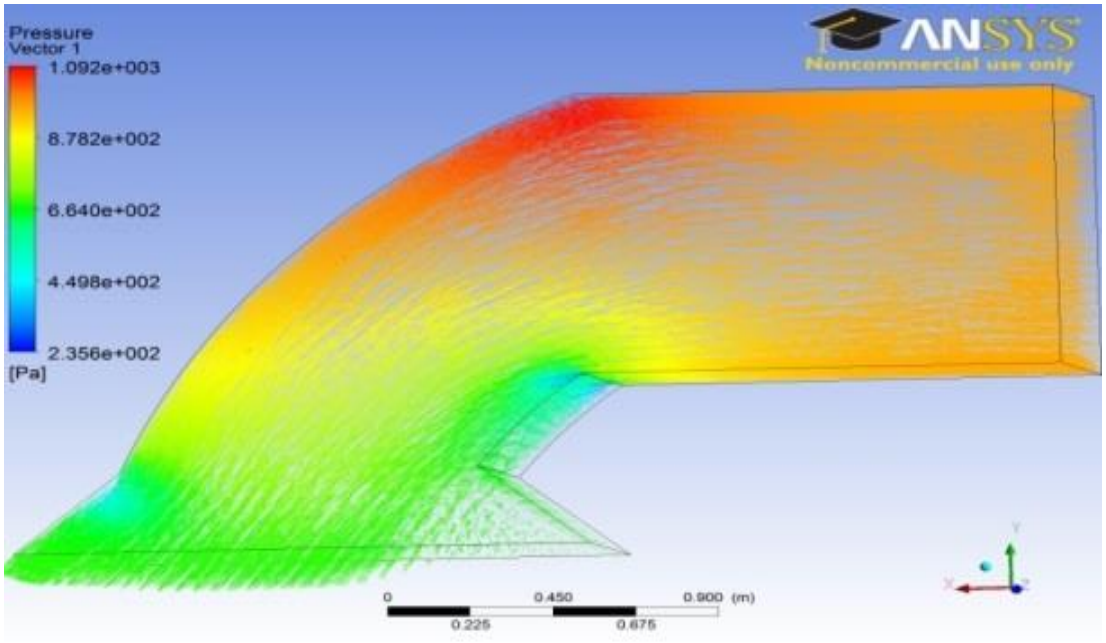

Figure 6.17. Pressure vectors through 45˚ elbow

The pressure contour before and after elbow's bend is illustrated in Figure 6.18. The result is shown in Table 6.8 for comparison with other scenarios.

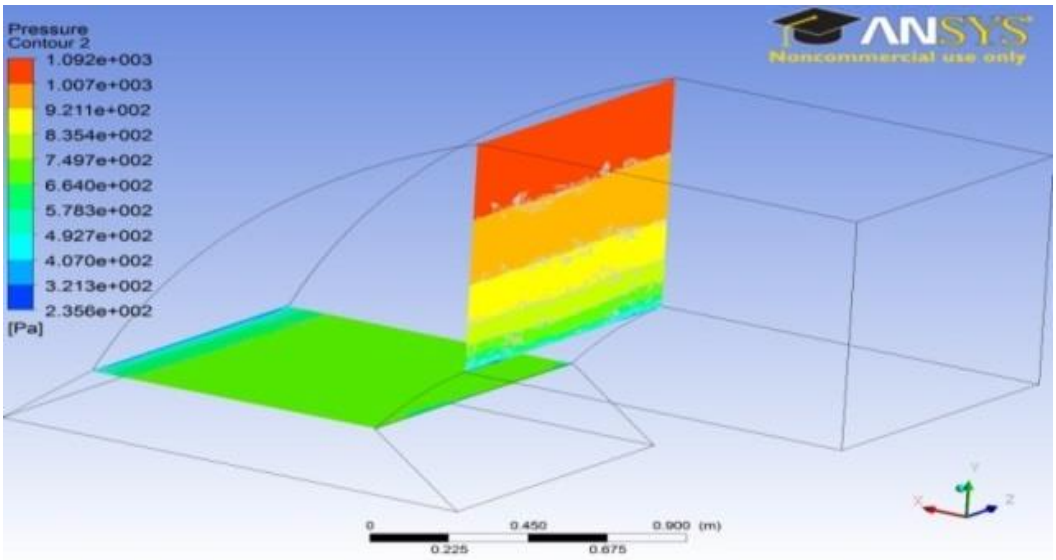

Figure 6.18. Pressure contours before and after the bend

In this simulation the pressure drop in comparison with the mine 90˚ elbow increased. However the outlet velocity was improved.

Table 6.8. 45˚ elbow CFD results

Scenario	3
Velocity Inlet (m/s)	18.9
Velocity outlet (m/s)	15.8
Velocity Difference (m/s)	3.1
Pressure Drop (Pa)	289

6.6.2.1.4 <u>Scenario 4, ideal design.</u> The Ideal numerical designed Scenario has been simulated according to the numerical approach. Height and width of the duct have been calculated at 1.5 and 0.64 m with a 90˚ bend angle. The hydraulic diameter and Reynolds number have been calculated at 0.9 and 1,122,237 respectively. Inlet velocity for this scenario is similar to the previous scenarios and has been embedded as 18.9 m/s.

The mesh has been generated and discretized approximately 64,000 tetrahedral control volumes. The Pressure distribution is shown in Figure 6.19.

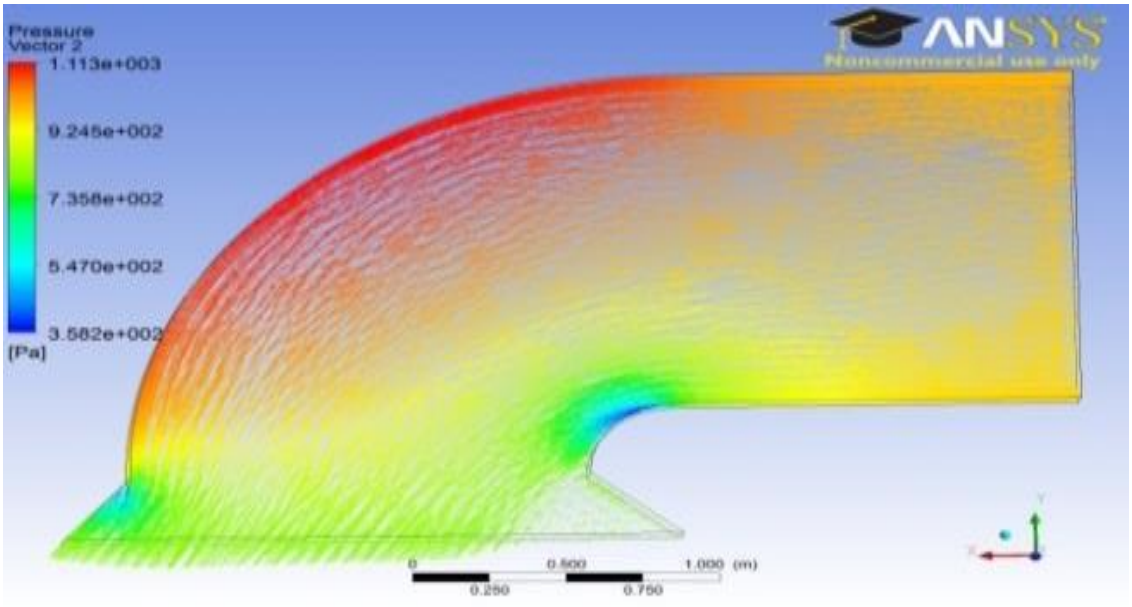

Figure 6.19. Pressure vectors through optimum elbow

The result of this scenario has been summarized in Table 6.9.

Table 6.9. Optimum elbow CFD results

Scenario	4
Velocity Inlet (m/s)	18.9
Velocity outlet (m/s)	16.7
Velocity Difference (m/s)	2.2
Pressure Drop (Pa)	175.7

The pressure contour before elbow's outlet is shown in Figure 6.20.

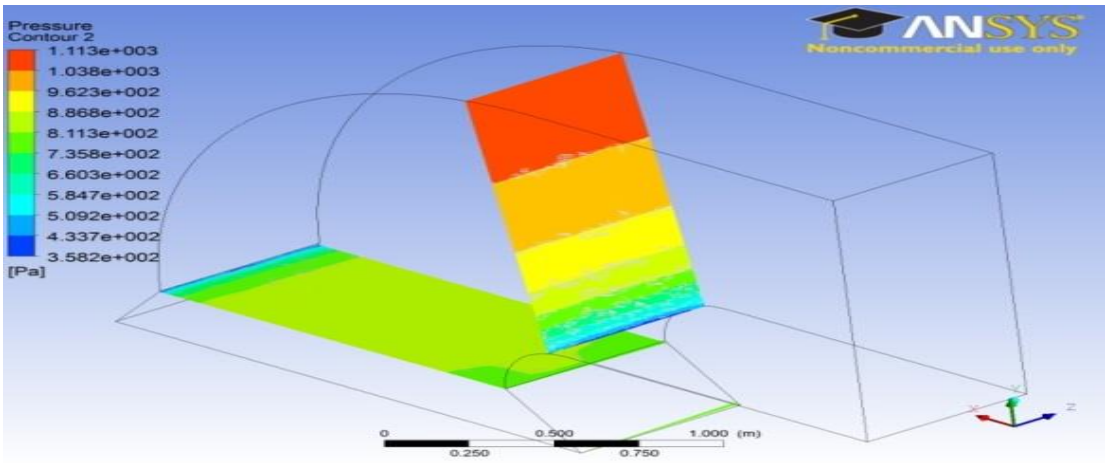

Figure 6.20. Pressure contours before and after the bend

6.6.2.1.5 General result and discussion. It is noteworthy from Scenario 1 that a decrease in inlet velocity is reflected in noticeably reduced pressure drop. Consistent with the data from table 6.6, pressure drop in the experimental results is more than the computational result. However the pressure drop differences for 12 m/s inlet velocity scenarios is 10.7 Pa. For an 18.9 m/s inlet velocity scenarios the pressure drop is calculated as 20 Pa. This study has shown that with just a change of elbow from 90˚ bend angle to 60˚ the pressure drop problem has been improved. The outlet velocity has been enhanced by changing the elbow 90˚ bend to 45˚ but this results in the pressure dropping significantly. An ideal design has not been achieved just by changing the elbow's bend angle**.** The ideal design has been accomplished when the height of the duct changed to 1.5m and the width to 0.64m with a smooth 90˚ bend angle. Due to formation of eddies at the end of the short bend angle in all scenarios; the diffuser form of outlet should be

changed. Numerous CFD results have been illustrated in Table 6.10. The result is shown in Figure 6.21.

Table 6.10. Various elbow's CFD results

Scenario	V_{Inlet} m/s	V_{outlet} m/s	ΔV (m/s)	P_{Drop} (Pa)
90˚ Elbow	18.9	12.12	6.78	217
60˚ Elbow	18.9	15.3	3.6	181
45˚ Elbow	18.9	15.8	3.1	289
Ideal Elbow	18.9	16.7	2.2	175.7

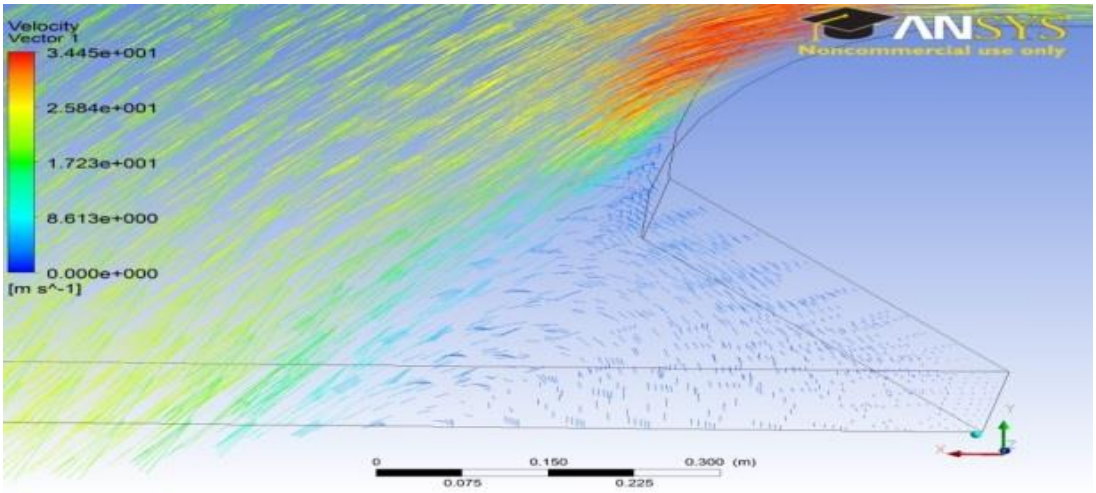

Figure 6.21. Eddies distribution vector at the elbow's outlet

6.6.2.2 Louver scenarios. Two different louver blade angles have been designed in line with mine's louver field measurements to investigate airflow behavior and compare the pressure drop and velocity with measured results.

The geometries of all scenarios have been simulated using AutoCAD and imported into the Workbench 14. The computational domain has been meshed and the grid generated with approximately 192,000 cells for the 60˚ blade angle and 200,000 tetrahedral control volumes for the 0˚ blade angle to the horizontal. The viscous model is set using the standard k-ε realizable model with standard wall functions for near wall treatment. Air physical properties are treated as constants with density of 1.225 kg/m^3 and viscosity of 1.7894 e-05 kg/m-s.

A kinematic viscosity 15.11 x10^{-6} m^2/s has been used in the Reynolds number calculation. 18.9 m/s air velocity has been applied to the velocity inlet as boundary

condition and no slip boundary conditions are applied to all of the wall boundaries. The thickness of the wall has been set to 1 mm. The blades of the louver have been specified as symmetrical, and a pressure outlet boundary condition was imposed at the louver outlet. The hydraulic diameter has been calculated 1.006.The SIMPLE algorithm was used as the solution method for the pressure-velocity coupling. The momentum was discretized using second order. The convergence criterion was set at 10e-05 for continuity, kinetic energy (k) and turbulent dissipation (ε) equations. The calculation has been run with 250 iterations.

6.6.2.2.1 60˚ angle louver. In this scenario blade angles of louver have been set to 60˚ and the geometry has been simulated using AutoCAD according to the Experimental Mine louver dimensions. . As shown in Figure 6.5 individual louvers blades vary in angle.

The geometry of 60˚ louver has been simulated to match the field measurements. The inlet velocity and hydraulic diameter have been set at 18.9 m/s and 1.02. The mesh has been generated approximately 192,000 tetrahedral control volumes. Reynolds number for this simulation has been calculated at 1,275,843. The pressure behavior of airflow across louvers is shown in Figure 6.22.

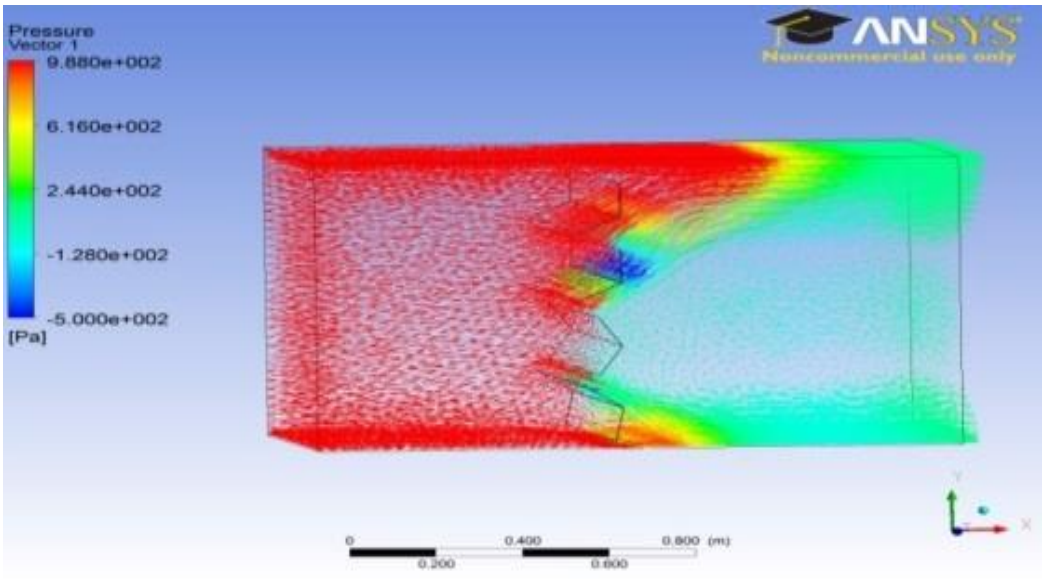

Figure 6.22. Pressure vectors across 60˚ angle louver

It is evident from Figure 6.22 that eddies were created in the center of the duct and a large proportion of air has passed along the top and bottom parts of the duct. This louver angle has had negative influence on the resulting airflow properties. Table 6.11 shows the result of this simulation according to 60˚ blade angle of the louver in comparison with experimental and numerical results when the Joy surface fan has been set at high speed. The direction of airflow was along x axis left to right as shown Figure 6.22.

Table 6.11. Correlation of computational, experimental and numerical results across 60˚ angle louver

Scenario	V_{Inlet} m/s	V_{outlet} m/s	ΔV m/s	P_{Drop} (Pa)
60˚ Louver computational	18.9	12.77	6.13	762.4
60˚ Louver experimental	18.9	12.3	6.4	845
60˚ Louver numerical	18.9	12.3	6.4	961.38

6.6.2.2.2 <u>Ideal louver.</u> The geometry of 0˚ angle louver has been simulated by AutoCAD in line with measured dimensions as shown in Figure 6.2. The inlet velocity and hydraulic diameter have been set at 18.9 m/s and 1.02. The generated mesh had approximately 200,000 tetrahedral control volumes Reynolds number for this scenario has been calculated at 1,275,843. The pressure behavior of airflow across louver is shown in Figure 6.23.

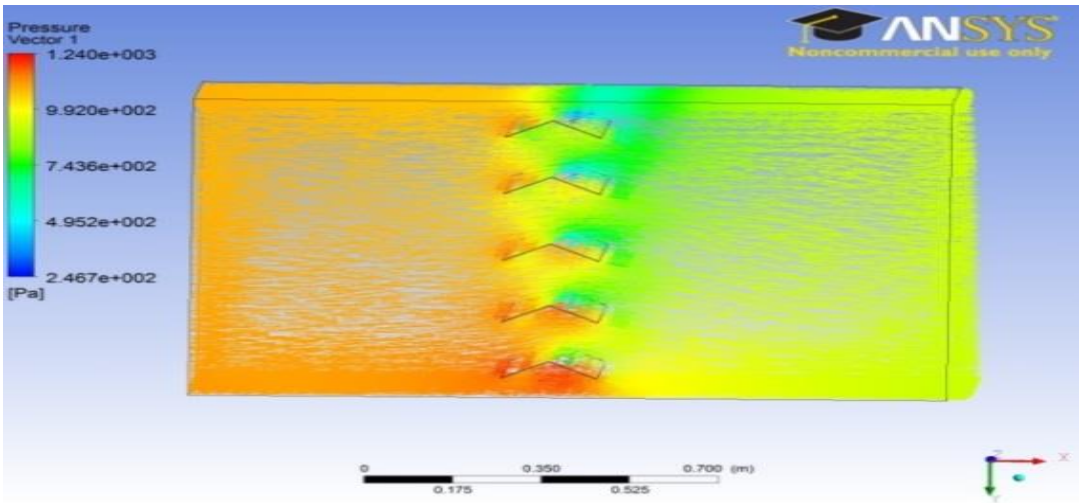

Figure 6.23. Pressure vectors across 0˚ angle louver

With the change of angle of louver blades to 0˚, the pressure drop decreased noticeably and the outlet velocity approached close to the inlet velocity. Results of this study in comparison with the experimental and numerical studies are shown in Table 6.12. Consistent with the data in the Table 6.12, this scenario has been selected as the best design for the position of the louver blades.

Table 6.12. Correlation of computational, experimental and numerical results across 0˚ angle louver

Scenario	V_{Inlet} m/s	V_{outlet} m/s	ΔV m/s	P_{Drop} (Pa)
0˚ Louver computational	18.9	18.4	0.2	84
0˚ Louver experimental	18.9	18.9	0	69
0˚ Louver numerical	18.9	18.9	0	72.1

6.7. CONCLUSION OF SECTION

The least pressure drop across the examined elbows and louver has been achieved when the height and width of the elbow changed to 1.5m and 0.64m with a smooth 90˚ bend angle and with the change of louver blade angle to 0˚ to the horizontal. Differences in the experimental and computational results of pressure drop have been calculated to be approximately 10% with the use of a 90˚ elbow and the 60˚ angle louver. An outlet velocity of 16.7 m/s has been achieved with use of the ideal elbow. The computational design results have shown that produced air velocity has decreased to 9.3 m/s when the 60˚ angle louver and the original mine elbow geometry was used in simulation.

The pressure drop has decreased when the inlet velocity through the elbow has been decreased sharply. Computationally calculated pressure drop results with the 60˚ angle louver and a 90˚ mine elbow have been determined as 979.4 Pa at the mine inlet shaft. With the change of louver blade angle to 0˚ and use of an ideal elbow the pressure drop has been decreased to 259.7 Pa. With the employment of these changes the pressure drop has been improved by 72.5% by the use of a CFD approach. The difference between experimental and numerical pressure drop results at a 0˚ angle louver is calculated as 4% while this difference for a 60˚ angle louver was 12%. The diffuser form of elbow at its outlet as shown in Figure 6.21 has produced eddies. The produced eddies have had a

negative influence on airflow behavior through the elbow. Hence the mine's elbow should be changed. This study has shown that both the louver and elbow can contribute to drop the produced pressure by a surface fan drastically. Various approaches have been utilized to decrease the pressure drop across the louver and the elbow. However none of them have eradicated the amount of pressure drop in the ducting in a fully-fledged way. One approach for eliminating the pressure drop across ducts on surface is to mount the main mine fan vertically on the shaft. This study has been carried out to allow a better understanding of flow behavior in surface ducting systems. It has also allowed the determination of the optimum operating conditions of the surface fan. As a result of these studies a vertical position has been selected for the design of the main mine fan position at the MS&T Experimental Mine.

7. CONCLUSION

With the use of both two surface and two booster fans the optimum ventilation network design has been achieved. The network efficiency has been increased by about 34% when the Joy and Alphair surface fans and two booster fans have been utilized. The air quantity has been improved by at least 25 m^3/s on all working faces. When 15 m^3/s has been achieved at working faces the network efficiency has been improved 40% and the network annual power cost has been decreased $ 20,000 in comparison with 1 surface and two booster fans. By mounting a new surface fan and subdividing the ventilation network into two segregated networks, the feasibility of various designs has been tested. With switching of inlets and outlets of both surface and booster fans, the pushing system has been changed to the pull system without changing the direction of fan blade. So, by this action, we have achieved a pull system without decrease in fan efficiency. Numerous results from this survey have shown that by adding each fan to the network the amount of air quantity has been improved noticeably. The optimum location of booster fans has been determined in line with achieving the optimum future layout for ventilation network. The appropriate blade angle for booster fans has been determined as 25˚. The Joy surface fan has been mounted on the fan house shaft and Alphair surface fan has been located on far west shaft of the mine with 15˚ bade angle. The new portal has been designed on the lower level of the mine to drain water from the eastern part and also to make an easy access to the bottom level. The air quantity, network efficiency and the network annual power cost determined the optimum design for the ventilation network for the next 100 years.

Fire behavior at three main important mine locations has been investigated in order to propose a layout to mitigate the fire hazards through the airways on future ventilation plan. It is noteworthy that distance from fire event and airflow direction has played a key role in establishing CO, CO_2 and temperature levels. In addition this study has shown that tires of vehicles are one of the most important factors in burning events. However the least consideration has been employed for choosing the tires of vehicles in the mines. The life time of tires is a major purchaser consideration. Consideration as to burning characteristics and other hazards has been neglected. In addition when all fans

have been turned off natural ventilation pressure plays a key role in determining fire distribution in the mine. Natural ventilation pressure is a crucial factor in hazardous situations. The highest amount of toxic CO gas has been monitored at 3000 ppm at the closest station to the fire when all fans have been turned off. The high monitored level of CO and CO_2 has shown that it is hard to inertize the fire at that part of the mine. The west working face lower level has been determined as the most difficult part of the mine for achieving solutions to safety issues. Noxious gases have been trapped at the mine by turning surface and booster fans off. That is why the natural ventilation study has been determined as the most important parameter to extinguish the fire in appropriate way. Numerous application such closing or opening different doors and shafts have been investigated to achieve the optimum procedure for controlling the fire. This study has shown that the best approach for diminishing the fire is not always turning the surface and booster fans off. The reversed direction of surface fans has been considered in this study which in a real mine is very hard to employ. The Emergency door between the east and a west part has been considered as the other option to manage the fire in incidents. This study has shown that the emergency plan ahead of any emergency is needed for every mine.

Elbows and louvers as major sources of pressure losses through ducting have been reported in most countries mines. A study has been carried out in the Experimental Mine to conclude that with the changes of louvers blade angles the total pressure loss in the duct decreased significantly when it was changed to 0˚ (completely open position) especially. However, we cannot ignore that louvers play a key role as an airflow modulator in ducts. They do this by increasing or decreasing the pressure loss through the louvers. It is self-evident that if you change the angle of the louver, the pressure loss will be changed as will the airflow. Fan power is wasted due to air shock loss in passage through the louvers. Fans may stall when a louver blade angle is set to give a high obstruction. With the reduction in pressure drop across the louver, the pressure drop across the elbow has proportionally increased. The amount of air quantity and needful pressure for the underground has been improved 64% experimentally. 60˚ blade angle has played a role as an impediment against airflow in the duct. The least pressure drop across louvers has been achieved with the change of blade angle to 0˚. The airflow quality at

elbow's inlet has been improved 89.6% numerically by changing the blade angle of louvers to 0˚. It is noteworthy from mine elbow result that with the decrease in inlet velocity, pressure drop has been decreased noticeably. Consistent with the mine elbow data differences in the experimental and computational results of pressure drop have been calculated approximately 10% with the use of a 90˚ elbow and the 60˚ louvers and also for 18.9 m/s inlet velocity scenarios is 8.4%. The least pressure drop across the examined elbows and louvers has been achieved when the height and width of the elbow changed to 1.5m and 0.64m respectively with a smooth 90˚ bend angle and with the change of louvers blade angle to 0˚ proportion to the surface. On account of produced eddies and zero pressure at the end of short bend angle, the diffuser form of outlet should be changed. Computational design results have shown that the produced air velocity has decreased to 9.3 m/s when 60˚ louvers and the original mine elbow geometry used in simulation. With the change of louver blade angle to 0˚ and use of an optimum elbow the pressure drop has been improved by 72.5% by the use of a CFD approach. Three-dimensional CFD models of louvers and elbow are useful in identifying the detailed flow characteristics through ducting systems. This study has shown that louvers and elbow can contribute to drop the produced pressure by surface fan drastically. A comprehensive research study has been undertaken and various solutions have been posed to decrease the amount of pressure drop across louvers and elbows. One way to eliminate pressure drop across ducts on surface is mounting the main mine fan vertically on the shaft. This study has been carried out for better understanding of flow behavior in surface ducting system and determining the position of surface fan. As a result a vertical position has been selected for the main mine fan position in Experimental Mine.

BIBLIOGRAPHY

1. Aldred, R., Spronston, J.H., and Pearce, R.J., 1984. *Air-conditioning and recirculation of mine air in North Nottinghamshire*. Mining Engineer London 143(273): 601-607.
2. Allen., C., Keen, B., 2008. *Ventilation on Demand (VOD) Project – Vale Inco Limited, Coleman Mine*, Proceedings of the 12th US/North American Mine Ventilation Symposium (Ed: K.G. Wallace), pp. 45-49, ISBN: 978-0-615-20009-5, Reno Nevada.
3. Anderson, J. D. Jr., 1995, Computational Fluid Dynamics, the Basics with Applications, Published by McGrawHill, Inc. New York. USA.
4. ANSYS, Inc., 2009, ANSYS FLUENT Getting Started Guide. ANSYS Workbench 14.0, ANSYS, Inc.
5. ANSYS, Inc., 2009, ANSYS FLUENT Theory Guide. ANSYS Workbench 14.0, ANSYS, Inc.
6. Ashelford, D., 2009. Remote Operation of Dilution Louvres, PowerPoint presentation, BHP Billiton.
7. Brake, D. J., 2013. *Fire Modelling in Underground Mines using Ventsim Visual VentFIRE Software*, Australian Mine Ventilation Conference / Adelaide, SA, Australia.
8. Calizaya, F., City, S. L., Stephens, M. and Gillies, A. D. S, 2010. *Utilization of Booster Fans in Underground Coal Mines*, *SME annual meeing*, 1–7.
9. Çengel, Y. A., 2006. Introduction to Thermodynamics and HeatTransfer, Second edition, The McGraw−Hill.
10. De Nevers, N., 2000. *Air Pollution Control Engineering.* Long Grove, Illinois: Waveland Press, Inc.
11. De Rosa, M., 2004a. Analyses of Mobile Equipment Fires for all U.S. Surface and Underground Coal and Metal/Non-metal Mining Categories, 1990-1999, NIOSH report IC 9467.
12. De Rosa, M., 2004b. Analysis of Mine Fires for All U.S. Metal/Nonmetal Mining Categories, 1990-2001, NIOSH Report IC 9476.
13. Eng, K. K. P., 2009. " New Ventilation Design Criteria For Underground Metal Mines Based Upon The "LIFE-CYCLE " Airflow Demand Schedule, PhD dissertation, Mining Engineering Department, University of British Columbia, Vancouver. Canada.
14. El-Nagdy, K. A., 2002. "Analysis of Complex Ventilation Networks In Multiple Fan Coal Mines". PhD dissertation, College of Engineering and Mineral Resources, West Virginia University, USA.

15. Fink, D.G. and Beatty, H.W., 1987. Standard Handbook for Electrical Engineers, 12th Edition, McGraw Hill Book Co, New York, USA.

16. Fleetwood, B.R., Burton, R.C., Pretoruis, B.C.B, and Holding, W., 1984. *Controlled recirculation of ventilation air at Loraine Gold Mines*, Limited. Association of the Mine Managers of South Africa, Circular 2, 1984.

17. Gamble, G. A., Ray, R. E., Americas, P. B. and York, N., 2009. *Differences In Design Considerations For Tunnel Vs . Mine Ventilation Fan Systems,* SME Annual Meeting, Denver, CO, Preprint 09-056.

18. Gillies, A. D. S, Wu, H, Reece, D and Hosking, R., 2004. U*se of Mine Fire Simulation for Emergency Preparedness*, Proceedings Qld Mining Industry Health and Safety Conference, pp 13-20 (Qld Resources Council).

19. Gillies, A. D. S., & Calizaya, F., 2012. *Use of Underground Booster Fans in Foreign Prominent Coal Mining Countries Compared With the Ban in the United States*, 14th United States/North American Mine Ventilation Symposium, 2012 – Calizaya and Nelson © *2012, University of Utah, Dept. of Mining Engineering* 475–480.

20. Gillies, S., Slaughter, C. and Wu, H. W., 2010. *Booster Fans – Some Considerations for their Usage in Underground Coal Mines*, 13th United States/North American Mine Ventilation Symposium , pp. 511–518.

21. Greyvenstein, G.P., Le Grange, L.A., and Meyer J.P., 1993, *The Optimization of Ventilation Ducting in an Upcast Mine Shaft TeeJunction and Fan Drift with Computational Fluid Dynamics*, Proc. 6th U.S. Mine Ventilation Symposium, June 21 -23, Salt Lake City, Utah, pp. 293-297.

22. Habibi, A,. 2013. "Utilization of Booster Fans in Underground Mines", Master thesis, Department of Mining and Nuclear Engineering at University Missouri S&T.

23. Habibi, A. and Gillies, A. D. S., 2012. *Effect of Booster Fan in Ventilation Networks – Computational and Experimental Approaches*, 14th United State/ North American Mine Ventilation Symposium, 2012, pp.83-89 (Nelson and Calizaya at 2012, University of Utah, Dept. of Mining Engineering).

24. Hansen, R., 2009. Literature survey – fire and smoke spread in underground mines.

25. Hansen, R., 2010b. Smoke spread calculations for fires in underground mines [online], report from Studies in Sustainable Technology Institute of Mälardalen University, Västerås. 58 p. Available from: <mdh.diva portal.org/smash/get/diva2:325849/FULLTEXT01> [Accessed: 27 January 2013].

26. Hardcastle, S.G., and Kocsis, C.K., 2004. The ventilation challenge. CIM Bulletin, 97(1080): 51-57.

27. Hartman, H.L., Mutmansky, J.M., Ramani R.J., and Wang, Y.J., 1997. Mine Ventilation and Air Conditioning. Third Edition, New York: John Wiley and Sons John Wiley & Sons.

28. Henning, J.G., and Wojtus, K., 2006. *Narrow Vein Mine Design at the Hoyle Pond Mine*. Placer Dome Limited, Porcupine Joint Venture, South Porcupine, Ontario – Private Communication.

29. Heerden, J., and Sullivan, P., 1993, *The Application of CFD For Evaluation of Dust Suppression and Auxiliary Ventilation Systems Used With Continuous Miners*, Proc. 6th U.S. Mine Ventilation Symposium, June 21 -23, Salt Lake City, Utah, pp. 293-297.

30. Jobling, S., Yates, C., Lowndes, I.S. and Yang, Z.Y., 2001. The Integration Of The Ventilation Networks Of The North Selby and Stillingfleet Mines. In S. Wasilewski (ed.), Proc. Of the 7th International Mine Ventilation Congress, Proc., Krakow, 17-22 June 2001, Katowice:EMAG.

31. Karlsson, B and Quintiere, J., 1999. Enclosure Fire Dynamics, 336 p (CRC Press).

32. Krog, R.B., 2002. "Assessment and Recommendation for the Ventilation System at the Golden Giant Mine*"*. Master of Science Thesis of Queen's University.Kingston, Ontario, Canada.

33. Kumar, G.V., Rao, G.V.K., and Rao, B.S., 1991. *Controlled Recirculation of Mine Air in a Large Bord and Pillar Coal Mine—an Economic Evaluation in the Indian Context.* Proceedings of the 5th US Mine Ventilation Symposium. Littleton, Colorado,SME.

34. Luxbacher G.W. and Ramani. R.V., 1979. *Optimization of Coal Mine Ventilation Systems.*Transactions, AIME. 286. 1801-1809.

35. Marks, J.R., 1989. *Rationale and Methodology in Designing Controlled Recirculation Ventilation Systems*. American Mining Congress Mining Convention, Underground Mining Session. September 20.

36. Martikainen, A.L., and Taylor,C.D., 2010. *Breaking the Ice on the Booster Fan Dilemma in US Underground Coal Mines*, Mining Engineering 62(10): 47-53, Denver, Colorado, USA.

37. McPherson, M. J., 1993. Subsurface Ventilation Engineering, First edition, CHAPMAN & HALL.

38. Meyer, C.F., 1993. *Controlled Recirculation of Mine Air in a South African Colliery*. Proceedings of the 6th US Mine Ventilation Symposium. Littleton, Colorado, SME.

39. Miller, D. S., 1990. Internal Flow Systems, 2nd Ed. BHRA (Information services), Bedford.

40. Moreby, R., 2009. Ventilation. *Australasian Coal Mining Practice*. Carlton, Victoria: Australasian Institute of Mining and Metallurgy.

41. Plessis, J. J. L., and Marx, W. M., 2008. *Main Fan Energy Management*, 12th U.S./North American Mine Ventilation Symposium 2008 – Wallace pp.441–446.

42. Rajaram, V., and Thimons, E. D., 1985 . *Reverse Performance Characteristics of ZMain Fans in an Oil Shale Mine* SME-AIME Annual Meeting, New York, New York, USA, pp. 1850-1853.

43. Ramani, R.V., 1992. Mine Ventilation. SME Mining Engineering Handbook. Littleton, Colorado: SME.

44. Rape, T., 2005. *"*Repair the Fan , Save Money*"*, Mining Engineering Journal (December), 31–33.

45. Ray, R. E., (n.d.). Design Cconsiderations For Main Exhaust Fan Systems at Underground Coal Mines, Proceeding of 6th International Mine Ventilation Congress, pp. 513-518.

46. Robinson, R., and Harrison, T., 1987. *Controlled Recirculation of Air at Wearmouth Colliery British Coal Corporation*. Proceedings of the 3rd Mine Ventilation Symposium. Littleton, Colorado: SME.

47. Rose, H.J.M., 1992. *"Recirculation of Air in Practice"*. Journal of the Mine Ventilation Society of South Africa 45(10): 172-174.

48. Smith, S. J., 1998. *"*Determination of k-factors of HVAC System Components Using Measurement and CFD Modelling*"*. PhD dissertation, 27. University of Nottingham, UK.

49. Stebbins, W. A., 2005. Guide to Selecting Adjustable-Speed Drive Systems, February 25.

50. Struble, G. R., Marks, J. R., and Brown, A. B., 1988. *Installation of a New Surface Fan at the Homestake Gold Mine, SME Annual Meeting, Denver, Colorado, USA 1988,* pp. 48-52.

51. Thyer, A., 2002. Development of a fire and explosion risk assessment methodology for underground mines [online], Science Group (Fire and Explosion), Health and Safety Laboratory. Report HSL/2002/24. 61 pp. Available from: <http://www.hse.gov. uk/research/hsl_pdf/2002/hsl02-24.pdf> [Accessed: 27 January 2013].

52. Turpin. R. A., and Weyher, L. H. E., 1977. I*nteractive Coal Mine Production Scheduling and Ventilation Planning Using a Time-Shared Computer*, 14th APCOM, SME-AZME**,** ed.by R. V. Ramani.

53. U.S. Department of Labor, 30 CFR Part 75, "Safety Standards for Underground Coal Mine Ventilation; Rule," 1992, Arlington, VA.

54. Ventsim Visual™ 3, 2014, Ventsim Visual ™ User Guide, Ventsim Company.

55. Wala, A. M., Yingling, J. C., Zhang, J., and Ray, R., 1993. *Validation Study of Computational Fluid Dynamics as a Tool For Mine Ventilation Design, SME Annual Meeing* , 520-525.

56. Wallace, B. K. G., Mcpherson, M. J., Brunner, D. J., and Kissell, F. N., 1990. Impact of Using Auxiliary Fans On Coal Mine Ventilation Efficiency and Cost, Bureau of Mines Report, Report of Investigations 9307.

57. Wallace K.G., 2001. *General Operational Characteristics and Industry Practices of Mine Ventilation Systems*, Proceedings of the 7th International Mine Ventilation

Congress (Ed: S. Wasilewski), pp 229-234, (Research and Development Centre for Electrical Engineering and Automation in Mining, Cracow, Poland.

58. Wang, Q., and Shang, D., 2009. *Design of Coal Mine Main Fan Performance Optimization*, Second Asia-Pacific Conference on Computational Intelligence and Industrial Applications (PACIIA 2009), pp.58–60.
59. Wang, Q., Wei, J., Yuan, R., and Zhu, C., 2009. *Scheme Design of Technology Improvement for Coal Mine ZMain Fan*. Second Asia-Pacific Conference on Computational Intelligence and Industrial Applications (PACIIA 2009), pp. 54–57.
60. Wempen, J. M., 2012. "Characterization of Air Recirculation In Multiple Fan Ventilation Systems", Masters thesis, Department of Mining Engineering at University of Utah, USA.
61. White, F. M., Fluid Mechanics, 2011, 7th Ed, Published by The McGraw-Hill Company, Inc. Chapter 6, pp. 379-382.
62. Zheng Yi., 2011. "Diesel Particulate Matter Dispersion Analysis in Underground Metal/Nonmetal MinesUsing Computational Fuid Dynamics". PhD dissertation, p.125. Missouri University of S&T. USA.
63. Zmrhal, V. and Schwarzer, J., 2009. *Numerical Simulation of Local Loss Coefficients of Ventilation Duct Fittings,* Eleventh International IBPSA Conference, Glasgow, Scotland, pp. 1761–1766.

VITA

Ali Haghighat completed his secondary education in Tehran, Iran in 2000. He attended Tehran Azad University and obtained his Bachelor degree in Mining Engineering in 2006. Mr. Haghighat joined Missouri University of Science and Technology in 2013 and received a Master of Science degree in Mining Engineering in August 2014. He has held the positions of Graduate Research Assistant and Graduate Teaching Assistant since June 2013.